A Szilikátipari Tudományos Egyesület lapja

építőanyag

Journal of Silicate Based and Composite Materials

A TARTALOMBÓL:

2020/6

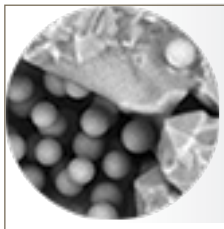

We are pleased to announce the organization of

ec-siliconf2

THE 2ND EUROPEAN CONFERENCE ON SILICON AND SILICA BASED MATERIALS

to be held in Hotel Palota in Miskolc-Lillafüred, Hungary, in October 4-8, 2021

The **ec-siliconf2** conference will be held in the wonderful palace of **Hotel Palota** in the exceptionally beautiful environment of **Beech Mountain** in **Miskolc-Lillafüred** in **Hungary**. In 2019 in the previous conference scientists had participated from **21** countries of **Asia, Europe, North- and South America** and **Africa**.

THE CONFERENCE SESSIONS

SESSION 1: Silicon and silica in inorganic and molecular chemistry
SESSION 2: Metallic silicon and silicon as an alloying agent
SESSION 3: Silicon (Si) and silica (SiO2) in medicine, therapy and health
SESSION 4: Silicon in micro and nanoelectronics and devices
SESSION 5: Silicon and silica in functional materials
SESSION 6: Silicon and silica in polymers
SESSION 7: Silicon and silica in ceramics and composites
SESSION 8: Silicon and silica in construction materials and glass
SESSION 9: Silicon and silica in biological systems and technologies
SESSION 10: Silicon and silica in smart materials and technologies
SESSION 11: Silicon and silica in minerals and rocks
SESSION 12: Testing and characterization methods, tools and errors
SESSION 13: Other results in research and development of silicon and silica and materials contain of them
SESSION 14: Other results in processing and application of silicon and silica and materials contain of them
SESSION 15: Miscellaneous in silicon and silica materials science

Registration abstract submission, and further information are available in:
www.ec-siliconf.eu

építőanyag

Journal of Silicate Based and Composite Materials

2020/6

TARTALOM

CONTENT

A finomkerámia-, üveg-, cement-, mész-, beton-, tégla- és cserép-, kő- és kavics-, tűzállóanyag-, szigetelőanyag-iparágak szakmai lapja
Scientific journal of ceramics, glass, cement, concrete, clay products, stone and gravel, insulating and fireproof materials and composites

A folyóiratot referálja · The journal is referred by:
MTA SZTAKI, ProQuest, Emerging Sources Citation Index, Google Scholar, INDEX COPERNICUS INTERNATIONAL, THOMSON REUTERS

A folyóiratban lektorált cikkek jelennek meg.
All published papers are peer-reviewed.
Kiadó · Publisher: Szilikátipari Tudományos Egyesület (SZTE)
Elnök · President: ASZTALOS István
1034 Budapest, Bécsi út 120.
Tel.: +36-1/201-9360 ▪ E-mail: epitoanyag@szte.org.hu
Tördelő szerkesztő · Layout editor: NÉMETH Hajnalka
Címlapfotó · Cover photo: GYURKÓ Zoltán

WWW.EPITOANYAG.ORG.HU
EN.EPITOANYAG.ORG.HU

Online ISSN: 2064-4477
Print ISSN: 0013-970x
INDEX: 2 52 50 ▪ 72 (2020) 185–230

Strength and consistency behaviour of replacement of cement with silicate-based geopolymer cement modified soft soil treated with crushed waste glasses for pavement underlain

Duc BUI VAN ▪ Faculty of Civil Engineering, and Research Group of Geotechnical Engineering, Construction Materials and Sustainability, Hanoi University of Mining and Geology, Vietnam ▪ buivanduc@humg.edu.vn

Kennedy Chibuzor ONYELOWE ▪ Department of Civil Engineering, Michael Okpara University of Agriculture, Nigeria ▪ konyelowe@mouau.edu.ng

Michael ONYIA ▪ Department of Civil Engineering, Faculty of Engineering, University of Nigeria ▪ michael.onyia@unn.edu.ng

Man NGUYEN XUAN ▪ Faculty of Civil Engineering, and Research Group of Geotechnical Engineering, Construction Materials and Sustainability, Hanoi University of Mining and Geology, Vietnam

Lam DAO PHUC ▪ Department of Structure-Materials, Civil Engineering Faculty University of Transport Technology ▪ lamdp@utt.edu.vn

Chidozie IKPA ▪ Department of Civil Engineering, Faculty of Engineering, Alex Ekwueme Federal University, Ndufu-Alike Ikwo, Ebonyi State, Nigeria

Somjai YUBONCHIT ▪ Professor of Civil Engineering, Rajamangala University of Technology Isan, Thailand ▪ d5540150@g.sut.ac.th

Adrian EBEREMU ▪ Professor of Civil Engineering, Ahmadu Bello University, Nigeria ▪ aeberemu@gmail.com

Kolawole OSINUBI ▪ Professor of Civil Engineering, Ahmadu Bello University, Nigeria ▪ kosinubi@yahoo.com

A. Bunyamin SALAHUDEEN ▪ Department of Civil Engineering, Faculty of Engineering, University of Jos, Nigeria ▪ basalahudeen@gmail.com

Agapitus AMADI ▪ Associate Professor of Civil Engineering, Federal University of Technology, Nigeria ▪ Agapitus.amadi@futminna.edu.ng

Michael MADUABUCHI ▪ Department of Civil Engineering, Michael Okpara University of Agriculture, Nigeria

Jesuborn OBIMBA-WOGU ▪ Department of Civil Engineering, Michael Okpara University of Agriculture, Nigeria

Ifeanyichukwu ONUOHA ▪ Department of Environmental Technology, School of Environmental Sciences, Federal University of Technology, Nigeria ▪ ifeanyichukwu.onuoha@futo.edu.ng

Zubair SAING ▪ Associate Professor of Civil Engineering, Universitas Muhammadiyah Maluku Utara, Indonesia ▪ zubairsaing@ummu.ac.id

Érkezett: 2020. 01. 23. ▪ Received: 23. 01. 2020. ▪ https://doi.org/10.14382/epitoanyag-jsbcm.2020.31

Abstract

The effect of quarry dust based geopolymer cement (QDbGPC) and ordinary Portland cement (OPC) replaced in the ratios of 0:0, 0:40, 5:35, 10:30, 15:25, 20:20, 25:15, 30:10, 35:5, and 40:0% by weight respectively was investigated. This was carried out under the influence of 4%, 8%, 12%, 16% and 20% by weight crushed waste glasses. This was conducted to study the effect of these materials on the consistency and strength characteristics of representative test soil in the laboratory. Preliminary test on the test soil shows that the soil is expansive, highly plastic with high clay content and classified as an A-7-6 soil group according to AASHTO classification system. It is also classified as poorly graded according to USCS. The treated exercise presented an improvement in the California bearing ratio, compaction and consistency characteristics in a steady and substantial pattern. The increased addition of the proportions of geopolymer cement caused increased values of CBR, G_s and decreased values of plasticity index. The unsuitable and problematic soft soil was improved to meet the requirements for a soil material to be used as a subgrade construction material. This is due to the composite blend of materials with high silicate contents responsible for strength gain. However, the replacement of ordinary Portland cement with silicate-based geopolymer cement will remove the dangers of CO_2 emission during construction works and present an environmentally friendly practice of soil re-engineering.

Keywords: California bearing ratio, compaction, silicate-based materials, crushed waste glasses, geopolymer cement, recycled solid waste materials, composite construction materials

Kulcsszavak: kaliforniai teherbírási érték, tömörítés, szilikát alapú anyagok, zúzott üveghulladék, geopolimer cement, újrahasznosított szilárd hulladékok, kompozit építőanyagok

1. Introduction

The improvement of the mechanical properties of soft soils has become increasingly necessary because of the role soils play in pavement constructions, more especially the underlain foundation structures [1-2]. Pavements are underlain structurally by soils borrowed or compacted in situ, during the foundation phase of flexible or rigid pavements [3-6]. Pavement facilities are important horizontal structures that contribute to the socioeconomic development and environmental accessibility of suburbs, urban centres, cities and nations. Unfortunately, in Nigeria and many other developing countries of the world, the failure rate of pavements is alarming [7]. Over 80 percent of the road pavements in Nigeria are in deplorable state due to primarily badly formed underlain. Worst in this category is located in the south-eastern and southern geopolitical regions of the country [8-9]. Pavement failures are initiated primarily by lateral deformation, which eventually initiate cracks like as presented in *Figs. 1* & *2* [2, 10]. These cracks give way for moisture migration to the underlain structure of the pavements. Further intake of moisture under hydraulically bound conditions causes the underlain subgrade to experience volume changes due swell-shrink cycles [11-12]. According to Herve *et al.* [1], these volume changes initiate greater degree of failure by shear and lateral heaving. This is the consequence of building pavements with weak and unstable underlain subgrade soils [1, 13-17]. The use of ordinary Portland cement in the weak soil stabilization protocols, on the other hand, generates strengthened structures prone to crack effects because of the brittle nature of ordinary cement stabilized soils [18]. Moreover, the use of ordinary Portland cement releases an equivalent amount of CO_2 into the atmosphere contributing to global warming and this is at a time when our planet is at the brink of environmental issues as a result of constant exposure to nonenvironmentally friendly construction procedures and practices [19-23]. The synthesis of geopolymer cement with quarry dust as the base material and its utilization in the improvement of the soft soil properties is currently being studied [23-29]. Soil conservation takes many methods and forms depending on its usage and various environmental reasons. This has proven as a sure way of conserving the soils for use as engineering material. However, new and other areas are also being explored to achieve soil stabilization with zero release of CO_2 into the environment [30-35]. Crushed waste glasses, also, are eco-friendly geomaterials derived from crushing waste glasses disposed by Glass Industries as scrap losses from glass production or poor handling [1, 36]. Waste glasses are also solid waste disposed by factories, homes and offices resulting from poor handling, accidents, etc. The utilization of ordinary Portland cement (OPC) and quarry dust based geopolymer cement (QDbGPC or GPC) in this work in a linear inverse replacement pattern was to determine the best geoengineering practices through which silicate-based or bio-based cements can partially or totally replace Portland cements, which inadvertently allow room for the disposal of the solid waste under consideration without exposing the environment or landfills to potential dangers [37-39]. This was conducted in that order to determine the replace-ability of the silicate-based geopolymer cement over ordinary Portland cement [2]. Also, the effect of introducing crushed waste glasses in an incremental order into the cemented test soil was also studied. It was a complex blending of various eco-friendly materials with a view to improving the California bearing ratio, consistency and compaction characteristics of the treated soft soil. According to Herve *et al.* [1] and Onyelowe *et al.* [36] the best practices of soil conservation could take this pattern for soils to be used as pavements underlain.

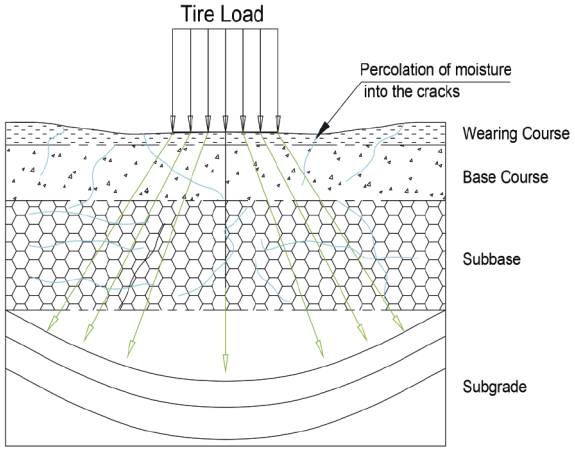

Fig. 1 Cross section of pavement with crack propagation at subgrade failure under traffic cyclic loading [2]
1. ábra Az útpálya keresztmetszete valamint a repedés terjedése az aljzat meghibásodásakor ciklikus forgalmi terhelés esetén

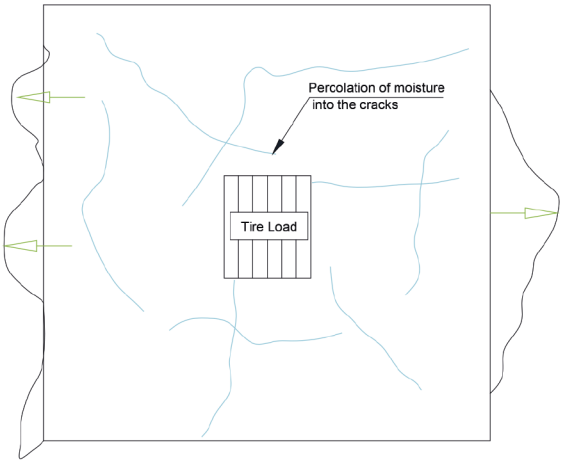

Fig. 2 Plan of pavement with crack propagation at subgrade failure under traffic cyclic loading [2]
2. ábra Az útpálya felülnézete valamint a repedés terjedése az aljzat meghibásodásakor ciklikus forgalmi terhelés esetén

2. Materials and methods

2.1 Materials preparation

400 g of test lateritic soil was collected from distributed in hilly areas such as Soc Son District, Hanoi City and Hoa Binh Province of Vietnam. The disturbed sample was taped to remove lumps, sundried for 4 days and stored for the stabilization experimentation. The quarry dust material is in several Crush Rock Industries Areas in Ninh Binh Province such as Gia Vien District, Hoa Lu District, Hanoi, Vietnam, which satisfies design conditions in accordance with TCVN

8857 [39]. It was also sundried to remove moisture and stored in silo bags for use. The waste glasses were collected from the dump sites across Hanoi. They were crushed with the 50kN crusher and also stored for use. The OPC used satisfied the requirement of cements used as binders in Vietnam construction industry [40-41]. The geopolymer cement (GPC) was synthesized with quarry dust (QD) and activator materials (Sodium Hydroxide (NaOH) and Sodium Silicate (Na_2SiO_3)). Based on previous findings on the synthesis of GPCs [28, 29, 31, 42-47], the quarry dust based Geopolymer was synthesized.

2.2 Experimental methods

The conventional tests that were conducted on the test soil for characterization and classification reasons are as follows;

i. Particle size distribution (PSD): this was conducted with vertically arranged sieve sizes mounted on an automatic shaker in accordance with BS 1377-2 and Nigerian General Specification [7, 48],
ii. Standard Proctor Compaction: this was conducted on the untreated soil with 2016 ELE Automatic Compactor Machine in accordance with BS 1377-2, and NGS [7, 48] and on the treated soil in accordance with BS 1924 [49],
iii. Consistency Limits: this was conducted using a 2013 cassagrande apparatus on the untreated soil in accordance with BS 1377-2, and NGS [7, 48] and on the treated soil specimens in accordance with BS 1924 [49],
iv. Specific Gravity test was conducted by Pycnometer method in accordance with BS 1377-2, and NGS [7, 48] and BS 1924 [49] for the untreated and the treated soils respectively,
v. Chemical Oxides Composition test on the test soils and the test materials with XRF method in accordance with BS 1377-2 and Nigerian GS [7, 48]
vi. And finally, California Bearing Ratio test (CBR): was conducted on the untreated and treated soils blended with 4, 8, 12, 16, and 20% CWG and linearly inversely replaced cements of QDbGPC and DOPC in a ratio pattern of 0:40, 5:35, 10:30, 15:25, 20:20, 25:15, 30:10, 35:5, and 40:0% by weight of solid. This was experimented with a 2015 S211 KIT CBR penetration machine, motorized 50kN ASTM used to load the penetration piston into the soil sample at a constant rate of 1.27 mm/min (1 mm/min to BS Spec.) and to measure the applied loads and piston's penetrations at determined intervals with which CBR values were computed using Eq. (1) and results were obtained. This was experimented in accordance with British standards, Vietnamese standards and AASHTO methods [48-54]

$$CBR = \frac{P_T}{P_S} x100 \quad (1)$$

Where;

P_T = corrected unit test load corresponding to the chosen penetration from load penetration curve,

P_S = the total standard load for the same depth of penetration which can be taken as 13.24 kN for 2.5 mm penetration and 19.96 kN for 5.0 mm penetration.

3. Results and discussions

3.1 General behavior and classification of test materials

The results of the experimental program have been presented in tables and graphs in the following pages. Test soil sample was investigated and characterized under the laboratory conditions with the preliminary test results presented in *Tables 1*, and *2* and *Fig. 3*. The soil was classified as A-7-6 group according to the AASHTO classification method [51]. It was equally classified according to USCS as poorly graded (GP) soil. Additionally, the soil was observed as having high clay content and high free swell index (FSI). It was also classified as highly plastic with plasticity index above 17% and expansive. *Table 3* presents that the test materials have high aluminosilicate content and possess pozzolanic properties [40]. *Table 3* and *Fig. 4* presents the oxide rates and bonding potentials of the test materials. This also satisfied that the material bonding is a very important factor in soil stabilization and strength development. This is because the soil and the admixture need to form a homogeneous and cohesive bond. Material requirement for cementitious materials states that the sum of the oxide rates of SiO_2, Al_2O_3, and Fe_2O_3 should not be less than 70%. The results of the analysed materials presented in *Table 3* show that the percentage of SiO_2 + Fe_2O_3 + Al_2O_3 for each of the materials is greater than 70%. This behaviour makes the test material samples highly pozzolanic [40]. This property was of great advantage because it brought about a high degree of interaction, pozzolanic reaction, carbonation reaction and bonding between the studied soil and the synthesized GPC.

Property description of test soils and units	Values
% Passing Sieve No 200	38
NMC (%)	13.49
LL (%)	46
PL (%)	21
PI (%)	25
SL (%)	8
FSI (%)	234
G_s	2.43
AASHTO Classification	A-7-6
UCSC	GP
MDD (g/cm³)	1.85
OMC (%)	16.2
CBR (%)	13
Colour	Reddish Grey

Table 1 Basic properties of test soils
1. táblázat A vizsgált talajok alapvető tulajdonságai

Materials	% Passing sieve (mm)										
	19	6.35	4.75	2.36	1.18	0.6	0.425	0.3	0.15	0.075	Pan
Test Soil	-	100	91	82	63	50	39	28	21	10	0
Quarry Dust	100	89	44	23	18	15	14	12	5	2	0
CWG	100	96	82	76	63	54	47	39	24	19	0

Table 2 Particle size distribution (PSD) of test materials
2. táblázat A vizsgált anyagok szemmegoszlása

Materials	Oxides Composition (content wt %)												
	SiO_2	Al_2O_3	CaO	Fe_2O_3	MgO	K_2O	Na_2O	TiO_2	LOI	P_2O_5	SO_3	IR	Free CaO
Test soil	76.56	15.09	2.30	2.66	0.89	2.10	0.33	0.07	-	-	-	-	-
Quarry Dust	63.48	17.72	5.56	1.77	4.65	2.76	0.01	3.17	0.88	-	-	-	-
CWG	73.5	0.78	8.11	-	1.79	2.09	11.0	-	1.89	-	-	-	0.8
DOPC	21.45	4.45	63.81	3.07	2.42	0.83	0.20	0.22	0.81	0.11	2.46	0.16	0.64

**IR is Insoluble Residue, LOI is Loss on Ignition, QD: Quarry Dust, DOPC: Dangote Ordinary Portland Cement, CWG: Crushed Waste Glasses*

Table 3 Oxides composition of the materials used in this paper
3. táblázat A cikkben használt anyagok oxidos összetétele

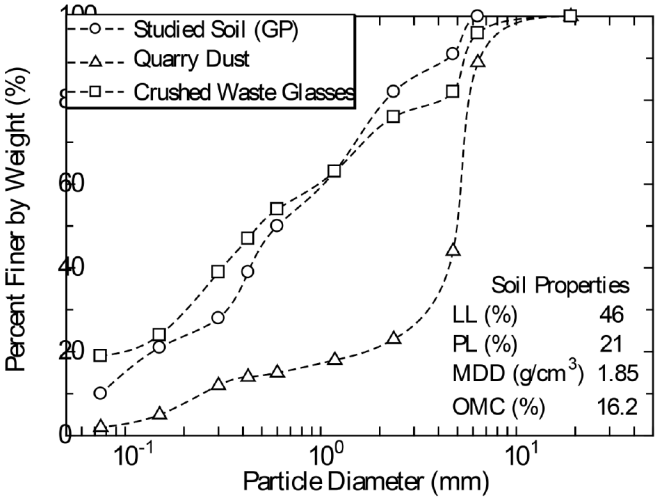

Fig. 3 Particle size distribution of studied materials
3. ábra A vizsgált anyagok szemmegoszlása

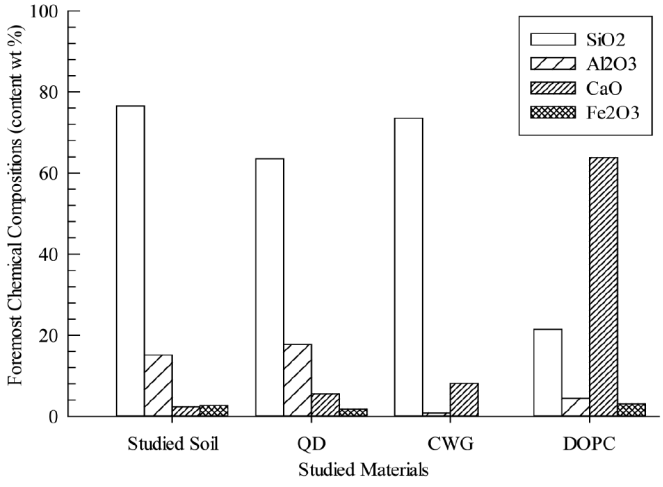

Fig. 4 Chemical oxides components in studied materials
4. ábra A vizsgált anyagok kémiai oxidos összetétele

3.2 Compaction behaviour of QDbGPC: DOPC treated soil with crushed waste glasses (CWG)

The compaction results are presented in *Table 4* and *Fig. 5*. The compaction behaviour is the densification process observed on the QDbGPC/ DOPC treated soil under the influence of added proportions of crushed waste glasses. The test soil was observed to be an unstable soil and was treated alternately with QDbGPC and DOPC in the ratios of 0:0, 0:40, 5:35, 10:30, 15:25, 20:20, 25:15, 30:10, 35:5, and 40:0% respectively. The effect of 4%, 8%, 12%, 16% and 20% by weight of crushed waste glasses over the cemented test soil was also observed. While 0:0% of the cements proportion by weight of solid served as the control point, the proportions of GPC increased from 5% in an increment of 5% while DOPC decreased from 40% at the rate of 5% also. The maximum dry density of the test soil increased with increased proportion of GPC and decreased proportion of DOPC. This consistently continued until 40:0% corresponding to GPC and DOPC respectively. The specific gravity also increased in that succession consistently. Alternatively, the optimum moisture content decreased with the same pattern. Notably, the introduction of the high content aluminosilicate crushed waste glasses improved the compaction characteristics of the test soil under the influence of the cements. This behaviour on the axes of the cements linear inverse replacement process was due to the introduction of a more bio-based cementing material, which is resistant to sulphate attacks, cracking and brittleness. Also, the bio-based cementing geomaterial i.e. the QDbGPC composite produced more silicate and aluminate to form CSH and CAH responsible for strength gain and densification [2, 56, 57, 58, 59]. It forms more elastic agglomeration and sequestrum and flocs to produce a more densified treated soil. Cation exchange reactions between the dissociated ions from the bio-based cementing material caused the increased density and specific gravity with increased proportions of GPC. These increased MDD were obtained at optimum moisture content [60].

3.3 Consistency behaviour of QDbGPC to DOPC treated soil with crushed waste glasses (CWG)

Table 5 and *Fig.6* present the consistency behaviour of the quarry dust based geopolymer cement linearly and inversely replace ordinary Portland cement treated soil under laboratory conditions under crushed waste glasses added to the treatment procedure. The addition of CWG into the cemented soil reduced the liquid limits, plastic limits and the plasticity index consistently. This behaviour however shows that further addition of CWG beyond the maximum 40% utilized in this exercise could have improved the consistency limits further. But very important to note was the improvements recorded with the linearly inversely introduction of the cements into the test soil. That is, while the bio-based geopolymer cement was increased in the treatment blend, the Portland cement was reduced and the effect of this treatment pattern was observed. Results have shown that increased quarry dust based geopolymer cement reduced the consistency limits from very high plastic condition to even very less plastic consistency. The

Proportion of Geopolymer to Ordinary Portland Cements (GPC/OPC)	Percentage of Crushed Waste Glasses (CWG) added (%)																	
	0%			4%			8%			12%			16%			20%		
	MDD	OMC	Gs	MDD	OMC	Gs	MDD	OMC	Gs	MDD	OMC	Gs	MDD	OMC	Gs	MDD	OMC	Gs
0:0	1.85	16.2	2.43	1.87	16.1	2.45	1.89	15.9	2.47	1.92	14.9	2.49	1.98	14.2	2.56	1.99	14.1	2.58
0:40	3.5	15.4	3.45	3.56	15.2	3.48	3.58	15.1	3.49	3.59	13.1	3.54	3.66	12.8	3.58	3.86	12.4	3.68
5:35	4.6	14.3	4.5	4.68	14.1	4.59	4.69	14	4.6	4.72	12.0	4.69	4.89	11.7	4.89	4.99	11.2	4.99
10:30	5.5	13.5	5.34	5.59	13.2	5.37	5.6	13.1	5.38	5.69	11.1	5.88	5.88	10.6	5.98	5.98	10.2	6.1
15:25	6.4	12.6	6.45	6.48	12.3	6.48	6.49	12.2	6.49	6.53	10.2	6.89	6.76	9.4	6.99	6.86	9.1	7.2
20:20	7.5	11.7	7.45	7.58	11.3	7.49	7.59	11.2	7.52	7.64	9.2	8.58	7.87	8.2	8.88	8.87	7.2	9.48
25:15	9.56	9.45	10.4	9.59	9.25	10.5	9.69	7.25	11.5	9.78	6.25	12.58	10.48	6.0	12.88	11.48	5.6	13.78
30:10	11.45	7.34	13.2	11.55	7.14	13.8	11.85	6.14	14.8	11.98	5.14	15.8	12.98	5.0	15.9	13.98	4.2	16.86
35:5	13.65	5.45	15.6	13.85	5.15	15.9	13.95	4.15	16.9	14.24	3.15	17.9	15.24	3.0	18.78	16.24	2.8	19.88
40:0	15.76	4.75	18.5	15.96	4.35	18.8	16.06	3.35	19.8	17.86	2.35	20.8	18.56	2.0	21.8	19.56	2.1	22.64

**MDD x10^{-1} and Gs x10^{-1}*

Table 4 Compaction behaviour of treated soil
4. táblázat A kezelt talajok tömörítési viselkedése

Proportion of Geopolymer to Ordinary Portland Cements (GPC/OPC)	Percentage of Crushed Waste Glasses (CWG) added (%)																	
	0%			4%			8%			12%			16%			20%		
	LL	PL	Ip	LL	PL	Ip	LL	PL	Ip	LL	PL	Ip	LL	PL	Ip	LL	PL	Ip
0:0	46	21	25	44	22	24	40	17	23	38	16	22	37	16	21	36	16	20
0:40	43	21	22	42	21	21	38	18	20	37	17	20	35	16	19	34	15	19
5:35	41	20	21	39	19	20	37	18	19	35	17	18	32	15	17	30	13	17
10:30	38	18	20	36	17	19	34	16	18	32	15	17	30	14	16	28	13	15
15:25	35	17	18	32	14	18	29	12	17	26	10	16	25	10	15	24	10	14
20:20	31	15	16	30	15	15	27	13	14	24	11	13	23	11	12	21	10	11
25:15	29	16	13	26	14	12	23	11	11	21	11	10	20	11	9	18	10	8
30:10	25	15	10	22	13	9	19	11	8	17	10	7	15	9	6	14	9	5
35:5	19	12	7	17	11	6	16	11	5	15	11	4	14	11	3	12	10	2
40:0	16	12	4	14	11	3	12	9	3	10	8	2	10	9	1	9	8	1

Table 5 Consistency behaviour of treated soil
5. táblázat A kezelés hatása a talajok konzisztenciájára

Plunger Penetration (mm)	Plunger Load (kN)								
	California bearing ratio behaviour of OPC+QDbGPC (%) treated soil with 0% CWG								
	0	0+40	5+35	10+30	20+20	25+15	30+10	35+5	40+0
0	0	0	0	0	0	0	0	0	0
0.5	1.2	1.5	1.8	2.1	4.4	8.4	12.4	16.5	20.5
1	1.3	1.6	1.9	2.2	4.5	8.5	12.5	16.6	20.6
1.5	1.5	1.7	2.0	2.3	4.6	8.6	12.6	16.7	20.7
2	1.7	1.8	2.1	2.4	4.7	8.7	12.7	16.8	20.8
2.5	1.8	1.9	2.2	2.5	4.8	8.8	12.8	16.9	20.9
3	2.0	2.1	2.3	2.6	4.9	8.9	12.9	17.0	21.0
3.5	2.1	2.2	2.4	2.7	5.0	9.0	13.0	17.1	21.1
4	2.2	2.3	2.5	2.8	5.1	9.1	13.1	17.2	21.2
4.5	2.3	2.4	2.6	2.9	5.2	9.2	13.2	17.3	21.3
5	2.4	2.5	2.7	3.0	5.3	9.3	13.3	17.4	21.4
5.5	2.6	2.7	2.8	3.1	5.4	9.4	13.4	17.5	21.5
6	2.7	2.8	2.9	3.2	5.5	9.5	13.5	17.6	21.6
6.5	2.9	2.9	3.0	3.3	5.6	9.6	13.6	17.7	21.7
7	3.2	3.3	3.4	3.5	5.7	9.7	13.7	17.8	21.8
7.5	3.6	3.7	3.8	3.7	5.8	9.8	13.8	17.9	21.9
8	3.8	3.9	4.0	4.1	6.2	9.9	13.9	18.0	22.0
8.5	4.1	4.2	4.3	4.4	6.5	10.0	14.0	18.1	22.1
9	4.3	4.4	4.5	4.6	6.7	10.1	14.1	18.2	22.2
9.5	4.4	4.5	4.6	4.7	6.8	10.2	14.2	18.3	22.3
10	4.5	4.6	4.7	4.8	6.9	10.3	14.3	18.4	22.4

Table 6 California bearing ratio behaviour of OPC+QDbGPC (%) treated soil with 0% CWG
6. táblázat OPC+QDbGPC-vel kezelt talaj kaliforniai teherbírási értéke (0% CWG esetén)

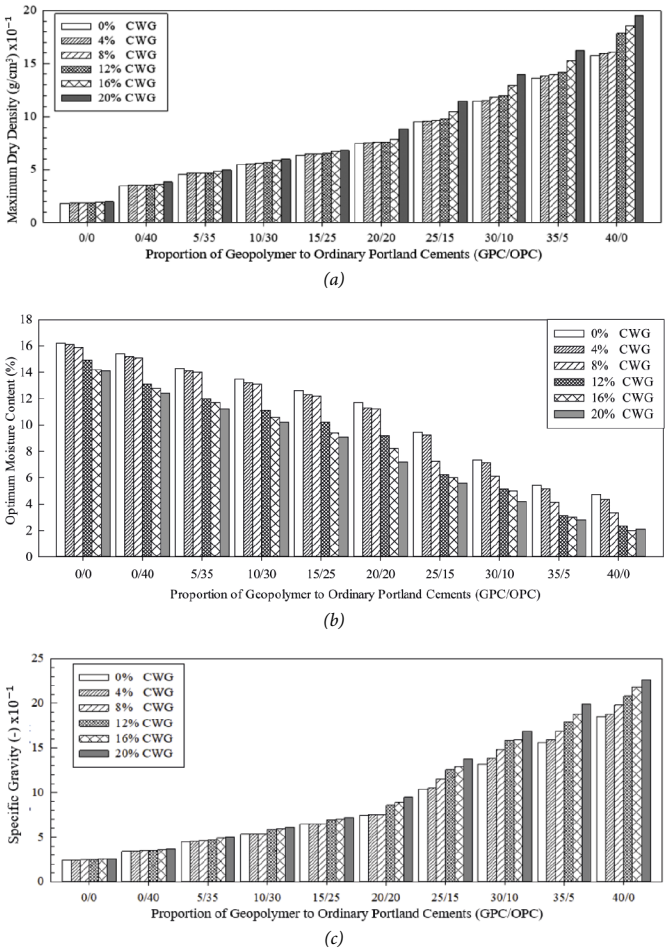

Fig. 5 Influences of crushed waste glasses on compaction behaviour of treated soil: (a) maximum dry density (x10⁻¹), (b) optimum moisture content, (c) specific gravity (x10⁻¹)

5. ábra Zúzott üveghulladék hatása a kezelt talajok tömörödési viselkedésén: (a) maximális száraz testsűrűség (x10⁻¹), (b) optimális nedvesség tartalom, (c) fajsúly (x10⁻¹)

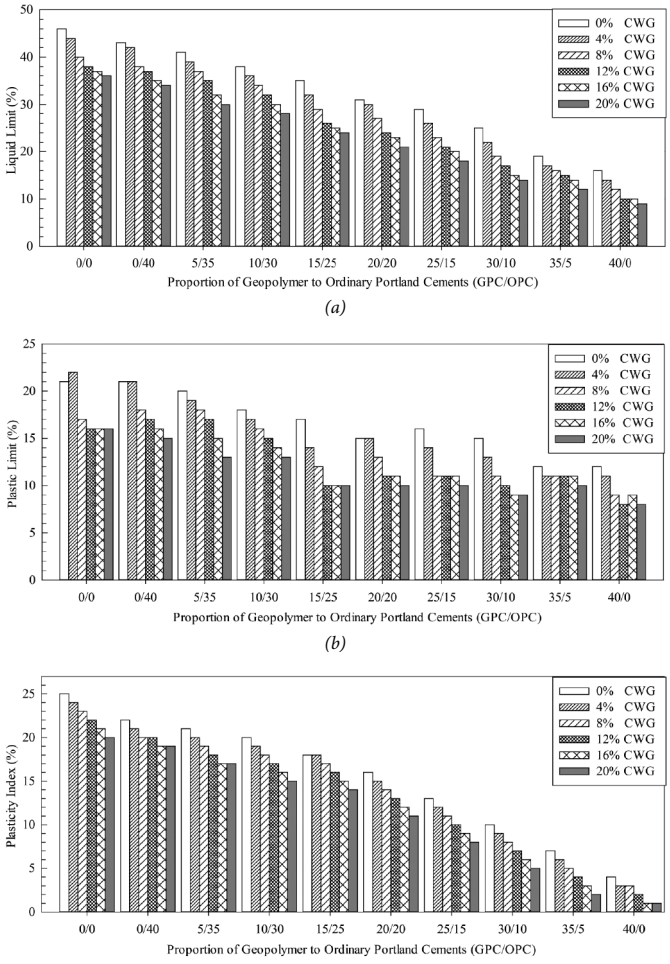

Fig. 6 Influences of crushed waste glasses on consistency behaviour of treated soil: (a) Liquid limits, (b) Plastic limit, and (c) Plasticity index

6. ábra Zúzott üveghulladék hatása a kezelt talajok konzisztenciájára: (a) Sodrási határ, (b) Folyási határ, (c) Plasztikus index

hydration of the stabilized mixture and its increased calcination and pozzolanic activity have contributed to the behaviour of the soil. And also due to molecular rearrangement in the formation of transitional compounds [2]. This improvement is due to the hydration of the highly silicate-based pozzolanic additives from the quarry dust based geopolymer cement (QDbGPC) with the treated soil matrix, which reduced the PI consistently thereby producing a stiff mixture of stabilized soil. Also, the release of more cations from the biomass based geomaterials and quarry dust during the cation exchange reaction has contributed to the behaviour of the stabilized mixture. This behaviour agrees with Little *et al.* [61], which showed that if water is used as pore fluid, the influence of the mechanical factors would remain same with a general decrease in LL and PI on addition of an admixture and binder. The prone to cracks and brittle behaviour of Portland treated soils has contributed to the improved consistency limits at reduced rates of the DOPC [2].

3.4 California bearing ratio behaviour of OPC plus QDbGPC treated soil with crushed waste glasses (CWG)

CBR test was conducted to determine the untreated and treated soils resistance to shear failure when subjected to axial loads. Traffic loads are axial dynamic loads pavement facilities are exposed to from vehicles of various sizes and penetration pressures. Pavements and pavement foundation fail by shear or lateral displacement (deformation). Hence it is important to observe the rigidity or stiffness of subgrade materials used as underlain structures. The CBR behaviour results of the underlain subgrade soil were presented in *Tables 6-12* and *Figs. 7 & 8*. The studied soil was observed to be an expansive soil and was treated alternately with QDbGPC and OPC in the ratios of 0:0, 0:40, 5:35, 10:30, 15:25, 20:20, 25:15, 30:10, 35:5, and 40:0% by weight respectively. The effect of 4%, 8%, 12%, 16% and 20% by weight of crushed waste glasses over the cemented test soil was also observed. While 0:0% of the cements proportion by weight of solid served as the control point, the proportions of GPC increased from 5% in an increment of 5% while OPC decreased from 40% at the rate of 5% also. There was a consistent improvement on the CBR value of the treated soil with increased QDGbGPC and reduced DOPC proportions. These improved CBR values were greater than 20%, and satisfy the material condition for use as improved subgrade material on Nigeria's dilapidated roads [7]. The consistently increased CBR values with the addition of QDGbGPC was due to the presence of adequate amount of calcium required for the formation of Calcium Silicate Hydrate (CSH) and Calcium Aluminate Hydrate

Plunger Penetration (mm)	Plunger Load (kN) California bearing ratio behaviour of OPC+QDbGPC (%) treated soil with 4% CWG								
	0	0+40	5+35	10+30	20+20	25+15	30+10	35+5	40+0
0	0	0	0	0	0	0	0	0	0
0.5	1.3	1.6	1.9	2.2	4.5	8.5	12.5	16.6	20.6
1	1.4	1.7	2.0	2.3	4.6	8.6	12.6	16.7	20.7
1.5	1.6	1.8	2.1	2.4	4.7	8.7	12.7	16.8	20.8
2	1.8	1.9	2.2	2.5	4.8	8.8	12.8	16.9	20.9
2.5	1.9	2.0	2.3	2.6	4.9	8.9	12.9	17.0	21.0
3	2.1	2.2	2.4	2.7	5.0	9.0	13.0	17.1	21.1
3.5	2.2	2.3	2.5	2.8	5.1	9.1	13.1	17.2	21.2
4	2.3	2.4	2.6	2.9	5.2	9.2	13.3	17.3	21.3
4.5	2.4	2.5	2.7	3.0	5.3	9.3	13.4	17.4	21.4
5	2.5	2.6	2.8	3.1	5.4	9.4	13.5	17.5	21.5
5.5	2.7	2.7	2.9	3.2	5.5	9.5	13.6	17.6	21.6
6	2.8	2.9	3.0	3.3	5.6	9.6	13.7	17.7	21.7
6.5	3.0	3.1	3.1	3.4	5.7	9.6	13.8	17.8	21.8
7	3.3	3.4	3.5	3.6	5.8	9.8	13.9	17.9	21.9
7.5	3.7	3.8	3.9	3.8	5.9	9.9	14.0	18.0	22.0
8	3.9	4.0	4.1	4.2	6.3	10.0	14.1	18.1	22.1
8.5	4.2	4.3	4.4	4.5	6.6	10.1	14.2	18.2	22.2
9	4.3	4.5	4.6	4.7	6.8	10.2	14.3	18.3	22.3
9.5	4.5	4.6	4.7	4.8	6.9	10.3	14.3	18.4	22.4
10	4.6	4.7	4.8	4.9	7.0	10.4	14.4	18.5	22.5

Table 7 California bearing ratio behaviour of OPC+QDbGPC (%) treated soil with 4% CWG
7. táblázat OPC+QDbGPC-vel kezelt talaj kaliforniai teherbírási értéke (4% CWG esetén)

Plunger Penetration (mm)	Plunger Load (kN) California bearing ratio behaviour of OPC+QDbGPC (%) treated soil with 8% CWG								
	0	0+40	5+35	10+30	20+20	25+15	30+10	35+5	40+0
0	0	0	0	0	0	0	0	0	0
0.5	1.4	1.7	2.1	2.3	4.6	8.6	12.6	16.7	20.7
1	1.5	1.8	2.2	2.4	4.7	8.7	12.7	16.8	20.8
1.5	1.7	1.9	2.3	2.5	4.8	8.8	12.8	16.9	20.9
2	1.9	2.1	2.3	2.6	4.9	8.9	12.9	17.0	21.0
2.5	2.1	2.1	2.4	2.7	5.0	9.0	13.0	17.1	21.1
3	2.2	2.3	2.5	2.8	5.1	9.1	13.1	17.2	21.2
3.5	2.3	2.4	2.6	2.9	5.2	9.2	13.2	17.3	21.3
4	2.4	2.5	2.7	3.0	5.3	9.3	13.3	17.4	21.4
4.5	2.5	2.6	2.8	3.1	5.4	9.4	13.5	17.5	21.5
5	2.6	2.7	2.9	3.2	5.5	9.5	13.6	17.6	21.6
5.5	2.8	2.9	3.0	3.3	5.6	9.6	13.7	17.7	21.7
6	2.9	3.0	3.0	3.4	5.7	9.7	13.8	17.8	21.8
6.5	3.1	3.2	3.2	3.5	5.8	9.8	13.9	17.9	21.9
7	3.4	3.5	3.6	3.7	5.9	9.9	14.0	18.0	22.0
7.5	3.8	3.9	4.0	4.1	6.0	10.0	14.1	18.1	22.1
8	4.0	4.1	4.2	4.3	6.4	10.1	14.2	18.2	22.2
8.5	4.3	4.4	4.5	4.6	6.7	10.2	14.3	18.3	22.3
9	4.4	4.6	4.7	4.8	6.9	10.3	14.4	18.4	22.4
9.5	4.6	4.7	4.8	4.9	7.0	10.4	14.5	18.5	22.5
10	4.7	4.8	4.9	5.0	7.1	10.5	14.6	18.6	22.6

Table 8 California bearing ratio behaviour of OPC+QDbGPC (%) treated soil with 8% CWG
8. táblázat OPC+QDbGPC-vel kezelt talaj kaliforniai teherbírási értéke (8% CWG esetén)

Plunger Penetration (mm)	Plunger Load (kN) California bearing ratio behaviour of OPC+QDbGPC (%) treated soil with 12% CWG								
	0	0+40	5+35	10+30	20+20	25+15	30+10	35+5	40+0
0	0	0	0	0	0	0	0	0	0
0.5	1.5	1.8	2.2	2.4	4.7	8.7	12.7	16.8	20.8
1	1.6	1.9	2.3	2.5	4.8	8.8	12.8	16.9	20.9
1.5	1.8	2.0	2.4	2.6	4.9	8.9	12.9	17.0	21.0
2	2.0	2.2	2.5	2.7	5.0	9.0	13.0	17.1	21.1
2.5	2.2	2.3	2.6	2.8	5.1	9.1	13.1	17.2	21.2
3	2.3	2.4	2.7	2.9	5.2	9.2	13.2	17.3	21.3
3.5	2.4	2.5	2.8	3.0	5.3	9.3	13.3	17.4	21.4
4	2.5	2.6	2.9	3.1	5.4	9.4	13.4	17.5	21.5
4.5	2.6	2.7	3.0	3.2	5.5	9.5	13.6	17.6	21.6
5	2.7	2.8	3.1	3.3	5.6	9.6	13.7	17.7	21.7
5.5	2.9	3.0	3.2	3.4	5.7	9.7	13.8	17.8	21.8
6	3.0	3.1	3.3	3.5	5.8	9.8	13.9	17.9	21.9
6.5	3.2	3.3	3.4	3.6	5.9	9.9	14.0	18.0	22.0
7	3.5	3.6	3.7	3.8	6.0	10.0	14.1	18.1	22.1
7.5	3.9	4.0	4.1	4.2	6.1	10.1	14.2	18.2	22.2
8	4.1	4.2	4.3	4.4	6.5	10.2	14.3	18.3	22.3
8.5	4.4	4.5	4.6	4.7	6.8	10.3	14.4	18.4	22.4
9	4.5	4.7	4.8	4.9	7.0	10.4	14.5	18.5	22.5
9.5	4.7	4.8	4.9	5.0	7.1	10.5	14.6	18.6	22.6
10	4.8	4.9	5.0	5.1	7.2	10.6	14.7	18.7	22.7

Table 9 California bearing ratio behaviour of OPC+QDbGPC (%) treated soil with 12% CWG
9. táblázat OPC+QDbGPC-vel kezelt talaj kaliforniai teherbírási értéke (12% CWG esetén)

Plunger Penetration (mm)	Plunger Load (kN) California bearing ratio behaviour of DOPC+QDbGPC (%) treated soil with 16% CWG								
	0	0+40	5+35	10+30	20+20	25+15	30+10	35+5	40+0
0	0	0	0	0	0	0	0	0	0
0.5	1.6	1.9	2.3	2.5	4.8	8.8	12.8	16.9	20.9
1	1.7	2.1	2.4	2.6	4.9	8.9	12.9	17.0	21.0
1.5	1.9	2.2	2.5	2.7	5.0	9.0	13.0	17.1	21.1
2	2.1	2.3	2.6	2.8	5.1	9.1	13.1	17.2	21.2
2.5	2.3	2.4	2.6	2.9	5.2	9.2	13.2	17.3	21.3
3	2.4	2.5	2.8	3.0	5.3	9.3	13.3	17.4	21.4
3.5	2.5	2.6	2.9	3.1	5.4	9.4	13.4	17.5	21.5
4	2.6	2.7	3.0	3.2	5.5	9.5	13.5	17.6	21.6
4.5	2.7	2.8	3.1	3.3	5.6	9.6	13.7	17.7	21.7
5	2.8	2.9	3.2	3.4	5.7	9.7	13.8	17.8	21.8
5.5	3.0	3.1	3.3	3.5	5.8	9.8	13.9	17.9	21.9
6	3.1	3.2	3.4	3.6	5.9	9.9	14.0	18.0	22.0
6.5	3.3	3.4	3.5	3.7	6.0	10.0	14.1	18.1	22.1
7	3.6	3.7	3.8	3.9	6.1	10.1	14.2	18.2	22.2
7.5	4.0	4.1	4.2	4.3	6.2	10.2	14.3	18.3	22.3
8	4.2	4.3	4.4	4.5	6.6	10.3	14.4	18.4	22.4
8.5	4.5	4.6	4.7	4.8	6.9	10.4	14.5	18.5	22.5
9	4.6	4.7	4.9	5.0	7.0	10.5	14.6	18.6	22.6
9.5	4.8	4.9	5.0	5.1	7.2	10.6	14.7	18.7	22.7
10	4.9	5.0	5.1	5.2	7.3	10.7	14.8	18.8	22.8

Table 10 California bearing ratio behaviour of DOPC+QDbGPC (%) treated soil with 16% CWG
10. táblázat OPC+QDbGPC-vel kezelt talaj kaliforniai teherbírási értéke (16% CWG esetén)

Plunger Penetration (mm)	Plunger Load (kN) California bearing ratio behaviour of OPC+QDbGPC (%) treated soil with 20% CWG								
	0	0+40	5+35	10+30	20+20	25+15	30+10	35+5	40+0
0	0	0	0	0	0	0	0	0	0
0.5	1.7	2.0	2.3	2.6	4.9	8.9	12.9	17.0	21.0
1	1.8	2.2	2.5	2.7	5.0	9.0	13.0	17.1	21.1
1.5	2.0	2.3	2.6	2.8	5.1	9.1	13.1	17.2	21.2
2	2.2	2.4	2.7	2.9	5.2	9.2	13.2	17.3	21.3
2.5	2.4	2.5	2.8	3.0	5.3	9.3	13.3	17.4	21.4
3	2.5	2.6	2.9	3.1	5.4	9.4	13.4	17.5	21.5
3.5	2.6	2.7	3.0	3.2	5.5	9.5	13.5	17.6	21.6
4	2.7	2.8	3.1	3.3	5.6	9.6	13.6	17.7	21.7
4.5	2.8	2.9	3.2	3.4	5.7	9.7	13.8	17.8	21.8
5	2.9	3.0	3.3	3.5	5.8	9.8	13.9	17.9	21.9
5.5	3.1	3.2	3.4	3.6	5.9	9.9	14.0	18.0	22.0
6	3.2	3.3	3.5	3.7	6.0	10.0	14.1	18.1	22.1
6.5	3.4	3.5	3.6	3.8	6.1	10.1	14.2	18.2	22.2
7	3.7	3.8	3.9	4.0	6.2	10.2	14.3	18.3	22.3
7.5	4.1	4.2	4.3	4.4	6.3	10.3	14.4	18.4	22.4
8	4.3	4.4	4.5	4.6	6.7	10.4	14.5	18.5	22.5
8.5	4.6	4.7	4.8	4.9	7.0	10.5	14.6	18.6	22.6
9	4.7	4.8	4.9	5.1	7.1	10.6	14.7	18.7	22.7
9.5	4.9	5.0	5.1	5.2	7.3	10.7	14.8	18.8	22.8
10	5.0	5.1	5.2	5.3	7.4	10.8	14.9	18.9	22.9

Table 11 California bearing ratio behaviour of OPC+QDbGPC (%) treated soil with 20% CWG
11. táblázat OPC+QDbGPC-vel kezelt talaj kaliforniai teherbírási értéke (20% CWG esetén)

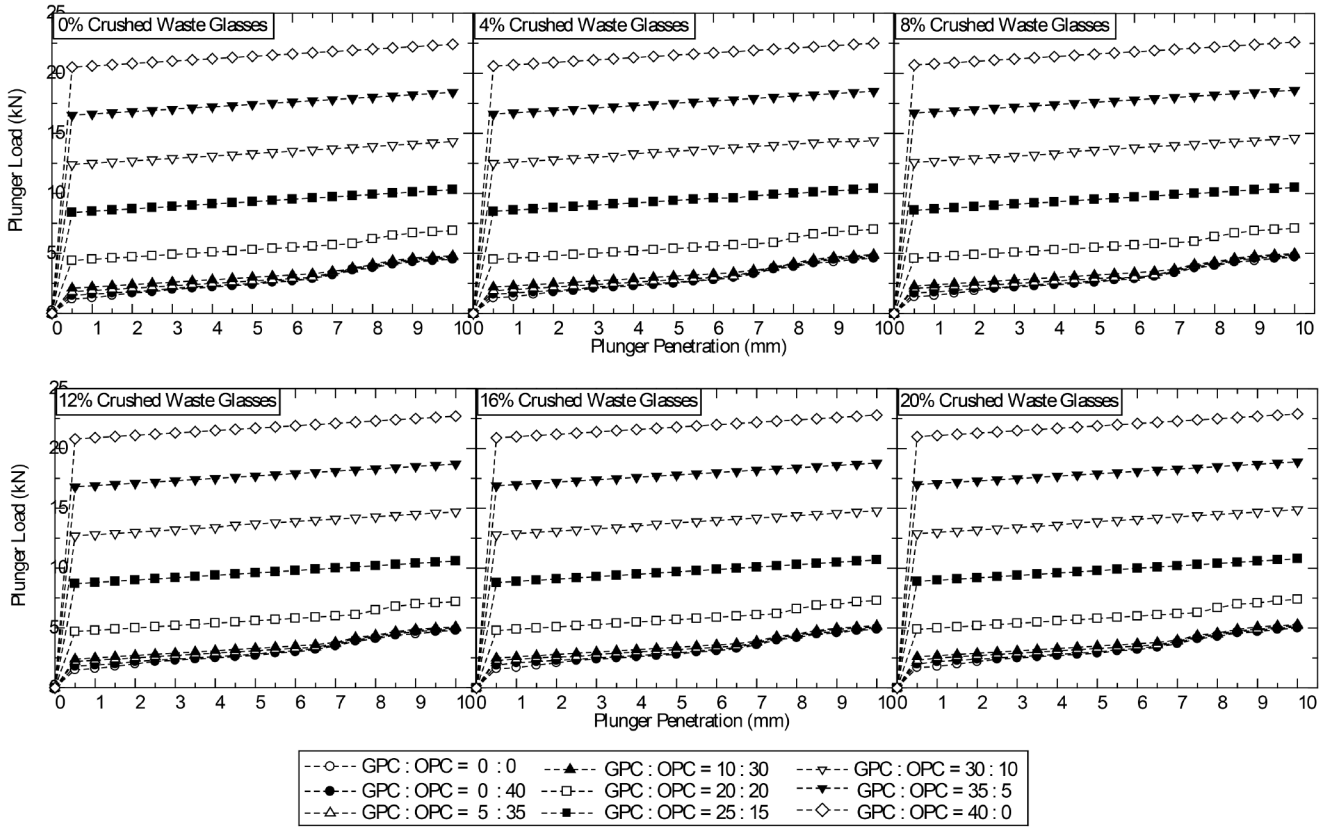

Fig. 7 Effect of crushed waste glasses proportion on the CBR behaviour of DOPC+QDbGPC (%) treated soil
7. ábra Zúzott üveghulladék arányának hatása a DOPC+QDbGPC-vel kezelt talaj kaliforniai teherbírási értékére

CWG Proportion by wt (%)	CBR of DOPC+QDbGPC (%) treated soil with CWG								
	0	0+40	5+35	10+30	20+20	25+15	30+10	35+5	40+0
0	13	14	17	19	36	66	97	128	158
4	14	15	17	20	37	67	97	128	159
8	16	16	18	20	38	68	98	129	159
12	17	17	20	21	39	69	99	130	160
16	17	18	20	22	39	69	100	131	161
20	18	19	21	23	40	70	100	131	162

Table 12 California bearing ratio of DOPC+QDbGPC (%) treated soil with CWG
12. táblázat CWG tartalmú DOPC+QDbGPC-vel kezelt talaj kaliforniai teherbírási értéke

(CAH), which are the major compounds responsible for the formation of sequestrum, flocs and strength development [1, 2]. The soil + QDbGPC blends at 40:0% by weight cementation met the minimum requirement for CBR value of 20 – 30% specified by Dogbey and Gidigasu [60] for materials suitability for use as base course materials when determined at MDD and OMC. Increase in CBR value, was an indication of the improvement observed in MDD, which is attributed to the compatibility of the grains of soil due to the increased cations released and the high pozzolanic and silicate properties of the QDbGPC such that greater polycondensation and densification were achieved.

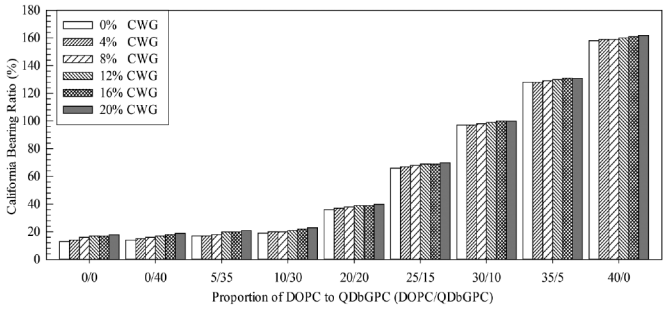

Fig. 8 California Bearing Ratio of DOPC+QDbGPC (%) treated soil with CWG
8. ábra CWG tartalmú DOPC+QDbGPC-vel kezelt talaj kaliforniai teherbírási értéke

5. Conclusions

The test soil treated alternately with QDbGPC and OPC in the ratios of 0:0, 0:40, 5:35, 10:30, 15:25, 20:20, 25:15, 30:10, 35:5, and 40:0% by weight respectively under the influence of 4%, 8%, 12%, 16% and 20% by weight crushed waste glasses over the cemented test soil was experimented in the lab and concluded as follows;

i. The preliminary test on the natural soil showed that the test soil was an expansive problem soil of highly plastic consistency unsuitable to be used as a pavement foundation material.

ii. The increase in the proportion of quarry dust based geopolymer cement and reduced ordinary Portland cement proportions improved the consistency, compaction and California bearing ratio characteristics of the soil

iii. The addition of crushed waste glasses also improved the tested properties of the soils of consistency and strength development.

iv. The use of 40:0% by weight of solid of the QDbGPC and DOPC respectively produced the highest improvement of the consistency and strength development characteristics of the treated soil.

v. This improvement has been achieved at zero release of CO_2 into the atmosphere (at 40:0% cementation) because the geopolymer cement is an ecofriendly geomaterials.

vi. Finally, the test exercise has generated a disposal mechanism for waste glasses and quarry dust as solid waste materials with an attendant improvement to soil reengineering for pavement foundation purposes in the composite blend of the silicate-based geopolymer cement.

Funding

This work was supported by the Ministry of Education and Training of Vietnam based on the decision No. 5652/QD-BGDDT on December 28, 2018 with project number B2019-MDA-08.

References

[1] Herve, P., et al. (2011): Desiccation cracking of soils, European Journal of Environmental and Civil Engineering, vol. 13: 7-8, pp. 869-888. https://doi.org/ 10.1080/19648189.2009.9693159

[2] Onyelowe, K. C. – Duc, Bui Van – Igboayaka, Clifford – Orji, Francis – Henry Ugwuanyi (2018d): Rheology of mechanical properties of soft soil and stabilization protocols in the developing countries-Nigeria. Materials Science for Energy Technologies. https://doi.org/10.1016/j.mset.2018.10.001

[3] Abood, T. T. – Kasa, A. B. – Chik, Z. B. (2007): Stabilization of Silty Clay Soil Using Chloride Compounds, JEST, Malaysia, vol. 2, pp. 102-103

[4] Onyelowe, K. C. (2016a). Kaolin Stabilization of Olokoro Lateritic Soil Using Bone Ash as Admixture, *International Journal of Constructive Research in Civil Engineering* (IJCRCE) Volume 2, Issue 1, PP 1-9

[5] Onyelowe, K. C. (2016c): Axial Load and Compaction Behavior of Pozzolan Stabilized Lateritic Soil with Coconut Shell Husk Ash and Palm Kernel Shell Husk Ash Admixtures, *International Journal of Innovative Studies in Sciences and Engineering Technology,* Volume 2, Issue 2

[6] Onyelowe, K. C. (2016e): Effect of Coconut Shell Husk Ash and Palm Kernel Shell Husk Ash on the Grading and Consistency Behaviour of Pozzolan Stabilized Oboro Lateritic Soil, *IISTE Journal of Civil and Environmental Research*, Vol.8, No.3, pp. 55-63. (www.iiste.org, www.researchgate.net).

[7] Nigeria General Specification/Federal Ministry of Works and Housing (1997). Testing for the selection of soil for roads and bridges, Vol. II.

[8] Onyelowe, K. C. (2012b): Soil Stabilization Techniques and Procedures; A Clue for the Developing world-Nigeria, *Global Journal of Engineering and Technology*, GJET, India. Vol.5 (1) 65-69.

[9] Onyelowe, K. C. (2012c): Geochemistry of Soil Stabilization, *ARPN Journal of Earth Sciences*, Vol. 1, Issue 2, Pp. 32-35.

[10] Edeh, Joseph Ejelikwu – Eberemu, Adrian Oshioname – Arigi, Abraham S. D. (2012): Reclaimed Asphalt Pavement Stabilized Using Crushed Concrete Waste as Highway Pavement Material, Advances in Civil Engineering Materials, 1 (1), 1–14, https://doi.org/10.1520/ACEM20120005.

[11] Onyelowe, K. C. – Duc Bui Van – Manh Nguyen Van (2018b): Swelling potential, shrinkage and durability of cemented and uncemented lateritic soils treated with CWC base geopolymer, International Journal of Geotechnical Engineering. https://doi.org/10.1080/19386362.2018.1462606

[12] Onyelowe, K. C. – Okafor, F. O. – Nwachukwu, D. G. (2012): Geophysical Use of Quarry Dust (as Admixture) as applied to Soil Stabilization and Modification-a review, *ARPN Journal of Earth Sciences*, PAKISTAN. 1(1).

[13] Onyelowe, K. C. (2017b): Nanosized palm bunch ash (NPBA) stabilisation of lateritic soil for construction purposes, *International Journal of Geotechnical Engineering*, TandF online, http://dx.doi.org/10.1080/19386362.2017.1322797

[14] Onyelowe, K. C. (2017c): Nanostructured Waste Paper Ash Stabilization of Lateritic Soils for Pavement Base Construction Purposes. *Electronic Journal of Geotechnical Engineering*, (22.09), pp 3633-3647. www.ejge.com

[15] Onyelowe, K. C. (2017d): Solid Wastes Management (SWM) in Nigeria and their Utilization in the Environmental Geotechnics as an Entrepreneurial Service Innovation (ESI) for Sustainable Development. Int J Waste Resour 7: 282. ISSN: 2252-5211.

[16] Onyelowe, K. C. (2017e): Nanosized Waste Paper Ash Stabilization of Lateritic Soil for Pavement Construction Purposes. *Proceedings of the 2017 Annual Conference on Engineering for Self Reliance of the School of Engineering & Engineering Technology (SEET), The Federal University of Technology, Akure, Nigeria, 11-13 July, 2017.*

[17] Onyelowe, K. C. (2018): Kaolin soil and its stabilization potentials as nanostructured cementitious admixture for geotechnics purposes, International Journal of Pavement Research and Technology (in press), https://doi.org/10.1016/j.ijprt.2018.03.001.

[18] Onyelowe, K. C. – Ubachukwu, O. A. (2015): Stabilization of Olokoro-Umuahia Lateritic Soil using Palm Bunch Ash (PBA) as Admixture, *Umudike Journal of Engineering and Technology* (UJET), Volume 1, Number 2, Pp. 67-77.

[19] Onyelowe, K. C. – Agunwamba, J. C. (2012b): Geotechnical Examination of the Geophysical Properties of Olokoro Lateritic Soil for Road Works, *Nigeria Journal of Technology*, NIJOTECH, Vol.31, No.3.

[20] Onyelowe, K. C. – Okafor, F. O. (2012): A Comparative Review of Soil Modification Mothods. *ARPN Journal of Earth Sciences*, PAKISTAN. 1(2).

[21] Onyelowe, K. C. – Okafor, F. O. (2013): Portland Cement/Quarry Dust Improvement of Olokoro Laterite for Road Base, *World Journal of Engineering Science* WJES, India. 1(4)133-143.

[22] Eberemu, Adrian O. – Amadi, Agapitus A. – Edeh, Joseph E. (2012):Diffusion of municipal waste contaminants in compacted lateritic soil treated with bagasse ash. Environmental Earth Sciences, https://doi.org/10.1007/s12665-012-2168-z

[23] Salahudeen, A. B. – Eberemu, A. O. – Osinubi, K. J. (2014): Assessment of Cement Kiln Dust-Treated Expansive Soil for the Construction of Flexible Pavements. Geotechnical and Geological Engineering, an International Journal, 32:923-931. https://doi.org/10.1007/s10706-014-9769-0

[24] Onyelowe, K. C. – Bui Van, D. (2018b): Predicting Subgrade Stiffness of Nanostructured Palm Bunch Ash Stabilized Lateritic Soil for Transport Geotechnics Purposes. Journal of GeoEngineering of Taiwan Geotechnical Society (in press). http://140.118.105.174/jge/index.php

[25] Onyelowe, K. C. – Bui Van, D. (2018c): Structural analysis of consolidation settlement behaviour of soil treated with alternative cementing materials for foundation purposes. Environmental Technology & Innovation, Vol. 11, pp. 125-141. https://doi.org/10.1016/j.eti.2018.05.005

[26] Onyelowe, K. C. – Onuoha, I. C. – Ikpemo, O. C. – Okafor, F. O. – Maduabuchi, M. N. – Kalu-Nchere, J. – Aguwa, P. (2017a): Nanostructured Clay (NC) and the Stabilization of Lateritic Soil for Construction Purposes. *Electronic Journal of Geotechnical Engineering*, (22.10), pp 4177-4196. www.ejge.com

[27] Onyelowe, K. C. – Ekwe, N. P. – Okafor, F. O. – Onuoha, I. C. – Maduabuchi, M. N. – Eze, G. T. (2017c): Investigation of the Stabilization Potentials of Nanosized-Waste Tyre Ash (NWTA) as Admixture with Lateritic Soil in Nigeria. *Umudike Journal of Engineering and Technology (UJET), Vol. 3, No. 1, Pp. 26 – 35. www.ujetmouau.com*

[28] Nikolov, A. – Rostovsky, I. – Nugteren, H. (2017): Geopolymer Materials Based on Natural Zeolite. *Case Studies in Construction Materials.* Vol. 6, Pp. 198-205. http://dx.doi.org/10.1016/j.cscm.2017.03.001

[29] Hamidi, R. M. – Man, Z. – Azizli, K. A. (2016): Concentration of NaOH and the Effect on the Properties of Fly Ash Based Geopolymer. 4th International Conference of Process Engineering and Advanced Materials; Procedia Engineering, Vol. 148, Pp. 189-193. http://dx.doi.org/10.1016/j.proeng.2016.06.568

[30] Bui Van, D. – Onyelowe, K. C. – Phi Van Dang – Dinh Phuc Hoang – Nu Nguyen Thi – Wu, W. (2018): Strength Development of Lateritic Soil Stabilized by Local Nanostructured Ashes, Proceedings of China-Europe Conference On Geotechnical Engineering, SSGG, pp. 782–786, 2018. https://doi.org/10.1007/978-3-319-97112-4_175

[31] Davidovits, J. (2013): Geopolymer Cement a review. Institute Geopolymer, F-02100 Saint-Quentin, France. [online]

[32] Behzad, K. – Huat, B. B. K. (2008): Peat Soil Stabilization sing Ordinary Portland Cement, Polypropylene Fibers, and Air Curing Technique, EJGE, USA, Vol.13, pp. l

[33] Onyelowe, K. C. – Onuoha, I. C (2016): Ordinary Portland Cement Stabilization of Amaoba-Umuahia Lateritic Soil using Snail Shell Ash, SSA as Admixture, *International Journal of Innovative Studies in Sciences and Engineering Technology*, Volume 2, Issue 1

[34] Onyelowe, K. C. – Ubachukwu, O. A. – Onuoha, I. C. – Ikpa, C – Umoren, P. (2016): Comparison between the Strength Characteristics of Pozzolan Stabilized Lateritic Soil of Coconut Shell Husk Ash and Palm Kernel Shell Husk Ash Admixtures, *American Research Journal of Civil and Structural Engineering*, Vol. 1, Issue 1, Pp. 1-8

[35] Škvára, F. – Jílek, T. – Kopecký, L. (2005): Geopolymer materials based on fly ash. *Ceram.-Silik*, 49(3), 195-204.

[36] Onyelowe, K. C. – Bui Van, D. – Dao-Phuc, L. – Onyelowe, F. – Ikpa, C. – Ezugwu, C. – Salahudeen, A. B. – Maduabuchi, M. – Obimba-Wogu, J. – Ibe, K. – Ihenna, L. (2020): Evaluation of index and compaction properties of lateritic soils treated with quarry dust based geopolymer cement for subgrade purpose. Epitőanyag– Journal of Silicate Based and Composite Materials, Vol. 72, No. 1, pp. 12–15. https://doi.org/10.14382/epitoanyag-jsbcm.2020.2

[37] Srinivasan, K. – Sivakumar, A. (2013): Geopolymer binders: a need for future concrete construction. *ISRN Polymer Science*, volume 2013, Article ID 509185, 8 pages. DOI: http://dx.doi.org/10.1155/2013/509185

[38] Van Bui, D. – Onyelowe, K. (2018): Adsorbed complex and laboratory geotechnics of Quarry Dust (QD) stabilized lateritic soils. *Environmental Technology & Innovation*, 10, 355-363. https://doi.org/10.1016/j.eti.2018.04.005

[39] Onyelowe, K. C. – Maduabuchi, M. N. (2017a): Palm Bunch Management and Disposal as Solid Waste and the Stabilization of Olokoro Lateritic Soil for Road Construction Purposes in Abia State, Nigeria. Int J Waste Resour Vol 7 Issue 2. https://doi.org/10.4172/2252-5211.1000279

[40] American Standard for Testing and Materials (ASTM) C618 (2014). Specification for Pozzolanas. ASTM International, Philadelphia, USA.

[41] TCVN 8859 (2011). Natural aggregates for road pavement layers. Vietnamese Specification for Material,s, Construction and Acceptance.

[42] Akbari, H. – Mensah-Biney, R. – Simms, J. (2015): Production of Geopolymer Binder from Coal Fly Ash to Make Cement-less Concrete. World of Coal Ash (WOCA) Conference in Nasvhille, TN-May 5-7. [online].

[43] Graber, E. R. – Fine, P. – Levy, G. J. (2006): Soil Stabilization in Semiarid and Arid Land Agriculture, Journal of Materials in Civil Engineering, ASCE, Vol.18. No.2, pp. 190-201

[44] Hasan, M. M. – Islam, M. R. – Tarefder, R. A. (2018): Characterization of subgrade soil mixed with recycled asphalt pavement. Journal of Traffic and Transportation Engineering, Vol. 5 (3), pp. 207-214. https://doi.org/10.1016/j.jtte.2017.03.007

[45] Little, D. N. – Males, E. H. – Prusinski, J. R. – Stewart, B. (2010): Cementitious Stabilization; Transportation in the New Millennium, Louisiana, USA, pp. 1-7.

[46] Ai, C. – Li, Q. J. – Qiu, Y. (2015). Testing and assessing the performance of a new warm mix asphalt with SMC. Journal of Traffic and Transportation Engineering, Vol. 2 (6), pp. 399-405. http://dx.doi.org/10.1016/j.jtte.2015.10.002

[47] Abdel-Gawwadm, H. A. – Abo-El-Enein, S. A. (2016): A Novel Method to Produce Dry Polymer Cement Powder. *HBRC Journal.* Vol. 12, Pp. 13-24. http://dx.doi.org/10.1016/j.hbrcj.2014.06.0018

[48] BS 1377 - 2, 3, (1990). Methods of Testing Soils for Civil Engineering Purposes, British Standard Institute, London.

[49] BS 1924, (1990). Methods of Tests for Stabilized Soil, British Standard Institute, London.

[50] TCVN 9504 (2012). Specification for construction and acceptance of water bound macadam layer. Vietnmese Standard Code for Concrete Materials.

[51] AASHTO (1993): Guide for Design of Pavement Structures. American Association of State Highway and Transportation Officials (AASHTO), Washington DC.

[52] AASHTO (2005): Standard Specification for Transportation Materials and Methods of Sampling and Testing, Part II Methods of Sampling and Testing 25th Edition. American Association of State Highway and Transportation Officials, Washington DC.

[53] AASHTO T 190-09 (2014): Standard method of test for resistance R-value and expansion pressure of compacted soils. American Association of State Highway and Transportation Officials, Washington DC.

[54] AASHTO T 307 (2014): Standard method of test for determining the resilient modulus of soils and aggregate materials. American Association of State Highway and Transportation Officials, Washington DC.

[55] TCVN 8858 (2011): Cement treated aggregates bases for road pavement. Vietnamese Specification for Construction and Acceptance.

[56] Wei, H. – Dong-yan, L. – Bao-yun, Z. – Yan-bo, F. – Yu-chao, X (2014): Study on the Rheological Properties and Constitutive Model of Shenzhen Mucky Soft Soil. Journal of Engineering Science and Technology Review 7 (3), pp. 55 – 61

[57] Zhu, G. – Zhu, L. – Yu, C. (2017): Rheology properties of soils; a review. International Symposium on Resource Exploration and Environmental Science, Earth and Environmental Science 64, pp. 1-8. https://doi.org/10.1088/1755-1315/64/1/012011.

[58] Srivastava, V. – Atul, Imam – Mehta, A. – Satyendranath, P. K. – Tripathi, M. K. (2018): Supplementary Cementitious Materials in Construction - An Attempt to Reduce CO_2 Emission. Journal of Environmental Nanotechnology, Volume 7, No.2, pp. 31-36. https://doi.org/10.13074/jent.2018.06.182306

[59] Smith, G. N. – Smith, I. G. N. (1998): Elements of Soil Mechanics, 7th Edition, Blackwell Science, Inc., USA.

[60] Gidigasu, M. D. – Dogbey, J. L. K. (1980): Geotechnical Characterization of Laterized Decomposed Rocks for Pavement Construction in Dry Sub-Humid Environment". 6th South East Asian Conference on Soil Engineering, Taipei, 1, 493-506.Garg, S.K. (2005). Soil Mechanics and Foundation Engineering, 6th Edition, Kharna Publishers, Delhi

[61] Onyelowe, K. C. – Bui Van, D. (2018a): Durability of nanostructured biomasses ash (NBA) stabilized expansive soils for pavement foundation, International Journal of Geotechnical Engineering, https://doi.org/10.1080/19386362.2017.1422909

Ref.:
Bui Van, Duc – **Onyelowe**, Kennedy Chibuzor – **Onyia**, Michael – **Xuan**, Man Nguyen – **Phuc**, Lam Dao – **Ikpa**, Chidozie – **Yubonchit**, Somjai – **Eberemu**, Adrian – **Osinubi**, Kolawole – **Salahudeen**, A. Bunyamin – **Amadi**, Agapitus – **Maduabuchi**, Michael – **Obimba-Wogu**, Jesuborn – **Onuoha**, Ifeanyichukwu – **Saing**, Zubair: *Strength and consistency behaviour of replacement of cement with silicate-based geopolymer cement modified soft soil treated with crushed waste glasses for pavement underlain*
Építőanyag – Journal of Silicate Based and Composite Materials, Vol. 72, No. 6 (2020), 186–197. p.
https://doi.org/10.14382/epitoanyag-jsbcm.2020.31

Review of stir casting technique and technical challenges for ceramic reinforcement particulate and aluminium matrix composites

Malek ALI
Educational Background: 2011, Ph.D. in Materials Engineering - University Science Malaysia (USM) Malaysia. Major: Nanotechnology. 2007, M.Sc. in Materials Engineering - University Science Malaysia (USM). 2000, B.Sc. in Materials Science- University of Technology, Iraq. Associate professor, Faculty of Aviation Sciences, Amman Arab University. Research experience in the following areas: Synthesis Advanced Nanomaterials. Metallurgy, Nano. Composites (Polymer, Ceramics, Metals), Corrosion and Energy. Manufacturing/Fabrication of Metallic.

Malek ALI ▪ Faculty of Aviation Sciences, Amman Arab University, Jordan ▪ malikali77@yahoo.com
Érkezett: 2020. 03. 29. ▪ Received: 29. 03. 2020. ▪ https://doi.org/10.14382/epitoanyag-jsbcm.2020.32

Abstract
Ceramic metal composites are promising advanced materials compared to conventional materials due to special properties such as: low weight, low cost, wear resistance, corrosion resistance, and high strength, etc. Stir casting is one of the lowest costs and simplest ways of making aluminium matrix composites. The main limitations of stir casting are poor distribution with combination of the reinforcement ceramic particles (agglomerations) in the metal matrix, porosities in composites during fabrication, and wettability of ceramic particles with molten metal's. Enhancement of stir casting parameters for Ceramic-Metals Matrix Composites (CMMCs) is the main objective for many studies. In this paper, the stir casting process will be discussed in detail with parameters affecting the homogeneous distribution of reinforcements, porosities in composites during fabrication, and the mechanical properties of the ceramic metal matrix composites.
Keywords: stir casting, ceramic reinforcement, aluminium matrix composites
Kulcsszavak: keveréses öntés, kerámia megerősítés, aluminium matrix kompozitok

1. Introduction

A composite material can be defined as a combination of the best properties of each of the component materials; each material retains its separate chemical, physical, and mechanical properties. The three major composites are: ceramic matrix composite (CMMC), metal matrix composite (MMC), and polymer matrix composite (PMC). The three composites have a different properties and production methods that portrays specific behavior and capabilities. The main advantages of composite materials are their high strength and stiffness, combined with low density, fatigue life, and high corrosion resistance. The reinforcing stage provides the strength and stiffness. In most cases, the reinforcement is harder, stronger, and stiffer than the matrix. The reinforcement is usually a fiber or a particulate with regular or irregular shape. Particulate reinforced composites usually contain less reinforcement (up to 40 to 50 volume percent) due to processing difficulties and brittleness [1]. There are several fabrication techniques available in manufacturing the CMMC materials. Fabrication methods can be divided into three types. These are solid phase processes, liquid phase process, and semi-solid fabrication process. Liquid phase process includes stir casting, liquid metal infiltration, squeeze casting, and spray code position [2,3]. Ceramics particles are good candidate as reinforcement materials such as oxides, carbides, and nitrides which are characterized by their strength and stiffness at ambient and elevated temperature. Choosing the manufacturing process for any MMCs is based on several factors such as the: maintenance of reinforcement strength, minimization of reinforcement damage, promotion of wetting and bonding between the matrix and reinforcement, ability to achieve the spacing and orientation of reinforcement with the matrix, and cost. With these several fabrication techniques, there are however problems associated with homogeneous distribution of reinforcement, and porosity in composites during fabrication, essential for optimum mechanical properties of MMC [4-10]. Literature survey indicate that various parameters of stir casting process such as: stirring speed and time, stirring blade angle, pouring temperature and solidification rate, reinforcement's percentage and size have major effect on fabrication of MMC. Enhancement of parameters of stir casting process for CMC is the main objective for many studies. Few of these works are concerned with parameters that are affected by homogeneous distribution of reinforcement, and porosities in composites during fabrication which are the essential for optimum mechanical properties of MMC [11].

2. Stir casting

Stir casting is currently the most popular commercial method of producing aluminum-based composites. Stir casting of MMCs was initiated in 1968 [12,13]. In this process, powder form as reinforcing phases are usually distributed into molten metal's by mechanical stirring as shown in *Fig. 1*. Non-uniform distribution, and porosity in casted CMMCs consider main disadvantages for stir casting process. Generally, the difference in density is between the liquid metal and the reinforcement and the consequent tendency to reinforce the sink or float, resulting in nonuniform distribution of the reinforcement in the solidified composite.

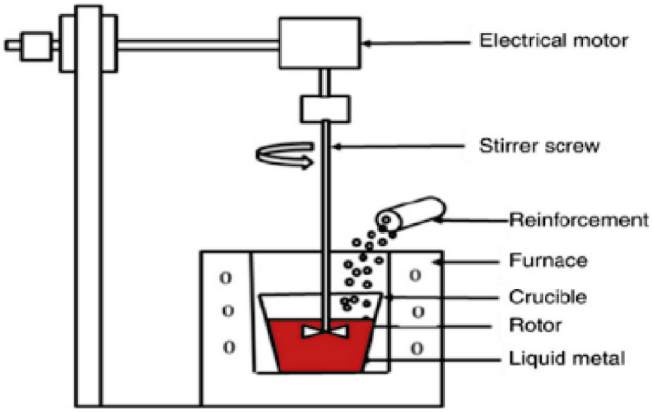

Fig. 1 Mechanical stirring
1. ábra Mechanikus keverés

3. Effect of stirring speed and time on distribution of particles and porosities in casted CMMCs

For most applications, a homogeneous distribution of the particles is desirable in order to maximize the mechanical properties. Prabu *et al.* [14] reported by microstructure analysis that during lower speed and lower stir time particle clustering occurred in some places, and some places were identified without SiC inclusion. By increasing the stirring speed and stirring time better homogeneous distribution of SiC in the Al matrix were found. Better distributions of SiC were found at 600 rpm and 10 min stirring time condition as shown in *Fig. 2*.

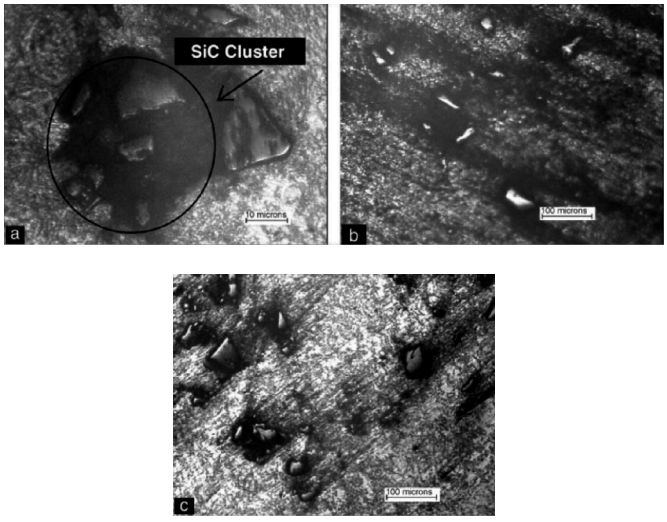

Fig. 2 Microstructure of Al–10%SiCp MMC fabricated at 600 rpm: (a) 5 min stirring; (b) 10 min stirring; (c) 15 min stirring
2. ábra 600 fordulat/perc sebességen készített Al–10%SiCp MMC mikroszerkezete: (a) 5 perc keverés után; (b) 10 perc keverés után; (c) 15 perc keverés után

Also, they reported that with higher speeds (700 rpm), more porosity has been observed in the microstructure which lead to minimize the mechanical properties. From *Fig. 3* Adetayo et al. [15] explained the influence of stirring speed on stir casting synthesis of 15 wt% silicon carbide particle reinforced aluminium alloy (SiCp-6061 Al) composite.

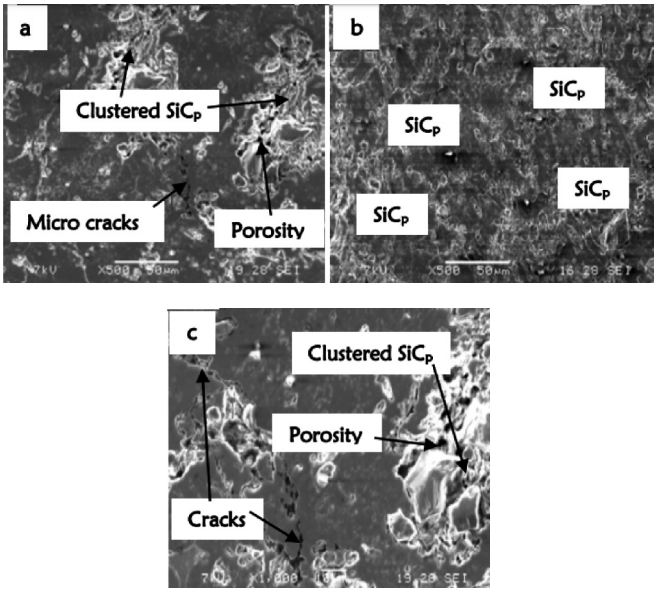

Fig. 3 Microstructure of 15 wt% SiCp Al composite processed at (a) 300 rpm (b) 500 rpm and (c) 700 rpm. The formation of composites, porosity, and micro cracks are indicated
3. ábra 15 wt% SiCp Al kompozit mikroszerkezete különböző fordulatszám esetén: (a) 300 (b) 500 és (c) 700 fordulat/perc. A kompozitok kialakulásának, repedéseknek és pórusok helye az ábrán jelezve

They reported that at 300 rpm, it is observed from the micrograph that regions of clustering and micro porosity are detected. Moreover, the distribution of SiC is not uniformly dispersed. This indicates that 300 rpm is insufficient to achieve homogenous distribution of SiCp in the Al alloy matrix. With higher stirring speed of 500 rpm, an improved distribution of the SiCp is achieved. Moreover, vortex formation is found to be minimized at 500 rpm stirring speed thereby stabilizing centrifugation which may lead to minimal stirring efficiency and potentially severe air entrainment at higher stirring condition. At higher stirring speed of 700 rpm, the porosity in the microstructure is more pronounced. This condition is attributed to the vigorous vortex formation due to high stirring speed which enables oxide skins, gases and contaminants to be entrained in the melt. Furthermore, the distribution of the SiCp is not effective enough due to the formation of undesirable conditions such as large porosity and gas entrapment. Also, Aqida *et al.* [16] explained that low rpm of the stirrer applies less shearing force on the matrix metal and there is no space for the reinforcement particles (dispersed phase) to distribute uniformly throughout the matrix. Moreover, the dispersed phase has the tendency to agglomerate and form clusters. This happens due to the absence of the required force to resist it. At higher speeds of the stirrer the shearing force applied on the matrix metal is higher which creates the passage for the dispersed phase to move inside through the vortex created by stirring. The energy supplied by high speed rotation of the stirrer is strong enough to disperse the particles of the dispersed phase which causes uniform distribution of the dispersed phase into the matrix. It was also founded out by the researchers that on increased stirrer speeds there is chance for the gas particles to move inside the matrix and increase the porosity [16]. Hashim *et al.* [17] reported that it has also been indicated that the reinforcement particles occupy inter dendritic and secondary

dendrite arm spacing; therefore, the finer the spacing or the finer the matrix grain size, the better is the particle distribution. Also, the processing temperature effects the viscosity of the melt. The particle distribution is subjective to the viscosity change. So, the stirring speed is considered as a crucial factor in the fabrication of MMCs. The stirring action should be slow to prevent the formation of vortex at the surface of the melt, and care must be taken not to break the surface too often, which could contaminate the bath with dross. Use of a slowly rotating, propeller like mechanical stirrer is preferred by some foundries. In fact, results of laboratory studies indicate that the mechanical property of the casting are maximized by continuous stirring versus intermittent (hand) stirring. When induction melting, the furnace's natural eddy current stirring action usually is sufficient to disperse the particles, although supplementary hand stirring (with the power off) also is recommended to ensure that no particles have congregated in potential "dead" zones [18]. According to R. S. Rana *et al.* [19] porosity is a casting defect and is undesirable as far as Aluminium matrix composite castings are concerned. However, the process parameters of holding times, stirring speed, and the position of the impeller affect the development of porosity. It has also been reported by Vaibhav Ingle *et al.* [20] that the structural defects during casting like porosity are a result of unsatisfactory casting technology. Hashimet *et al.* [21] reported that the occurrence of porosity cannot be ruled out however, it can definitely be minimized. Porosity formation is caused by:

i. Gas entrapment during vigorous stirring,
ii. Air bubbles entering the slurry either independently or as an air envelope to the reinforcement particles,
iii. Water vapor (H_2O) on the surface of the particles,
iv. Hydrogen evolution, and
v. Shrinkage during solidification.

Generally, this non uniformity and porosity are generated due to, difference in density between the liquid metal and the reinforcement, oxide skins, and formation of gases. Therefore, and optimum stirring speed and time are required in order to achieve uniform distribution in the matrix with less porosity. Also uniform distribution in the matrix with less porosity can be improved by: keep the viscosity within the allowed limit, alloys with minimum reactivity to the reinforcement must be used, covering the melt with an inert gas atmosphere to reduce the oxidation, giving heat treatment to the reinforcement particles to remove gas layer around the particle surface which impedes wetting between the particles and molten metal's, and stirring of the melt to minimize the settling of particles due to density difference [22-25]. Based on the studies highlighted, the stirring speed is recognized as an important process parameter for processing aluminum composite [26-29].

4. Effect of stirring blade number with angle on distribution of particles and porosities in casted CMMCs

The blade angle (*Fig. 4*) and number of blades are prominent factor which formed the vortex by the stirring on solid-liquid mixing to transfers reinforcements particles into the melt from the liquid surface and lead to uniform distribution. Therefore, selection of a suitable blade angle, and numbers of blades are crucial to acquire good level of axial flow and shearing action [30].

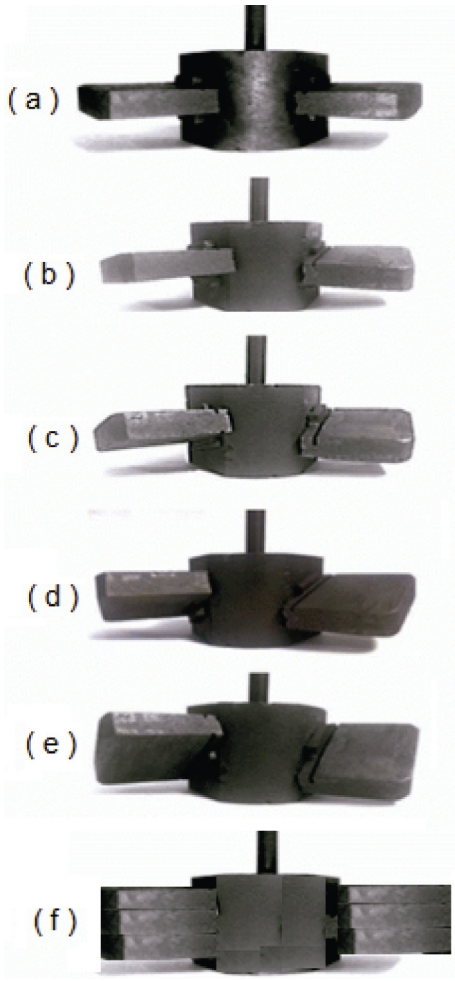

Fig. 4 Three blades stirrer, showing different blade angles (a) 0°, (b) 30°, (c) 45°, (d) 60°, (e) 75°, and (f) 90°
4. ábra Három pengés keverők, kiemelve azok különböző penge dőlési szögét: (a) 0°, (b) 30°, (c) 45°, (d) 60°, (e) 75° és (f) 90°

To investigate the effect of blade angle, researchers used water model and CFD model. They selected blade angle as 15, 30, 45, 60 and 90°. In a water model Ravi *et al.* [31] investigated the effect of impeller blade angle over the distribution of solid particles in the liquid. They found at low angle (α=15°) particles are dispersed below the stirrer. Impeller with blade angle (α=30°) performed well and shows uniform dispersion without concentration of particles. Whereas, impeller with high blade angle (α>30°), most of the solid particles concentrate at just below the tip of the impeller blade which results more radial variation. Thus, 30° was concluded as optimal value of blade angle with respect to stirrer axis which is in good agreement with FEM Model by Sahu and Lu. They attempted to reduce stagnant and dead zones in the flow pattern with blade angle 30, 45, 60 and 90° with respect to the impeller axis. Inactive zone in the cylindrical portion and bottom portion of the crucible are said stagnant zone and dead

zone respectively [32, 33]. Also S. Naher, D. Brabazon, L. *et al.* [34] observed that at 100 rpm and with 0 and 30 degree blade angles no uniform dispersion resulted, but with 45 and 60 degree blade angles there was full particulate dispersion. It is further observed for all stirring speeds that dispersion rates increase with increasing blade angle. The turbine blade also produces dispersion times similar to the best found for the flat bladed stirrers (Naher). They founded the uniform dispersion time for 10% SiC particles for different stirrer types and stirring speeds in water of viscosity 1 mPas. Whereas no dispersion occurred for the higher viscosity glycerol/water mixtures below 150 rpm. it was found that for most cases the 60 degree angle produced the lowest dispersion times. The turbine stirrer again produced the lowest dispersion time. Very similar results were observed for the higher viscosity (300, 500, 800 and 1000 mPas) glycerol/water mixtures tested. High blade angle (α>90°) lead to high level of shearing flow and consume high power as well. Shearing action ensure the solid particle suspension in the melt but without axial suction pressure it is difficult to suck solid particles into the melt. The axial flow can be increased by decreasing the blade angle and significant axial flow was seen close to the liquid surface when the blade angle decreased to 30° [32, 33, 34]. Moreover, stirring time plays an important role over the distribution of solid particles and power consumption by the stirring motor. Kevin Kurian Paul and Sijo MT [28] reported that the Al-20 wt.% SiC composite samples by stir casting with 4 Blade Stirrer have high tendency to form particle cluster than 3, and 2 Blade Stirrer due to the homogeneity in mixing Sic additions to the composite which acts as a reinforcement for the aluminium matrix. Also, they confirmed that mechanical properties show greater strength and hardness for four blade stirrers than two blade and five blades. Many researchers [35,38] reported that the increasing vortex height as shown in *Fig.* 5 depend on stirring speed and viscosities of mixtures. Much greater vortex height observed in high stirring speeds and low mixtures viscosities.

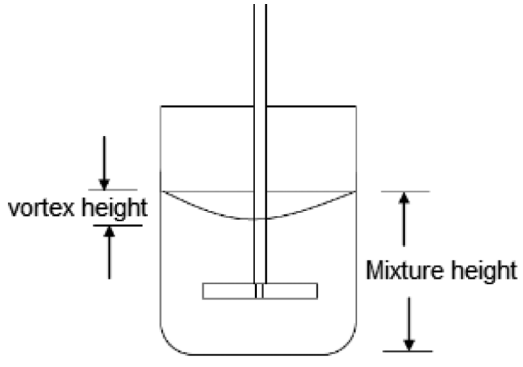

Fig. 5 Vortex and mixture heights
5. ábra Örvény- és keverékmagasság

Skibo *et al.* [37] proved that vigorously stirring in the melt so as to mix the reinforcement particles incorporated in the melt introduces a greater proportion of gas into the slurry. High velocity of slurry, due to higher stirring speeds forms a vortex on the surface of the slurry. The formation of a vortex on the surface was quite helpful in the movement of ceramic particles into the slurry of alloy and reinforcements. This was attributed to the pressure difference created between the inner and the outer surface of melt, which pulls the ceramic particles into the melt. This has been reiterated by Ghosh and Ray [38] that the extent of porosity in a cast composite depends on the state of agitation and it can be reduced by the control of certain process variables. A vortex created during the stirring can suck the air or gas bubbles in to the liquid metal. As the results, the particles were attached with air bubbles to form the particles cluster in the matrix. At higher temperature (>800 ˚C), more particles cluster are found in the composite bar [39].

5. Effect of solidification rate on distribution of particles and porosities in casted CMMCs

In general, the solidification rate effect on distribution of reinforcement particles, grains size of metals matrix, and porosity which are essential to achieve optimum mechanical properties. The solidification rate is one of the most important factors that affects the reinforcement distribution in composites fabricated by gravity casting and has been investigated in depth both theoretically and experimentally. When the cooling rate is higher than the critical rate, the reinforcement distributes homogeneously in the composite. To improve the properties of composite, should reduce the stirring temperature, and solidify the liquid metal rapidly, or add alloying elements into the matrix alloy [40,41]. Muthazhagan *et al.* [42] observed by micro structure results of Al-B4C-Graphite composite revealed uniform distribution of reinforcements at a medium cooling rate of solidification whereas solidification at a slow cooling rate resulted in settlement of reinforcement at the bottom of the composite due to density variation of boron carbide, graphite and aluminium. Also, there is enough time for settling down of reinforcement particles at the bottom. Solidification at faster cooling rates resulted in entrapment of particles at the top of the composite. Solidification at faster cooling rates after a homogeneous distribution of the particles in matrix with minimum porosity formation is required to achieve optimum mechanical properties. Also A.Labib *et al.* [43] reported that the result of Al/Si-10 vol.% SiC composite properties are basically controlled by the solidification rate. Higher solidification rates promote homogeneous distribution of the SiC particles. Also M. Makhlouf *et al.* [44] confirmed that the cooling rate has a marked effect on the grains size, morphology, and distribution of all the microstructural constituents. Increasing cooling rate refines all microstructural features in size, changes the morphology of some reinforcement particles, and decreases the size of all intermetallic compounds regardless of their type. The rate of solidification in Al/Si composite depends on a balance between the rate of heat flow from the liquid to the solid through the interface and the latent heat of fusion released during solidification. The thermal conductivities of Al and Si in their pure form are 205 and 83 W/mK respectively, and their latent heats of fusion are 396 and 1411 J/g respectively. Since the difference between the magnitude of the thermal conductivity of pure Al and pure Si and the difference between the magnitude of the latent heat of fusion of pure Al and pure Si are large, Al will solidify and shrinkage much faster than Si as shown in *Fig. 6(a)*.

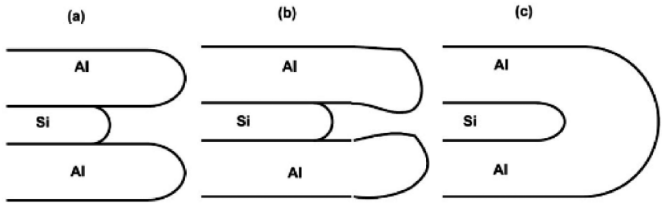

Fig. 6. Solidification in cast Al–Si alloys [53]
6. ábra Al-Si ötvözetek szilárdulási folyamata [53]

By fast cooling the different in cooling rate between Al and Si decreased which lead to solidified the Al completely over Si particle as in *Fig. 3(b)* and *(c)*.

Pradeep Rohatgi *et al.* [45] also reported that the thermal conductivity and heat diffusivity of particles are generally less than those of the melt, and during the cooling process, the temperature of the particles will be higher than that of the melt. In such cases, it is difficult for the primary phase to nucleate at the particle surfaces. Thermal analysis showed that the unreinforced alloys exhibited undercooling for primary-phase nucleation, whereas the composites generally did not show any significant undercooling. The grain size of the composites is often smaller than that of the unreinforced alloy under identical casting conditions. Solute diffusion is impeded during growth due to the barrier effects of particles [46]. Solidification at faster cooling rates resulted in entrapment of porosity throw-out the composite whereas slow cooling rate form composite with less porosity due to enough time for releasing air bubbles during solidification. Generally, this non uniformity and porosity are generated due to, difference in density between the liquid metal and the reinforcement, oxide skins, and formation of gases. Also, uniform distribution in the matrix with less porosity can be improved by: keep the viscosity within the allowed limit, alloys with minimum reactivity to the reinforcement must be used, covering the melt with an inert gas atmosphere to reduce the oxidation [47].

6. Effect of reinforcement's weight percentage, particles size and on distribution of particles and porosities in casted CMMCs

The volume fraction, and particle size also influence the composite particle distribution. Anjan *et al.* [48] was prepared Al-SiC composites containing 5%, 10% and 15% weight fractions of silicon carbide particles by stir casting technique. The effects of volume fraction of SiC particles and its dispersion on the properties of Al/SiC composites were investigated. Anjan *et al.* Reported based on experimental evaluation that tensile strength and hardness were significantly improved by the addition of SiC particles, and clustering of silicon carbide particles in aluminum matrix were observed in microstructure and porosity level increased with increase in SiC Content. Also, Khalid Mahmood [49] Reported that percentage of SiC should be selected is in line with the information comprehensively reviewed. Also, by using fine particle size, the problem arising from the centrifugal force can also be minimized that produces segregation in the melt due to which the non-uniform properties are attained [50]. By decreasing alumina particle size from micrometer to nanometer, more frequent interactions occur between Al and hard particles. Moreover, decreasing alumina particle size from micrometer to nanometer led to the reduction of alumina inter-particles distance. Decreasing the distance between alumina particles will increase required tension for dislocation movement between alumina particles and, consequently, enhancement of composite strength [50]. Microstructural analysis of the developed composites indicates that coarse size garnet mineral particles are uniformly distributed in the matrix of LM13 alloy compared to fine size particles. However, particle clustering is observed for fine size reinforced composites [51]. With higher percentage of reinforcements which were stirred for relatively longer time during their processing, have an increased amount of air bubbles sucked into the molten metal vortex. It was found that there is a positive correlation between the particle volume percentage incorporated in a composite and the porosity content of that composite. According to Surrappa [52], in cast metal matrix composites the occurrence of porosity can be attributed invariably to the amount of H_2 gas present in the melt, oxide film on the surface of the ceramic particle, which is drawn into the molten metal at the time of stirring. Vigorously stirred melt or vortex tends to entrap gas into the molten mixture. Nripjit *et al.* [53] also found that the porosity of the reinforced composite is more as compared to unreinforced alloys and goes on increasing with the increase in the volume fraction of the reinforcements in aluminium alloy matrices. In general, with increasing reinforcement weight percentage, and decreasing particles size a significant improvement in the mechanical properties were observed. On the other hand, a sharp reduction in the mechanical properties were observed which was finer particulate and high mass fraction addition level due to high possibility of agglomeration and porosity [54]. Wettability is another significant problem when producing cast metal matrix composites. Wettability can be defined as the ability of a liquid to spread on a solid surface to improve wetting of ceramic particles are:

1. increasing the surface energies of the solid,
2. decreasing the surface tension of the liquid matrix alloy, and
3. decreasing the solid+liquid interfacial energy at the particle matrix interface.

The proper dispersion of reinforcement materials was affected by pouring rate, pouring temperature and gating systems. This paper provides a comprehensive factor that effect on distribution of particles and porosities in casted CMMCs. several authors reported that uniform distribution of the reinforcement particles with less porosity is necessary for the improvement in the properties of MMCs like hardness, toughness, tensile strength etc. [55-58].

7. Conclusions

Stir casting is currently the most popular commercial method of producing aluminum-based composites. In this process, powder form as reinforcing phases are usually distributed into molten metal's by mechanical stirring. Non-uniform distribution, and porosity in casted CMMCs consider main disadvantages for stir casting process.

- During lower speed and lower stir time particle clustering occurred in some places, and some places were identified without inclusion.
- By increasing the stirring speed and stirring time better homogeneous distribution of SiC in the Al matrix were found.
- At higher stirring speed of 700 rpm, the porosity in the microstructure is more pronounced. This condition is attributed to the vigorous vortex formation due to high stirring speed which enables oxide skins, gases and contaminants to be entrained in the melt.
- Optimum stirring speed and time are required in order to achieve uniform distribution in the matrix with less porosity. Also uniform distribution in the matrix with less porosity can be improved by: keep the viscosity within the allowed limit, alloys with minimum reactivity to the reinforcement must be used, covering the melt with an inert gas atmosphere to reduce the oxidation, giving heat treatment to the reinforcement particles to remove gas layer around the particle surface which impedes wetting between the particles and molten metal's, and stirring of the melt to minimize the settling of particles due to density difference.
- Selection of a suitable blade angle, and numbers of blades are crucial to acquire good level of axial flow and shearing action.
- With 45- and 60-degree blade angles there was full particulate dispersion. It is further observed for all stirring speeds that dispersion rates increase with increasing blade angle.
- Dispersion rates increase with increasing blade angle, whereas no dispersion occurred for the higher viscosity glycerol/water mixtures below 150 rpm.
- Most cases the 60-degree angle produced the lowest dispersion times.
- High blade angle (α>90°) lead to high level of shearing flow and consume high power as well. Shearing action ensure the solid particle suspension in the melt but without axial suction pressure it is difficult to suck solid particles into the melt.
- The axial flow can be increased by decreasing the blade angle and significant axial flow was seen close to the liquid surface when the blade angle decreased to 30° [39, 40, 41].
- Solidification at faster cooling rates after a homogeneous distribution of the particles in matrix with minimum porosity formation is required to achieve optimum mechanical properties.
- Solidification at faster cooling rates resulted in entrapment of particles at the top of the composite in some cases.
- Solidification at faster cooling rates resulted in entrapment of porosity throw-out the composite whereas slow cooling rate form composite with less porosity due to density and the enough time for releasing air bubbles during solidification.
- Solidification at a slow cooling rate resulted in settlement of reinforcement at the bottom of the composite due to density variation of boron carbide, graphite and aluminium.
- With increasing reinforcement weight percentage, and decreasing particles size a significant improvement in the mechanical properties were observed. On the other hand, a sharp reduction in the mechanical properties were observed which was finer particulate and high mass fraction addition level due to high possibility of agglomeration and porosity.

References

[1] Maha, S. H. 2017. Composites Classification and Manufacturing Operations: A Review. International Journal of Advance Research 3:1708- 1713.

[2] Ratan, K., K. S. Er.Sushil. 2018. Thermal Property Evaluation of Heat Treated Aluminium Metal Matrix Composite Material. International Journal of Engineering Development and Research 6:2321-9939. https://www.ijedr.org/papers/IJEDR1801033.

[3] Pradeep, K. S., J. Satheesh. 2018. A Study on Tensile, Hardness, and Impact Strength using Al7075as Matrix Material and by using different Reinforcement: A Review. International Research Journal of Engineering and Technology 07: 2395-0056. https://doi.org. t/archives/V5/i7/IRJET-V5I7166.

[4] Ali, M., F. Samer. 2014. Synthesis and Characterization of Aluminum Composites Materials Reinforced with TiC Nano- Particles. Jordan Journal of Mechanical and Industrial Engineering 8:244-250. http://jjmie.hu.edu.jo/vol%2010-4/JJMIE-2016-10-4.

[5] Bahrami, A., N. Soltani, M.I. Pech-Canul, C. A. Gutiérrez. 2015. Development of metal-matrix composites from industrial/agricultural waste materials and their derivatives. critical reviews in environmental science and technology 1:166. https://doi.org/10.1080/10643389.2015.1077067.

[6] Skolianos, S. 1996. Mechanical Behavior of Cast SiC p-Reinforced Al-4.5%Cu-1.5%Mg Alloy. Materials Science and Engineering 210:76-82. https://doi.org/10.1016/0921-5093(95)10043-1

[7] GLOWSKI, M. S., A.WRONA, I. NEJMAN, M. RICHERT. 2018. Microstructural evaluation of Re particle reinforced composite on aluminium surface by friction stir processing. Journal of Silicate Based and Composite Materials 70:181-185. https://doi.org/10.14382/epitoanyag-jsbcm.2018.32

[8] Sergey, N., Svetlana P. *BUYAKOVA, Maria CHATZINIKOLAIDOU.* 2015. Rheology and porosity effect on mechanical properties of zirconia ceramics. Journal of Silicate Based and Composite Materials 67:150-158. https://doi.org/10.14382/epitoanyag-jsbcm.2015.26

[9] Ahmad, S. N. A. S., J. Hashim, M. I. Ghazali. 2007. Effect of Porosity on Tensile Properties of Cast Particle Reinforced MMC. Journal of Composite Materials 41:575-589. https://doi.org/10.1177/0021998306066720

[10] Madhav Reddy S., A. Chennakesava Reddy. 2006. Effects of Porosity on Mechanical Properties of Zirconium Oxide/AA1100 Alloy Metal Matrix Composites. National Conference on Materials and Manufacturing Processes 2:124-128. https://jntuhceh.ac.in/web/tutorials/faculty/1318_TiO-6061.

[11] Vemula, V. V., Sanjay K. C.2018. The effect of process parameters in Aluminum Metal Matrix Composites with Powder Metallurgy. Manufacturing 5:13. https://doi.10.1051/mfreview/2018001

[12] J. Wiley & Sons, "Technology & Engineering – Handbook of Composite Reinforcements ", P 344-355, 30-Nov-1992.

[13] Calin, R., M. Pul, and Z. Pehlivanli. 2012. The Effect of Reinforcement Volume Ratio on Porosity and Thermal Conductivity in Al-Mgo Composites. Materials Research 15:1057-1063. https://doi.org/10.1590/s1516-14392012005000131

[14] Prabu, S. B., L. Karunamoorthy, S.Kathiresan, B. Mohan. 2006. Influence of stirring speed and stirring time on distribution of particles in cast metal matrix composite. Journal of Materials Processing Technology 171:268-273. https://doi.org/10.1016/j.jmatprotec.2005.06.071

[15] Adetayo, A., Adebisi, M. Abdul, B. N. Mohammed. 2017. Influence of Stirring Speed on Microstructure and Wear Morphology of SiCp-6061Al Composite. International Journal of Engineering Materials and Manufacture 1:21-26. https://doi.org/10.26776/ijemm.01.01.2016.05

[16] Aqida, S.N., M.I. Ghazali, J. Hashim .2003. The Effects Of Stirring Speed and Reinforcement Particles on Porosity Formation in Cast MMC. Journal Mechanical 16:22-30. https://doi.org/10.11113/jt.v40.395

[17] Hashim, J., Looney L, M.S.J. Hashmi. 1999. Metal matrix composite Production by the stir casting method. Journal of Materials Processing Technology 92:1-7. https://doi.org/10.1016/s0924-0136(99)00118-1

[18] Davis, J., Aluminum and Aluminum Alloys. Technology & Engineering, Handbook, P 164, 1993.

[19] Rana, R. S., P. Rajesh. 2012. Review of recent Studies in Al matrix composites. International Journal of Scientific & Engineering Research 3:2229-5518. https://doi.org/www.ijser.org/researchpaper.

[20] Vaibhav, I., S. Madhukar. 2017. Defects,Root Causes in Casting Process and Their Remedies: Review. Int. Journal of Engineering Research and Application 3:47-54. https://doi.org/10.9790/9622-0703034754

[21] Hashim, J. 1999. Microstructure and Porosity Studies of Cast Al-SiCp Metal Matrix Composite. Jurnal Teknologi. 31:1-12.

[22] Sajjadi, S. A., H. R. Ezatpour, H. Beygi. 2001. Microstructure and mechanical properties of Al-Al_2O_3 micro and nano composites fabricated by stir casting. Materials Science and Engineering A 528:8765–8771. https://doi.org/10.1016/j.msea.2011.08.052

[23] Ratna, B. S., G. Pradeep, R. Kumar, P. Hemendra, D. Ravikumar. 2016. Magnesium Based Surface Metal Matrix Composites by Friction Stir Processing. Journal of Magnesium and Alloys 4:52–61. https://doi.org/10.1016/j.jma.2016.02.001

[24] Amouri, K., Sh. Kazemi , A. Momeni, M. Kazazi. 2016. Microstructure and Mechanical Properties of Al- nano/micro SiC Composites Produced by Stir Casting Technique. Materials Science & Engineering A 674:569-578. https://doi.org/10.1016/j.msea.2016.08.027

[25] Yu, W., X. Wang, H. Zhao, C. Ding, Z. Huang, H. Zhai, Z. Guo, S. Xiong. 2017. Microstructure, Mechanical Properties and Fracture Mechanism of Ti_2AlC Reinforced AZ91D Composites Fabricated by Stir Casting‖. Journal of Alloys and Compounds 702:199-208. https://doi.org/10.1016/j.jallcom.2017.01.231

[26] Marinho, R., L. Horiuchi, C. P. Augusto. 2018. Effect of stirring speed on conversion and time to particle stabilization of poly (vinyl chloride) produced by suspension polymerization process at the beginning of reaction. Brazilian Journal of Chemical Engineering 35:631-640. https://doi.org/10.1590/0104-6632.20180352s20160453

[27] Jailani, A., S.M. Tajuddin. 2012. Mechanical Properties of Stirred SiC Reinforced Aluminium Alloy: Stir Casting With Different Composition of SiC, Blade Angle and Stirring Speed. Advanced Materials 622-623:1335-1339. https://doi.org/10.4028/www.scientific.net/amr.622-623.1335

[28] Paul, K. K., MT. Sijo. 2015. Effect of Stirrer Parameter of Stir casting on Mechanical Properties of Aluminium Silicon Carbide Composite. International Journal Of Modern Engineering Research (IJMER), 5:43-49. https://archive.org/stream/Httpijmer.

[29] Jokhio, M. h., Muhammad ibrahim panhwar, Mukhtiar ali unar. 2011. Manufacturing of aluminum composite material using stircasting process. Mehran university research journal of engineering & technology 30:53-64.

[30] Bihari, B., A. K. Singh. 2017. An Ove rview on Different Processing Parameters in Particulate Reinforced Metal Matrix Composite Fabricated by Stir Casting Process Preparation of Aluminium Matrix Composite by Using Stir Casting Method. Int. Journal of Engineering Research and Application 7:42-48. https://doi.org/10.9790/9622-0701034248

[31] Ravi, KR., V.M. Sreekumar, RM. Pillai. 2005. Optimization of mixing parameters through a water model for metal matrix composites synthesis. Materials and Design 28:871- 881. https://doi.org/10.1016/j.matdes.2005.10.007.

[32] Lu, J., Z. Lu. 2010. Optimization of stirring parameters through numerical simulation for the preparation of aluminum matrix composite by stir casting process. Journal of Manufacturing Science and Engineering 132:1-7. https://doi.org/10.1115/1.4002851

[33] Sahu, MK., RK. Sahu. 2017. Optimization of stirring parameters using CFD simulations for HAMCs synthesis by stir casting process. Transactions of the Indian Institute of Metals.70:2563-2570. https://doi.org/10.1007/s12666-017-1119-5

[34] Naher, S., D. Brabazon, L. Looney. 2003. Simulation of the stir casting process. Journal of Materials Processing Technology 143:567–571. https://doi.org/10.1016/s0924-0136(03)00368-6

[35] Rajavathsavai, D., A. Khapre, B. Munshi. 2014. Numerical Study of Vortex Formation inside a Stirred Tank. international Journal of Chemical, Molecular, Nuclear, Materials and Metallurgical Engineering 8: 1421-1426.

[36] Devi, T., B.Kumar. 2017. Vortex depth analysis in an unbaffled stirred tank with concave blade impeller. Chem. Technol.11:301–307. https://doi.org/10.23939/chcht11.03.301

[37] Skibo, M., P.L.Morris, D.J. Lloyd. 1988. Structure and properties of liquid metal proceeded SiC reinforced aluminum", Cast reinforced metal composites. Materials Park, OH: ASM International :257-261.

[38] Ghosh, P.K, S. Ray. 1988. Porosity in a cast composite. Indian J.Technol., 26:83

[39] Bharath, V., Madev Nagaral, V Auradi, S. A. Kori.2014. Preparation of 6061Al-Al2O3 MMC's by Stir Casting and Evaluation of Mechanical and Wear Properties. Procedia Materials Science 6: 1658 – 1667. https://doi.org/10.1016/j.mspro.2014.07.151

[40] Singh, A., ID. Yoshiaki Osawa, H. Somekawa, T. Mukai. 2018. Effect of Solidification Cooling Rate on Microstructure and Mechanical Properties of an Extruded Mg-Zn-Y Alloy. Metals 8:337. https://doi.org/10.3390/met8050337

[41] Liang, G., Y. Ali, G. You, Ming, X. Zhang. 2018. Effect of cooling rate on grain reinforcement of cast aluminium alloys. Materialia, 3:113-121. https://doi.org/10.1016/j.mtla.2018.08.008

[42] Muthazhagan, C., K. Rajkumar. 2015. Effect of Cooling Rate on Distribution of Boron Carbide and Graphite in Al 6061 Composites During Solidification. International Journal of Applied Engineering Research 10:1429-1433.

[43] Labib, A., H. Liu, F.H. Samuel. 1993. Effect of solidification rate (0.1–100°C s−1) on the microstructure, mechanical properties and fractography of two AlSi-10vol.%SiC particle composite castings. Materials Science and Engineering 160:181-90. https://doi.org/10.1016/0921-5093(93)90500-e

[44] Makhlouf, M.M. and H.V. Guthy. 2001. The Al-Si Eutectic Reaction: Mechanisms and Crystallography. J. Light Metals 1:199–218. https://doi.org/10.1016/s1471-5317(02)00003-2

[45] Rohatgi, P. B. Schultz. 2008. Solidification During Casting of Metal-Matrix Composites. ASM Handbook, Volume 15: Casting, Pages 390-397. https://doi.org/10.31399/asm.hb.v15.a0005227

[46] Liu, Y., P.K. Rohatgi, S. Ray. 2008. Characteristics of Aluminum-50 volpct Graphite Composite,Metall. Mater.Trans. A 24:151–159. https://doi.org/10.1007/bf02669612

[47] Amouri, K., Sh. Kazemi, A. Momeni, M. Kazazi. 2016. Microstructure and Mechanical Properties of Al- nano/micro SiC CompositesProduced by Stir Casting Technique. Materials Science & Engineering A. 674:569-578. https://doi.org/10.1016/j.msea.2016.08.027

[48] Ajago, P., B. N. Anjan, R. N. Marigoudar, G. V. Preetham Kumar. 2018. Effect of SiC Reinforcement on Microstructure and Mechanical Properties of Aluminum Metal Matrix Composite. IOP Conf. Series: Materials Science and Engineering 376:012057. https://doi.org/10.1088/1757-899x/376/1/012057

[49] Ghauri, K. M., L. Ali, A. Ahmad, R. Ahmad, K. M. Din, I. A. Chaudhary, R. A. Karim. 2013. Synthesis and Characterization of Al/SiC Composite Made by Stir. Pak. J. Engg. & Appl. Sci.12:102-110.

[50] Tahamtan, S., M. Emamy, A. Halvaee. 2014. Effects of reinforcing particle size and interface bonding strength on tensile properties and fracture behavior of Al-A206/alumina micro/nano composites . Journal of Composite Materials 48: 3331. https://doi.org/10.1177/0021998313509860

[51] Sharma, A., S. Kumara, , R. Arorab, O.P. Pandeyc. 2015. Effect of Particle Size on Wear Behavior of Al–Garnet Composites. Journal Particulate Science and Technology 33: 234–239. https://doi.org/10.1080/02726351.2014.954686

[52] Surrappa, M.K. 1997. J. Mater. Process. Technol. 63:325

[53] Nripjit, A.K., Tyagi, N.Singh, A.Singh.2007. Advancesin Applied research 4:240.

[54] Yehia, M., Youssef, M. A. El-Sayed. 2016. Effect of Reinforcement Particle Size and Weight Fraction on the Mechanical Properties of SiC Particle Reinforced Al Metal Matrix Composites. International Review of Mechanical Engineering 10:1970 - 8734. https://doi.org/10.15866/ireme.v10i4.9509

[55] Clyne, T. W. 1996. Physical Metallurgy: Metallic Composite Materials. UK: Elsevier Science

[56] Whitehouse, A. F. 2000. Creep of Metal Matrix Composites. Comprehensive Composite Materials 3:371-418. https://doi.org/10.1016/b0-08-042993-9/00014-0

[57] Skolianos, S. 1996. Mechanical Behavior of Cast SiC p-Reinforced Al-4.5%Cu-1.5%Mg Alloy. Materials Science and Engineering: A 210:276-82. https://doi.org/10.1016/0921-5093(95)10043-1

[58] Jung, A., H. J. Maier, H. J. Christ. 2000. High-Temperature Fatigue Behaviour and Microstructure of a Dispersoid-Strengthened and SiC-Reinforced Aluminium Alloy. Microstructure and mechanical properties of metallic high-temperature materials: 34-49. https://doi.org/10.1520/stp15260s

Ref.:
Ali, Malek: *Review of stir casting technique and technical challenges for ceramic reinforcement particulate and aluminium matrix composites*
Építőanyag – Journal of Silicate Based and Composite Materials, Vol. 72, No. 6 (2020), 198–204. p.
https://doi.org/10.14382/epitoanyag-jsbcm.2020.32

Refractive index variations of glass microfragments by annealing – forensic applications

Tamás VÖRÖS
received his PhD from the Eötvös Loránd University, Hungary, in 2019. His research field was inorganic and structural chemistry. Now he works in the Laboratory of Forensic Physics and Inorganic Analytics in the HIFS, his research topic is forensic glass investigation.

Krisztina TAKÁCS
Expert pharmaceutical laboratory technician and expert instrumental analyst in the Hungarian Institute for Forensic Sciences, recent research interest: forensic examination of glasses.

Péter RÉGER
received his MSc in Budapest University of Technology and Economics, Faculty of Chemical Technology and Biotechnology. His research topic is glass comparative analysis based on elemental composition and refractive index.

Tamás VÖRÖS ▪ Department of Physics and Chemistry,
Hungarian Institute for Forensic Sciences, Hungary ▪ vorost@nszkk.gov.hu
Krisztina TAKÁCS ▪ Department of Physics and Chemistry,
Hungarian Institute for Forensic Sciences, Hungary ▪ takacsgyne@nszkk.gov.hu
Péter RÉGER ▪ Department of Physics and Chemistry,
Hungarian Institute for Forensic Sciences, Hungary ▪ regerp@nszkk.gov.hu

Érkezett: 2020. 04. 17. ▪ Received: 17. 04. 2020. ▪ https://doi.org/10.14382/epitoanyag-jsbcm.2020.33

Abstract
Annealing, as a possible glass investigating method was used for the first time in the Hungarian Institute for Forensic Sciences (HIFS). Glass is a frequently examined evidence type in forensic investigations. In the case of glass microfragments, the most common method for characterization is the measurement of the refractive index (RI). This characteristic value changes after heating up and cooling down the fragments according to the degree of the internal structural stress. The extent of this change (ΔRI) can be used in glass characterization and investigation. In the present study, first 25–25–25 toughened, nontoughened plate and container glasses were investigated. It has been found that, based on the ΔRI values, these glass types are distinguishable. Furthermore, the type of an unknown glass sample most likely can be determined. In real forensic cases it has been shown that a) more reliable information on the possible origin can be obtained if the refractive index measurements are supplemented with the examination of the RI values after annealing; b) if fragments have RI values very close to each other, the origin may be clarified using ΔRI, especially in those cases when the control samples with the same refractive indices are different types of glasses. The experiments were carried out on fragments in the range of ~100 µm.
Keywords: glass, crime evidence, delta RI, annealing, forensic discrimination
Kulcsszavak: üveg, bűncselekmény bizonyítéka, RI változás, felfűtés, forenzikus megkülönböztetés

1. Introduction

Glass is a frequently examined material [1, 2], and it is also important – as crime evidence – in forensic laboratories [3]. In the case of criminal activities including glass breaking, small fragments may transfer to the clothing of the persons standing nearby, and glass fragments can also be found on the objects used for the breaking. To associate a person or an object with the crime scene, a comparison of the control sample(s) and the recovered fragments from the clothes or objects is required. A useful comparison method is the measurement of the refractive index, which has the advantage over other techniques, e.g. X-Ray Fluorescence Spectrometry (XRF), Inductively Coupled Plasma – Mass Spectrometry (ICP-MS) or Scanning Electron Microscopy with Energy Dispersive Spectroscopy (SEM/EDS), that it can be applied for glass fragments smaller than 100 µm in one dimension. However, the discrimination force of the refractive index (RI) is usually not as good as of the above-mentioned techniques. A possible way of improving the discrimination is the process of annealing. Glass has internal structural stress due to its thermal disequilibrium, which depends on the type of the glass. Because of the manufacturing process, toughened glass has greater internal structural stress compared to the non-toughened glasses. Annealing (heating up followed by a very slow cooling) minimizes this stress, which results in an increase in the RI values, so the difference between the post- and the preannealed RI values (ΔRI) is a characteristic feature of the stress level in the investigated glass [4]. Locke and Hayes have shown that the ΔRI value is in the range of 0.00173–0.00206 for toughened, 0.00086–0.00144 for non-toughened float, patterned or plate glass, while 0.00073 for container glass [5]. Work performed by Cassista and Sandercock [6], Locke and Rockett [7], Winstanley and Rydeard [8], and Marcouiller [9] has been also shown and confirmed that toughened glass can be classified by annealing. It was also shown that the increase of the heating time (6–12–24 hours) increases the measured ΔRI value [10].

The aim of our work was to carry out annealing experiments for the first time in the Hungarian Institute for Forensic Sciences, including the investigation of 25–25–25 toughened, nontoughened plate and container glasses, and testing the discrimination power of the annealing method in real cases.

2. Methods

Refractive indices were measured by the oil immersion method using the GRIM®3 system made by Foster&Freeman. A narrow-band pass filter (589 nm) was used to choose the appropriate wavelength and to block the other lines of the light source. All investigated glass microfragments were mounted onto separate microscope slides, covered with a few drops of silicone oil (Locke Scientific Oil B), crushed with a dissecting needle and covered with a thin glass cover plate. The fragments

Container glasses			Plate glasses			Toughened glasses		
RI_{before}	RI_{after}	ΔRI	RI_{before}	RI_{after}	ΔRI	RI_{before}	RI_{after}	ΔRI
1.51959	**1.51993**	**34·10⁻⁵**	1.51729	1.51842	113·10⁻⁵	1.51995	1.52186	191·10⁻⁵
1.52339	1.52375	36·10⁻⁵	1.52066	1.52143	77·10⁻⁵	**1.51961**	**1.52160**	**199·10⁻⁵**
1.52477	1.52509	32·10⁻⁵	1.51683	1.51751	68·10⁻⁵	1.52053	1.52255	202·10⁻⁵
1.52346	1.52377	31·10⁻⁵	1.51417	1.51515	98·10⁻⁵	1.52109	1.52311	202·10⁻⁵
1.52527	1.52547	20·10⁻⁵	1.51773	1.51881	108·10⁻⁵	1.52291	1.52471	180·10⁻⁵
1.52446	1.52470	24·10⁻⁵	1.51383	1.51485	102·10⁻⁵	1.52102	1.52309	207·10⁻⁵
1.52546	1.52576	30·10⁻⁵	1.51571	1.51681	110·10⁻⁵	1.52436	1.52619	183·10⁻⁵
1.52047	1.52081	34·10⁻⁵	1.51853	1.51944	91·10⁻⁵	1.52149	1.52355	206·10⁻⁵
1.52200	1.52235	35·10⁻⁵	1.51894	1.51993	99·10⁻⁵	1.51762	1.51951	189·10⁻⁵
1.52385	1.52423	38·10⁻⁵	1.51761	1.51855	94·10⁻⁵	1.52426	1.52621	195·10⁻⁵
1.52426	1.52448	22·10⁻⁵	1.51530	1.51633	103·10⁻⁵	1.52447	1.52632	185·10⁻⁵
1.52300	1.52331	31·10⁻⁵	1.52097	1.52182	85·10⁻⁵	1.52237	1.52435	198·10⁻⁵
1.52412	1.52440	28·10⁻⁵	1.52077	1.52140	63·10⁻⁵	1.52437	1.52632	195·10⁻⁵
1.52400	1.52435	35·10⁻⁵	1.51433	1.51524	91·10⁻⁵	1.52006	1.52201	195·10⁻⁵
1.52140	1.52180	40·10⁻⁵	1.52101	1.52172	71·10⁻⁵	1.51911	1.52110	199·10⁻⁵
1.52379	1.52407	28·10⁻⁵	1.52207	1.52278	71·10⁻⁵	1.51677	1.51843	166·10⁻⁵
1.52409	1.52435	26·10⁻⁵	1.51907	1.51970	63·10⁻⁵	1.52119	1.52288	169·10⁻⁵
1.52395	1.52430	35·10⁻⁵	1.52076	1.52152	76·10⁻⁵	1.52181	1.52360	179·10⁻⁵
1.52369	1.52394	25·10⁻⁵	1.52409	1.52469	60·10⁻⁵	1.51508	1.51686	178·10⁻⁵
1.52386	1.52424	38·10⁻⁵	1.51715	1.51798	83·10⁻⁵	1.51917	1.52098	181·10⁻⁵
1.52387	1.52417	30·10⁻⁵	1.51688	1.51765	77·10⁻⁵	1.51920	1.52109	189·10⁻⁵
1.52603	1.52625	22·10⁻⁵	1.52115	1.52184	69·10⁻⁵	1.52010	1.52206	196·10⁻⁵
1.52554	1.52583	29·10⁻⁵	1.51983	1.52048	65·10⁻⁵	1.52096	1.52299	203·10⁻⁵
1.52340	1.52374	34·10⁻⁵	**1.51946**	**1.52016**	**70·10⁻⁵**	1.51803	1.51984	181·10⁻⁵
1.52335	1.52358	23·10⁻⁵	1.51912	1.51979	67·10⁻⁵	1.52023	1.52206	183·10⁻⁵

Table 1 Average refractive indices of 25–25–25 container, plate and toughened glasses before (RI_{before}) and after (RI_{after}) annealing, and the difference of these values (ΔRI)
1. táblázat 25-25 db öblös-, sík- és biztonsági üveg átlagos optikai törésmutatója hőkezelés előtt (RI_{before}) és azt követően (RI_{after}), valamint ezen értékek különbségei (ΔRI)

were observed with a phase-contrast microscope as the temperature of the slides was varied at ramp-rate of 4 °C min^{-1}. The average RI value was determined from the measured matching temperature using a calibration curve determined by the measurements of 10 glass standards (Locke Scientific).

The annealing was carried out by using an OMSZÖV OH63 type furnace, which was heated up to the required temperature (see the exact values at the appropriate chapters in the Results section) during ~1 hour. The temperature was then held at the chosen degree for 4.0 hours in each experiment, and it was controlled by a GANZ DKT NiCr-Ni thermometer. As no installation existed for temperature programming, the rate of cooling was limited to that achieved by turning off the supply of the furnace. After an overnight cooling, the temperature was under 200 °C, and at this stage the furnace was opened. In the annealing experiments, a porcelain combustion boat or a homemade stainless steel sample holder with holes of 6 mm in diameter and 3 mm deep were used.

The investigated glasses, which were cleaned before the investigation using 96 V/V% ethanol, are mentioned in the appropriate chapters of the Results section.

3. Results

3.1 ΔRI of different glass types

Altogether 25 container glasses (5 colorless, 10 green, and 10 brown beer or wine bottles purchased in Hungary), 25 colorless plate glasses, and 25 toughened glasses (5 colorless, 10 pale green, and 10 green) were investigated. Each sample was crushed, and one bulk fragment was chosen from each glass. This fragment was broken into two equal parts, and the average RI value of one was measured (RI_{before}). The other part was annealed (up to 700 °C) followed by the RI determination (RI_{after}). These values are shown in *Table 1*.

According to the data shown in *Table 1*, the ΔRI values are in the range of 0.00020–0.00040 for container glasses, 0.00060–0.00113 for plate glasses, and 0.00166–0.00207 for toughened glasses. In the last case, the measured values are almost the same as observed by Locke and Hayes [5]. In contrast, the values for the plate and the container glasses are ~$30·10^{-5}$ smaller compared to the results by Locke and Hayes. The observed ΔRI values form three distinct groups as it is shown in *Fig. 1*. Although different types of glasses

could be almost the same RI_{before} values, according to the ΔRI values these glasses are distinguishable (see the bold values in *Table 1*). Moreover, the type of an unknown glass sample most likely can be determined.

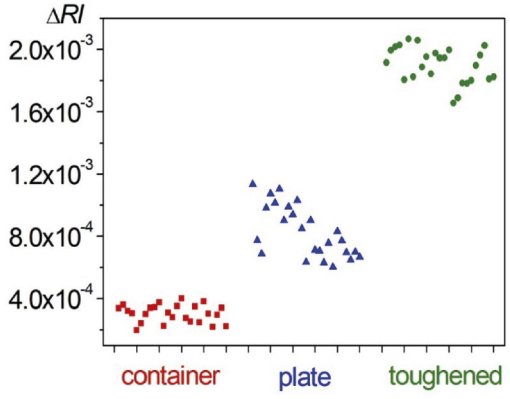

Fig. 1 The difference of the average refractive indices (ΔRI) of 25–25–25 container, plate, and toughened glasses after (RI_{after}) and before (RI_{before}) annealing
1. ábra 25-25 db öblös-, sík- és biztonsági üveg felfűtést követően (RI_{after}) és azt megelőzően (RI_{before}) mért átlagos optikai törésmutatójának különbségei (ΔRI)

3.2 ΔRI – an additional data for recovered microfragments

In the case of glass microfragments, the comparison of the recovered and the control samples in forensic laboratories usually based on only one information – the refractive index. In order to support the comparison from another side, the measurement of the ΔRI values could be important additional information. It is important to note that ΔRI can be measured also in the case of fragments smaller than 100 μm, which samples are not large enough for Micro X-Ray Fluorescence Spectrometry (μ-XRF) or Laser Ablation Inductively Coupled Plasma - Mass Spectrometry (LA-ICP-MS) investigations.

In one of our cases in 2019, first the refractive index of the control toughened glass sample was measured. It has been shown in many studies that the average RI value of the fragments from the surface can be a little bit different from the values of the bulk fragments [11, 12]. According to this, the average RI value of a bulk and a surface fragment was measured. As it is shown in *Table 2*, a ~$20 \cdot 10^{-5}$ difference was observed, which is consistent with the previous literature data. Based on the average refractive indices and on the range of RI values, our initial statement was that two of the recovered fragments could originate from the bulk, and two from the surface of the control sample. In the next step, both the bulk and the surface fragment of the control sample together with the four recovered fragments were annealed up to 450 °C. The lower temperature was chosen for two reasons: a) in the case of one glass fragment annealed up to 700 °C in the previous experiment a significant deformation was observed, which we would like to avoid in the experiments with recovered fragments; b) our aim was to examine how much the refractive index changes when lower temperature is applied. The measured average RI value after annealing together with the minimum and maximum values are also shown in *Table 2* and *Fig. 2*. It is clearly visible, that the data of the recovered fragments and the control sample is the same not just before, but after annealing. This makes it even more certain that each of the recovered four microscale glass fragments can originate from the control sample. Furthermore, it is interesting to note that the average ΔRI values are the same for the bulk and the surface fragments of the control sample ($85 \cdot 10^{-5}$), and – as it was expected – smaller than the observed RI changes for toughened glasses annealed up to 700 °C.

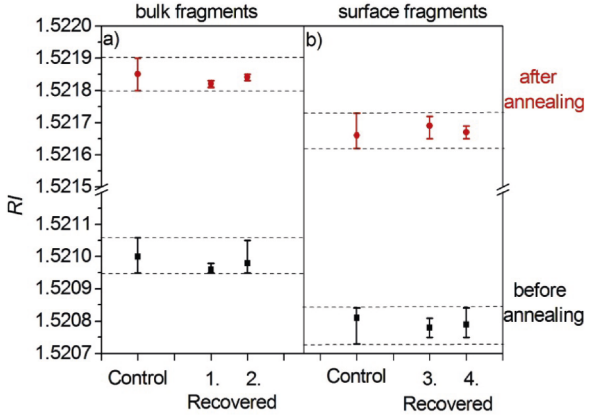

Fig. 2 The average RI values together with the range observed for a) bulk and b) surface fragments of the control sample and for four recovered microscale glass fragments before (black) and after (red) annealing in one of the examined cases in the HIFS
2. ábra Egy, az NSZKK-ban vizsgált ügyben érkezett összehasonlító minta a) tömbi és b) felszíni szemcséjének, valamint a rázalékban talált négy darab bűnjelszemcsének az átlagos optikai törésmutató értéke a mérési tartománnyal együtt felfűtés előtt (fekete) és azt követően (piros)

	Before annealing			After annealing			$\Delta RI_{average}$
	$RI_{average}$	$RI_{min.}$	$RI_{max.}$	$RI_{average}$	$RI_{min.}$	$RI_{max.}$	
Control (bulk)	1.52100	1.52095	1.52106	1.52185	1.52180	1.52190	$85 \cdot 10^{-5}$
Recovered (1.)	1.52096	1.52095	1.52098	1.52182	1.52181	1.52183	$86 \cdot 10^{-5}$
Recovered (2.)	1.52098	1.52095	1.52105	1.52184	1.52183	1.52185	$86 \cdot 10^{-5}$
Control (surface)	1.52081	1.52073	1.52084	1.52166	1.52162	1.52173	$85 \cdot 10^{-5}$
Recovered (3.)	1.52078	1.52075	1.52081	1.52169	1.52165	1.52172	$91 \cdot 10^{-5}$
Recovered (4.)	1.52079	1.52075	1.52084	1.52167	1.52165	1.52169	$88 \cdot 10^{-5}$

Table 2 The average, minimum, and maximum RI values observed for the bulk and surface fragments of the control sample and for four recovered microscale glass fragments before and after annealing together with the differences of the $RI_{average}$ values in one of the examined cases in the HIFS
2. táblázat Egy, a Nemzeti Szakértői és Kutató Központban (NSZKK) vizsgált ügyben érkezett összehasonlító minta tömbi és felszíni szemcséjének, valamint a rázalékban talált négy darab bűnjelszemcsének az átlagos optikai törésmutató értéke, az egyes szemcséknél mért legkisebb és legnagyobb optikai törésmutató értékek felfűtés előtt és azt követően, valamint a felfűtést követően és azt megelőzően mért átlagos RI értékek különbségei

3.3 Discrimination by ΔRI

It has been shown in earlier investigations [13], and also in our experiments (see *Table 1*) that different types of glasses from different sources can have very similar RI values. As it is shown in *Table 1* (see the values in bold) the average RI value measured before annealing of one of the container, plate, and

toughened glasses (1.51959, 1.51946, 1.51961) may be so close to each other that the clear distinction based on the refractive indices is not possible. A similar situation was observed in one of our other cases, in which eight windows of a car were broken by a suspect. Four out of the eight control samples (indicated as 1.2., 1.5., 1.7., 1.8.) have similar average RI values, while the other four samples have different refractive indices as it is shown in *Table 3*. According to our measurements, two recovered fragments can originate from the control samples 1.2. and 1.5., and their average RI values are also close to the appropriate values of control samples 1.7. and 1.8. In order to clarify their origin, both the recovered fragments and the four control samples were annealed up to 650 °C. As it is shown in *Table 3*, the average RI changes in the case of 1.2., 1.7., and 1.8. samples are $187 \cdot 10^{-5}$, $179 \cdot 10^{-5}$, and $179 \cdot 10^{-5}$, respectively. These values are in accordance with our previous measurements for toughened glasses. However, in the case of 1.5., the ΔRI value is much smaller, $82 \cdot 10^{-5}$, which corresponds to the value measured for plate glasses. (As it is turned out later, the car was out of use, and one of its windows was replaced by a plate glass.) Additional result of this experiment was that annealing up to 650 °C or 700 °C causes similar changes in the refractive indices.

Examining the two recovered fragments, the first fragment has 1.52159 average RI value after annealing, which means $87 \cdot 10^{-5}$ change in the refractive index. Thus, it can be clearly seen that this fragment very likely originates from control sample 1.5., and cannot originate from any of the other control samples. The second examined recovered fragment was very small, so only one measurement could be carried out after annealing, which resulted in an RI value of 1.52169. This value is in the RI range (1.52153–1.52170) of control sample 1.5. after annealing, and significantly different from the other control samples examined by annealing. It means that the second investigated recovered fragment can also likely originate from sample 1.5. The results of this experiment are shown both in *Table 3* and *Fig. 3*.

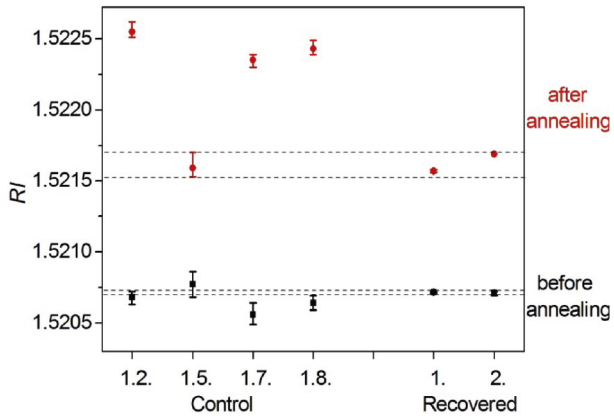

Fig. 3 *The average RI values together with the range observed for four control samples and for two recovered microscale glass fragments before (black) and after (red) annealing in one of the examined cases in the HIFS*

3. ábra *Egy, az NSZKK-ban vizsgált ügyben érkezett négy darab összehasonlító minta és két darab bűnjelszemcse átlagos optikai törésmutató értéke a mérési tartománnyal együtt felfűtés előtt (fekete) és azt követően (piros)*

		Before annealing			After annealing			
		$RI_{average}$	$RI_{min.}$	$RI_{max.}$	$RI_{average}$	$RI_{min.}$	$RI_{max.}$	$\Delta RI_{average}$
Control samples	1.1.	1.52301	1.52295	1.52304	not investigated	–	–	–
	1.2.	1.52068	1.52063	1.52072	1.52255	1.52251	1.52262	$187 \cdot 10^{-5}$
	1.3.	1.51795	1.51789	1.51799	not investigated	–	–	–
	1.4.	1.52357	1.52352	1.52364	not investigated	–	–	–
	1.5.	1.52077	1.52068	1.52086	1.52159	1.52153	1.52170	$82 \cdot 10^{-5}$
	1.6.	1.52146	1.52141	1.52153	not investigated	–	–	–
	1.7.	1.52056	1.52049	1.52064	1.52235	1.52230	1.52239	$179 \cdot 10^{-5}$
	1.8.	1.52064	1.52059	1.52069	1.52243	1.52239	1.52249	$179 \cdot 10^{-5}$
Recovered (1.)		1.52072	1.52071	1.52072	1.52159	1.52158	1.52160	$87 \cdot 10^{-5}$
Recovered (2.)		1.52071	1.52069	1.52072	1.52169	1.52169	1.52169	$98 \cdot 10^{-5}$

Table 3 *The average, minimum, and maximum RI values observed for eight control samples and two recovered fragments before annealing and in six cases after annealing together with the differences of the $RI_{average}$ values*

3. táblázat *Nyolc darab összehasonlító minta és két darab bűnjelszemcse átlagos optikai törésmutató értéke, valamint az egyes szemcséknél mért legkisebb és legnagyobb optikai törésmutató értékek felfűtés előtt és összesen hat esetben azt követően, valamint a felfűtést követően és azt megelőzően mért átlagos RI értékek különbségei*

4. Conclusions

The change in the refractive indices by annealing caused by the various structural stresses present in different types of glasses represents a possibility for glass origin examination which was not previously used in the Hungarian Institute for Forensic Sciences (HIFS). In accordance with previous investigations, our experiments have also shown that the type of an unknown glass fragment can be determined by annealing. So far, comparative analysis of microscale glass fragments in the HIFS has been performed only by refractive index measurements. By supplementing these investigations with the examination of the RI values after annealing, even more reliable information on the possible origin can be obtained. For those fragments which have more or less the same RI values the origin may be clarified, especially in those cases when the control samples with the same refractive indices are different types of glasses. A further advantage of the annealing experiments is that the ΔRI value can be measured on fragments in the range of ~100 μm, which are not large enough for comparison based on elemental analysis. In conclusion, annealing is a good additional opportunity for the examination of glass microfragments, which is – based on our experiments – applicable in the Hungarian Institute for Forensic Sciences.

Acknowledgement

The authors acknowledge the colleagues of the Department of Physics and Chemistry of the Hungarian Institute for Forensic Sciences for their contribution to this work.

References

[1] Gömze, L. A. – Gömze, L. N. – Kocserha, I. – Géber, R.: Typical defects on automobile windscreens at the interfaces of silver coatings, copper filaments and glasses, Építőanyag – Journal of Silicate Based and Composite Materials, 64, 64–66, 2012. http://dx.doi.org/10.14382/epitoanyag-jsbcm.2012.12

[2] Rénes, M. – Jakab, A. – Nehme, K. – Nehme, S. G.: Laboratory experiments of point fixed glasses, Építőanyag – Journal of Silicate Based and Composite Materials, 67, 62–65, 2015. http://dx.doi.org/10.14382/epitoanyag-jsbcm.2015.10

[3] Curran, J. M. – Hicks, T. N. – Buckleton, J. S.: Forensic Interpretation of Glass Evidence, CRC Press, 2000.

[4] Locke, J. – Sanger, D. G. – Roopnarine, G.: The identification of toughened glass by annealing, Forensic Science International, 20, 295–301, 1982. https://doi.org/10.1016/0379-0738(82)90131-1

[5] Locke, J. – Hayes, C. A.: Refractive index measurements across glass objects and the influence of annealing, Forensic Science International, 26, 147–157, 1984. https://doi.org/10.1016/0379-0738(84)90071-9

[6] Cassista, A. R. – Sandercock, P. M. L.: Effects of Annealing on Toughened and Non-Toughened Glass, Canadian Society of Forensic Science Journal, 27, 171–177, 1994. https://doi.org/10.1080/00085030.1994.10757033

[7] Locke, J. – Rockett, L. A.: The application of annealing to improve the discrimination between glasses, Forensic Science International, 29, 237–245, 1985. https://doi.org/10.1016/0379-0738(85)90117-3

[8] Winstanley, R. – Rydeard, C.: Concepts of annealing applied to small glass fragments, Forensic Science International, 29, 1–10, 1985. https://doi.org/10.1016/0379-0738(85)90028-3

[9] Marcouiller, J. M.: A Revised Glass Annealing Method to Distinguish Glass Types, Journal of Forensic Sciences, 35, 554–559, 1990. https://doi.org/10.1520/JFS12861J

[10] Locke, J. – Hayes, C. A. – Sanger, D. G.: The design of equipment and thermal routines for annealing glass particles, Forensic Science International, 26, 139-146, 1984. https://doi.org/10.1016/0379-0738(84)90070-7

[11] A. W. N. Newton, J. M. Curran, C. M. Triggs, J. S. Buckleton, The consequences of potentially differing distributions of the refractive indices of glass fragments from control and recovered sources; Forensic Science International, 140, 185–193, 2004. https://doi.org/10.1016/j.forsciint.2003.11.030

[12] Zoro, J. A. – Locke, J. – Day, R. S. – Badmus, O. – Perryman, A. C.: An investigation of refractive index anomalies at the surfaces of glass objects and windows, Forensic Science International, 39, 127–141, 1988. https://doi.org/10.1016/0379-0738(88)90085-0

[13] Lambert, J. A. – Evett, I. W.: The refractive index distribution of control glass samples examined by the Forensic Science Laboratories in the United Kingdom, Forensic Science International, 26, 1–23, 1984. https://doi.org/10.1016/0379-0738(84)90207-X

Ref.:

Vörös, Tamás – **Takács**, Krisztina – **Réger**, Péter: *Refractive index variations of glass microfragments by annealing – forensic applications*

Építőanyag – Journal of Silicate Based and Composite Materials, Vol. 72, No. 6 (2020), 205–209. p.

https://doi.org/10.14382/epitoanyag-jsbcm.2020.33

Formulation of predictive model for the compressive strength of oyster shell powder-cement concrete using Scheffe's simplex lattice theory

Obiekwe A. UBACHUKWU ▪ Department of Civil Engineering,
Michael Okpara University of Agriculture, Nigeria ▪ obiubachukwu@yahoo.com
Fidelis O. OKAFOR ▪ Department of Civil Engineering,
University of Nigeria, Nigeria ▪ fidelis.okafor@unn.edu.ng

Érkezett: 2020. 03. 24. ▪ Received: 24. 03. 2020. ▪ https://doi.org/10.14382/epitoanyag-jsbcm.2020.34

Abstract

This empirical study was carried out to formulate and validate a predictive model for the compressive strength of oyster shell powder-cement concrete using Scheffe's simplex lattice theory, so as to ensure economic usage of readily available oyster shells. A total of 90 cubes of concrete were cast to formulate and validate the model for the compressive strength of oyster shell powder (OSP)-cement concrete using Scheffe's (5, 2) simplex lattice theory. The formulated model was tested for adequacy using the Student t-test. It was observed that the model results agree with those of the experiments. Hence, the model is adequate and can predict the compressive strength, given the mix proportions. The model gave highest compressive strength of 30.81 N/mm^2 corresponding to mix ratio of 0.54:0.815:2.045:3.925:0.185 for water, cement, sand, granite and OSP respectively. The developed model also gave minimum compressive strength of 17.85 N/mm^2 corresponding to mix ratio of 0.525:0.825:2.2:4.05:0.175 for water, cement, sand, granite and OSP respectively. With this formulated model, any point on the simplex can easily be derived.

Key words: concrete, oyster shells, compressive strength, Scheffe, simplex
Kulcsszavak: beton, osztriga héj, nyomószilárdság, Scheffe, szimplex

Obiekwe A. UBACHUKWU
is a lecturer and Master of Structural Engineering at Michael Okpara University of Agriculture, Department of Civil Engineering, Umudike, Abia State-Nigeria. His research interest include, but not limited to Characterization and optimization of Civil engineering materials, Soil-Structure Interaction, Modelling of structures and structural materials, structural dynamics and stability. He is a registered engineer.

Fidelis O. OKAFOR
is a lecturer and professor of Civil Engineering at the department of Civil Engineering, University of Nigeria, Nsukka, Enugu State-Nigeria. His major area of interest is Materials and Highway Engineering. Hes also serves as reviewer for several reputable international journals.

1. Introduction

When a product is formed by mixing together two or more ingredients, the product is called a mixture and the ingredients are called mixture components [1]. In the case of concrete (mixture) and mixture components (cement, sand, granite, water and admixture or supplementary cementitious material), there is need to develop a way of optimally combining these ingredients, with a view to economizing our scarce resources, without compromise on the rheological and hardened properties of concrete produced. According to [2], it is important to find the optimum dosage and substitution ratio, because application of supplementary cementing materials over the optimum amount may reduce the performance, both in strength and durability parameters. One of the purposes of a mixture experiment is to find the best proportion of each component and the best value of each process variable, in order to optimize a single response or multiple responses simultaneously. A comprehensive methodology for mixture experiment was first proposed by [3, 4]. Scheffe introduced the {q,m}simplex lattice design and simplex centroid designs. If the number of components is not large and a high order polynomial is needed in order to accurately describe the response surface; then, a simplex lattice design can be used [5]. Scheffe's model is most times referred to as mixture model. They differ from the usual regression model due to correlation among all components in the mixture designs. Another difference is that the intercept term in the model is not usually included in the regression model [6]. Scheffe expressed the functional relationship between the investigated property and mixture components. Scheffe's ideas endure as primary recourse for practitioners of mixture experiments [7]. In a bid to reduce air and water pollutions, global warming, cost of construction and environmental nuisance, some researchers have used oyster shell powder as supplementary cementitious material to produce ecologically and economically friendly concrete [8-13]. The use of supplementary cementing materials in concrete may help in reducing the large carbon dioxide emission that result from production of Portland cement [14]. However, none of those researchers was able to come up with a model to optimize these mixture components as a predictor of compressive strength, given the mix proportion and vice versa. Hence, the present study will focus on model formulation and validation of oyster shell powder-cement concrete using the Scheffe's simplex lattice theory.

2. Materials and methods

2.1 Materials

Dangote brand of ordinary Portland cement was used in this research and it conformed to the requirements of [15]. The sand was sourced from Imo River in Imo State. It was sieved through 10 mm British standards test sieve to remove cobbles. The sand was sharp and free from deleterious substances and conforms to the requirements of [16]. The granite was sourced from the quarry site at Ishiagu, Ebonyi State, Nigeria. The maximum size of aggregate used for this work is 20 mm diameter. It was thoroughly flushed with water to reduce the level of impurities

and organic matter that might have intruded during quarrying; to conform to requirements [17]. The water used for the study was obtained from borehole. The water was clean and free from any visible impurities. It conformed to the requirements of [18]. The water does not contain harmful constituents in such quantities as may be detrimental to the setting, hardening and durability of the concrete. Oyster Shell Powder was obtained from oyster shells littered at Okwagwe River, Delta State, after washing, sun drying, crushing and sieving with 150 µm sieve. A total of 90 cubes of concrete were cast and cured for 28 days. 15 runs with three replicates each for the model compressive strength and 15 runs with three replicates each for validation of the model (control).

2.2 Method

2.2.1 Design of experiment

The OSP-cement concrete is made up of five components: water, cement, sand, granite and OSP which we can designate as X_1, X_2, X_3, X_4 an d X_5 respectively. Where, X_i represents the volume fraction of component. The volume fractions of the components sum to one, and the region defined by this constraint is the regular tetrahedron (or simplex) shown in *Fig. 1*.

Each vertex of the tetrahedron represents the pure component. For example, the vertex labelled X_1 is the pure water mixture with $X_1 = 1$, $X_2 = 0$, $X_3 = 0$, $X_4 = 0$ and $X_5 = 0$ or (1,0,0,0,0).

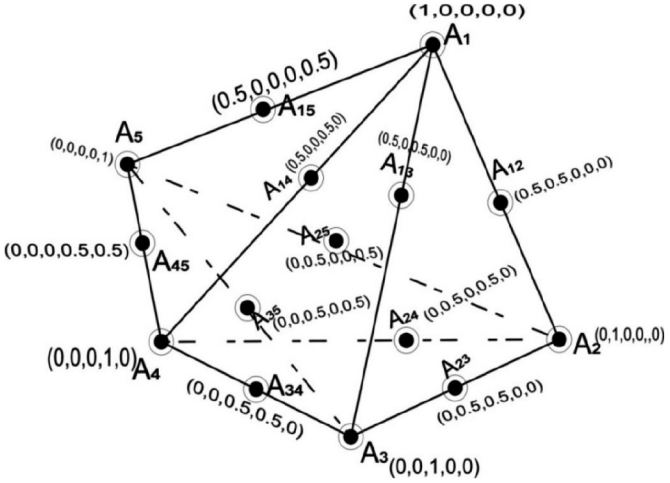

Fig. 1. A (5, 2) Scheffe's simplex lattice with 15 experimental runs
1. ábra (5,2) méretű Scheffe szimplex rács 15 vizsgálati ponttal

All responses (properties) of interest would be measured for each mixture in the design and modelled as a function of the components. Here, polynomial functions will be used. The number of coefficients, *n*, of the polynomial is determined using equation

$$n = \frac{(q+m-1)!}{(q-1)!*m!} \quad (1)$$

Where, *q* is the number of components of the mixture, and m is the degree of the polynomial. Thus, for *q=5* and *m=2* as in second degree polynomial, *n=15* signifying that for a (*q,m*) = (5,2) simplex design, we have 15 coefficients of the polynomial function; thus, 15 experimental runs.

The mixture constraint, according to [3] implies that

$$0 \le X_i \le 1, \text{ for } i = 1,2,\ldots..,q \quad (2)$$

For a five – component mixture,

$$X_1 + X_2 + X_3 + X_4 + X_5 = 1 \quad (3)$$

The linear polynomial model for a response y is

$$Y = b^*_o + b^*_1X_1 + b^*_2X_2 + b^*_3X_3 + b^*_4X_4 + b^*_5X_5 + e \quad (4)$$

Where b^*_i are constants and *e*, the random error term, represents the combined effects of all variables not included in the model. The form of Eq. (4) is called the Scheffe's linear mixture polynomial. If there is curvature in the system, a polynomial of higher degree such as the second order model should be sought. Hence, the quadratic model is given by Eq. (5).

$$Y = b^*_o + b^*_1X_1 + b^*_2X_2 + b^*_3X_3 + b^*_4X_4 + b^*_5X_5 + b^*_{12}X_1X_2 + b^*_{13}X_1X_3 + b^*_{14}X_1X_4 + b^*_{15}X_1X_5 + b^*_{23}X_2X_3 + b^*_{24}X_2X_4 + b^*_{25}X_2X_5 + b^*_{34}X_3X_4 + b^*_{35}X_3X_5 + b^*_{45}X_4X_5 + b^*_{11}X_1^2 + b^*_{22}X_2^2 + b^*_{33}X_3^2 + b^*_{44}X_4^2 + b^*_{55}X_5^2 + e \quad (5)$$

The challenge which any model developed using polynomial in Eq. (4) is that the developed model will always give an expected response, even when all the components are absent (zero). This limitation is due to the presence of b_o and e, random error in the polynomials [19]. Scheffe's model of Eq. (5) overcomes this weakness. Transformation of Eq. (5) gives Eq. (6) below

$$\hat{Y} = \beta_1X_1 + \beta_2X_2 + \beta_3X_3 + \beta_4X_4 + \beta_5X_5 + \beta_{12}X_1X_2 + \beta_{13}X_1X_3 + \beta_{14}X_1X_4 + \beta_{15}X_1X_5 + \beta_{23}X_2X_3 + \beta_{24}X_2X_4 + \beta_{25}X_2X_5 + \beta_{34}X_3X_4 + \beta_{35}X_3X_5 + \beta_{45}X_4X_5 \quad (6)$$

Eq. (6) is the regression equation for the (5, 2) Scheffe's second degree canonical polynomial. The determination of the values of the coefficients in Eq. (6) will complete the model equation. Where:

$$Y_1 = \beta_1,\ Y_2 = \beta_2,\ Y_3 = \beta_3,\ Y_4 = \beta_4,\ Y_5 = \beta_5,$$
$$\beta_{12} = 4Y_{12} - 2Y_1 - 2Y_2,\ \beta_{13} = 4Y_{13} - 2Y_1 - 2Y_3,$$
$$\beta_{14} = 4Y_{14} - 2Y_1 - 2Y_4,\ \beta_{15} = 4Y_{15} - 2Y_1 - 2Y_5,$$
$$\beta_{23} = 4Y_{23} - 2Y_2 - 2Y_3,\ \beta_{24} = 4Y_{24} - 2Y_2 - 2Y_4,$$
$$\beta_{25} = 4Y_{25} - 2Y_2 - 2Y_5,\ \beta_{34} = 4Y_{34} - 2Y_3 - 2Y_4,$$
$$\beta_{35} = 4Y_{35} - 2Y_3 - 2Y_5,\ \beta_{45} = 4Y_{45} - 2Y_4 - 2Y_5 \quad (7)$$

2.2.2 Concrete mix ratios for the formulation of regression model

According to [20], the relationship between the actual and the pseudo mix ratios are given by

$$\{Z\} = [A]\ \{X\} \quad (8)$$
$$\{X\} = [A^{-1}]\{Z\} \quad (9)$$

Where *Z*, *A*, and *X* are respectively the real mix ratios, coefficient of relation matrix and pseudo mix ratios. The value of matrix A will be obtained from the first five real mix ratios. The first five mix ratios are: Z_1[0.45:0.95:2.00:4.00:0.05], Z_2[0.48:0.90:1.85:3.75:0.10], Z_3[0.5:0.85:2.15:4.15:0.15], Z_4[0.55:0.80:2.25:3.95:0.20], Z_5[0.60:0.75:1.75:3.65:0.25] and the corresponding pseudo mix ratios at the vertices of the tetrahedron (simplex) are X_1[1:0:0:0:0], X_2[0:1:0:0:0], X_3[0:0:1:0:0], X_4[0:0:0:1:0], X_5[0:0:0:0:0:1] as shown in *Fig. 1*.

This quadratic model involves 15 parameters, so design will be at least 15 points in order to fit the model. However, multiple points or complete replicates are required to provide sufficient degrees of freedom to test the adequacy of the fit.

Matrix *A* is the transpose of the first five mix ratios and these are as shown below:

$$[A] = \begin{vmatrix} 0.45 & 0.48 & 0.5 & 0.55 & 0.60 \\ 0.95 & 0.90 & 0.85 & 0.80 & 0.75 \\ 2.00 & 1.85 & 2.15 & 2.25 & 1.75 \\ 4.00 & 3.75 & 4.15 & 3.95 & 3.65 \\ 0.05 & 0.10 & 0.15 & 0.20 & 0.25 \end{vmatrix}$$

With the substitution of the other pseudo mix ratios at the midpoint of the simplex into Eq. (8), we obtain the 10 remaining real mix ratios. Hence, the mix ratios, both real and pseudo at the vertices and midpoints of the tetrahedron are as given in *Table 1*.

In order to statistically test the validity of the regression model for the compressive strength of OSP-cement concrete, fifteen additional mixes (control) were made as given in *Table 2*.

The results obtained from the 28-compressive strength for model formulation were fitted into the regression equation to form the regression model. The model was validated using the results of 28-day compressive strength obtained using the control mix ratios.

Points	Real mix ratios					Pseudo mix ratios				
	Water Z_1	Cement Z_2	Sand Z_3	Granite Z_4	OSP Z_5	Water X_1	Cement X_2	Sand X_3	Granite X_4	OSP X_5
Y_1	0.45	0.95	2.00	4.00	0.05	1.0	0.0	0.0	0.0	0.0
Y_2	0.48	0.90	1.85	3.75	0.10	0.0	1.0	0.0	0.0	0.0
Y_3	0.50	0.85	2.15	4.15	0.15	0.0	0.0	1.0	0.0	0.0
Y_4	0.55	0.8	2.25	3.95	0.20	0.0	0.0	0.0	1.0	0.0
Y_5	0.60	0.75	1.75	3.65	0.25	0.0	0.0	0.0	0.0	1.0
Y_{12}	0.465	0.925	1.925	3.875	0.075	0.5	0.5	0.0	0.0	0.0
Y_{13}	0.475	0.90	2.075	4.075	0.100	0.5	0.0	0.5	0.0	0.0
Y_{14}	0.500	0.875	2.125	3.975	0.125	0.5	0.0	0.0	0.5	0.0
Y_{15}	0.525	0.850	1.875	3.825	0.150	0.5	0.0	0.0	0.0	0.5
Y_{23}	0.490	0.875	2.000	3.950	0.125	0.0	0.5	0.5	0.0	0.0
Y_{24}	0.515	0.850	2.050	3.850	0.150	0.0	0.5	0.0	0.5	0.0
Y_{25}	0.540	0.825	1.800	3.700	0.175	0.0	0.5	0.0	0.0	0.5
Y_{34}	0.525	0.825	2.200	4.050	0.175	0.0	0.0	0.5	0.5	0.0
Y_{35}	0.550	0.800	1.950	3.900	0.200	0.0	0.0	0.5	0.0	0.5
Y_{45}	0.575	0.775	2.000	3.800	0.225	0.0	0.0	0.0	0.5	0.5

Table 1 Concrete mix ratios for model formulation
1. táblázat A modellalkotáshoz használt beton összetétel arányok

Point	Real mix ratios					Pseudo mix ratios				
	Water Z_1	Cement Z_2	Sand Z_3	Granite Z_4	OSP Z_5	Water X_1	Cement X_2	Sand X_3	Granite X_4	OSP X_5
C_1	0.495	0.875	2.0625	3.9625	0.1250	0.25	0.25	0.25	0.25	0.0
C_2	0.5075	0.8625	1.9375	3.8875	0.1375	0.25	0.25	0.25	0.0	0.25
C_3	0.5200	0.8500	1.9625	3.8375	0.1500	0.25	0.25	0.0	0.25	0.25
C_4	0.525	0.8375	2.0375	3.9375	0.1625	0.25	0.0	0.25	0.25	0.25
C_5	0.5325	0.8250	2.0000	3.8750	0.1750	0.0	0.25	0.25	0.25	0.25
C_6	0.5160	0.8500	2.000	3.9000	0.1500	0.2	0.2	0.2	0.2	0.2
C_7	0.4840	0.8900	2.0250	3.9650	0.1100	0.3	0.3	0.3	0.1	0.0
C_8	0.4890	0.8850	1.9750	3.9350	0.1150	0.3	0.3	0.3	0.0	0.1
C_9	0.5040	0.8700	2.0050	3.8750	0.1300	0.3	0.3	0.0	0.3	0.1
C_{10}	0.5100	0.8550	2.0950	3.9950	0.1450	0.3	0.0	0.3	0.3	0.1
C_{11}	0.5190	0.8400	2.0500	3.9200	0.1600	0.0	0.3	0.3	0.3	0.1
C_{12}	0.5400	0.8150	2.0450	3.9250	0.1850	0.1	0.0	0.3	0.3	0.3
C_{13}	0.534	0.8300	1.9550	3.8050	0.1700	0.1	0.3	0.0	0.3	0.3
C_{14}	0.519	0.8450	1.9250	3.8650	0.1550	0.1	0.3	0.3	0.0	0.3
C_{15}	0.504	0.8600	2.0750	3.9550	0.1400	0.1	0.3	0.3	0.3	0.0

Table 2 Concrete mix ratios (control) for model validation
2. táblázat A modell validálásához használt beton összetétel arányok

Response	Replicate	Average mass (kg)	Volume (m^3)	Crushing load (N)	Compressive strength (N/mm^2)	Average compressive strength (N/mm^2)
Y1	A	8.20	0.003375	400000	17.78	19.48
Y1	B			490000	21.78	
Y1	C			425000	18.89	
Y2	A	8.72	0.003375	590000	26.22	29.01
Y2	B			730000	32.44	
Y2	C			638000	28.36	
Y3	A	8.28	0.003375	450000	20.00	19.56
Y3	B			430000	19.11	
Y3	C			440000	19.56	
Y4	A	8.38	0.003375	500000	22.22	21.93
Y4	B			460000	20.44	
Y4	C			520000	23.11	
Y5	A	8.33	0.003375	400000	17.78	19.21
Y5	B			482000	21.42	
Y5	C			415000	18.44	
Y12	A	8.48	0.003375	650000	28.89	30.81
Y12	B			730000	32.44	
Y12	C			700000	31.11	
Y13	A	8.68	0.003375	700000	31.11	27.41
Y13	B			550000	24.44	
Y13	C			600000	26.67	
Y14	A	8.77	0.003375	670000	29.78	25.93
Y14	B			530000	23.56	
Y14	C			550000	24.44	
Y15	A	8.70	0.003375	580000	25.78	24.74
Y15	B			570000	25.33	
Y15	C			520000	23.11	
Y23	A	8.77	0.003375	505000	22.44	23.48
Y23	B			535000	23.78	
Y23	C			545000	24.22	
Y24	A	8.77	0.003375	615000	27.33	26.59
Y24	B			585000	26.00	
Y24	C			595000	26.44	
Y25	A	8.63	0.003375	540000	24.00	23.70
Y25	B			510000	22.67	
Y25	C			550000	24.44	
Y34	A	8.18	0.003375	455000	20.22	17.85
Y34	B			385000	17.11	
Y34	C			365000	16.22	
Y35	A	8.15	0.003375	440000	19.56	18.89
Y35	B			420000	18.67	
Y35	C			415000	18.44	
Y45	A	8.42	0.003375	425000	18.89	18.30
Y45	B			402000	17.87	
Y45	C			408000	18.13	

Table 3 The 28-day compressive strength values for model formulation
3. táblázat A model alkotáshoz használt 28 napos nyomószilárdság értékek

Response (control)	Replicate	Average weight (kg)	Volume (m^3)	Crushing load (N)	Compressive strength (N/mm^2)	Average compressive strength (N/mm^2)
C1	A	8.52	0.003375	480000	21.33	21.85
C1	B			500000	22.22	
C1	C			495000	22.00	
C2	A	7.45	0.003375	640000	28.44	24.59
C2	B			510000	22.67	
C2	C			510000	22.67	
C3	A	8.45	0.003375	540000	24.00	22.59
C3	B			470000	20.89	
C3	C			515000	22.89	
C4	A	8.68	0.003375	610000	27.11	24.59
C4	B			525000	23.33	
C4	C			525000	23.33	
C5	A	8.65	0.003375	550000	24.44	24.44
C5	B			580000	25.78	
C5	C			520000	23.11	
C12	A	8.33	0.003375	540000	24.00	25.26
C12	B			580000	25.78	
C12	C			585000	26.00	
C13	A	8.20	0.003375	575000	25.56	25.93
C13	B			580000	25.78	
C13	C			595000	26.44	
C14	A	8.57	0.003375	570000	25.33	26.67
C14	B			620000	27.56	
C14	C			610000	27.11	
C15	A	8.47	0.003375	560000	24.89	24.79
C15	B			595000	26.44	
C15	C			518000	23.02	
C23	A	8.07	0.003375	505000	22.44	22.67
C23	B			510000	22.67	
C23	C			515000	22.89	
C24	A	8.07	0.003375	457000	20.31	19.14
C24	B			420000	18.67	
C24	C			415000	18.44	
C25	A	8.23	0.003375	340000	15.11	19.04
C25	B			495000	22.00	
C25	C			450000	20.00	
C34	A	8.33	0.003375	470000	20.89	19.73
C34	B			462000	20.53	
C34	C			400000	17.78	
C35	A	8.47	0.003375	490000	21.78	21.11
C35	B			505000	22.44	
C35	C			430000	19.11	
C45	A	8.23	0.003375	410000	18.22	18.30
C45	B			380000	16.89	
C45	C			445000	19.78	

Table 4 The 28-day compressive strength values for model validation (control)
4. táblázat A model validálásához használt 28 napos nyomószilárdság értékek

β_1	β_2	β_3	β_4	β_5	β_{12}	β_{13}	β_{14}	β_{15}	β_{23}	β_{24}	β_{25}	β_{34}	β_{35}	β_{45}
19.48	29.01	19.56	21.93	19.21	26.28	31.56	20.89	21.57	-3.20	4.50	-1.63	-11.56	-1.99	-9.10

Table 5. Coefficients of Scheffe's second degree polynomial for the regression model
5. táblázat Scheffe másodfokú polinomjának együtthatói a regressziós modellhez

3. Regression model for the compressive strength of OSP-cement concrete

The results of 28-day compressive strength for model formulation of OSP-Cement concrete are a given in *Table 3*.

Similarly, the results of 28-day compressive strength for model validation of OSP-cement concrete are a given in *Table 4*.

From Eq. (7), the coefficients of the Scheffe's second degree polynomial are given in *Table 5*.

Substituting the values of these coefficients into Eq. (6) yields

$$\hat{Y} = 19.48X_1 + 29.01X_2 + 19.56X_3 + 21.93X_4 + 19.21X_5 + 26.28X_1X_2 + 31.56X_1X_3 + 20.89X_1X_4 + 21.57X_1X_5 - 3.20X_2X_3 + 4.50X_2X_4 - 1.63X_2X_5 - 11.56X_3X_4 - 1.99X_3X_5 - 9.10X_4X_5 \quad (10)$$

Eq. (10) is the regression model for the compressive strength of oyster shell powder-cement concrete using the Scheffe's simplex lattice theory.

4. Model Validations

4.1 Replication Variance

Mean responses, Y and the variances of replicates, S_i^2 in *Table 9* were obtained from Eq. (11).

$$Y = \frac{\sum_{i=1}^{n} Y_i}{n} \quad (11)$$

$$S_i^2 = \left[\frac{1}{n-1}\right]\left[\sum Y_i^2 \left[\frac{1}{n(\sum Y_i)^2}\right]\right] \quad (12)$$

Where: $1 \leq i \leq n$

Expansion of Eq. (12) gives Eq. (13)

$$S_i^2 = \left[\frac{1}{n-1}\right][\sum_{i=n}^{n}[Y_i - Y]^2] \quad (13)$$

Where Y_i = responses; Y = mean of the responses for each control point; n = number of parallel observations at every point; $n - 1$ = degree of freedom; Si^2 = variance at each design point. For all the design points, N, the degree of freedom, V_e is given by

$$V_e = \sum N - 2 = 30 - 2 = 28 \quad (14)$$

Where:

N is the number of points.

$S_y^2 = 103.24/28 = 3.687$

Where S_i^2 is the variance at each point

$S_y = 1.92$

The results of the compressive strength obtained for the formulation and validation of the model based on Scheffe's lattice theory are given in *Table 7*.

4.2 Test of adequacy of the model

The test for adequacy of the model was done using Student's t-test at 95% confidence level on the compressive strength at the control points subject to these two hypotheses.

Null hypothesis

There is no significant difference between the laboratory tests and model predicted strength results.

Alternative hypothesis

There is a significant difference between the laboratory test and model predicted strength results.

4.2.1 Student's t-test

Table 8 shows the parameters with which the student's t-test will be done. We did a two-tailed test (inequality) and if $t_{Stat} > t_{Critical}$ two-tailed, we reject the null hypothesis.

$$t_{Stat} = \frac{\sum(\mathbf{lab-model})}{\sqrt{\frac{(15*\sum((\mathbf{lab-model})^2)-(\sum(\mathbf{lab-model}))\text{^}2}{(15-1)}}} = \frac{(16.61)}{\sqrt{\frac{(15*92.24)-(16.61)}{(15-1)}}} = 1.868$$

$\alpha = 0.05$ and 0.025 for two tail; DF = 15-1 = 14 (t-distribution table).

$t_{Critical} = 2.145$

$t_{Stat} < t_{Critical}$

From the calculations, $t_{Stat} = 1.868$ and $t_{Critical}$ two-tailed = 2.145, so $t_{Critical} > t_{Stat}$. Therefore, we accept the null hypothesis.

5. Conclusions

The present study was geared towards the formulation and validation of model to predict the compressive strength of OSP-cement concrete, given the mix proportions and vice versa, based on Scheffe's simplex lattice theory. From the foregoing results, the following conclusions are hereby drawn:

i. The statistical tests conducted to validate the Scheffe's lattice model formulated for OSP-cement blended concrete for 28-day compressive strength was found to be adequate for the model.

ii. A good agreement was found between the predicted and experimental values of the 28-day compressive strength, leading to the adoption of null hypothesis.

iii. The model gave highest compressive strength of 30.81 N/mm² corresponding to mix ratio of 0.54:0.815:2.045:3.925:0.185 for water, cement, sand, granite and OSP respectively and the minimum compressive strength of 17.85 N/mm² corresponding to mix ratio of 0.525:0.825:2.2:4.05:0.175 for water, cement, sand, granite and OSP respectively.

iv. Using the model, compressive strength of all points in the simplex can be derived.

Funding

This research did not receive any specific grant from funding agencies in the public, commercial, or not-for-profit sectors.

Response	Replicate	Response Y_i (N/mm²)	$\sum Y_i$	Y	$\sum Y_i^2$	S_i^2
Y1	A	17.78	58.44	19.48	1147.11	4.26
Y1	B	21.78				
Y1	C	18.89				
Y2	A	26.22	87.02	29.01	2544.28	10.00
Y2	B	32.44				
Y2	C	28.36				
Y3	A	20.00	58.67	19.56	1147.65	0.20
Y3	B	19.11				
Y3	C	19.56				
Y4	A	22.22	65.78	21.93	1445.93	1.84
Y4	B	20.44				
Y4	C	23.11				
Y5	A	17.78	57.64	19.21	1115.16	3.77
Y5	B	21.42				
Y5	C	18.44				
Y12	A	28.89	92.44	30.81	2855.11	3.23
Y12	B	32.44				
Y12	C	31.11				
Y13	A	31.11	82.22	27.41	2276.54	11.52
Y13	B	24.44				
Y13	C	26.67				
Y14	A	29.78	77.78	25.93	2039.11	11.33
Y14	B	23.56				
Y14	C	24.44				
Y15	A	25.78	74.22	24.74	1840.40	2.04
Y15	B	25.33				
Y15	C	23.11				
Y23	A	22.44	70.44	23.48	1655.85	0.86
Y23	B	23.78				
Y23	C	24.22				
Y24	A	27.33	79.78	26.59	2122.42	0.46
Y24	B	26.00				
Y24	C	26.44				
Y25	A	24.00	71.11	23.70	1687.31	0.86
Y25	B	22.67				
Y25	C	24.44				
Y34	A	20.22	53.56	17.85	964.89	4.41
Y34	B	17.11				
Y34	C	16.22				
Y35	A	19.56	56.67	18.89	1071.06	0.35
Y35	B	18.67				
Y35	C	18.44				
Y45	A	18.89	54.89	18.30	1004.83	0.28
Y45	B	17.87				
Y45	C	18.13				

C1	A	21.33	65.56	21.85	1432.94	0.21
C1	B	22.22				
C1	C	22.00				
C2	A	28.44	73.78	24.59	1836.64	11.13
C2	B	22.67				
C2	C	22.67				
C3	A	24.00	67.78	22.59	1536.25	2.49
C3	B	20.89				
C3	C	22.89				
C4	A	27.11	73.78	24.59	1823.90	4.76
C4	B	23.33				
C4	C	23.33				
C5	A	24.44	73.33	24.44	1796.15	1.78
C5	B	25.78				
C5	C	23.11				
C12	A	24.00	75.78	25.26	1916.49	1.20
C12	B	25.78				
C12	C	26.00				
C13	A	25.56	77.78	25.93	2016.89	0.21
C13	B	25.78				
C13	C	26.44				
C14	A	25.33	80.00	26.67	2136.10	1.38
C14	B	27.56				
C14	C	27.11				
C15	A	24.89	74.36	24.79	1848.79	2.94
C15	B	26.44				
C15	C	23.02				
C23	A	22.44	68.00	22.67	1541.43	0.05
C23	B	22.67				
C23	C	22.89				
C24	A	20.31	57.42	19.14	1101.18	1.04
C24	B	18.67				
C24	C	18.44				
C25	A	15.11	57.11	19.04	1112.35	12.56
C25	B	22.00				
C25	C	20.00				
C34	A	20.89	59.20	19.73	1174.01	2.90
C34	B	20.53				
C34	C	17.78				
C35	A	21.78	63.33	21.11	1343.26	3.11
C35	B	22.44				
C35	C	19.11				
C45	A	18.22	54.89	18.30	1008.44	2.09
C45	B	16.89				
C45	C	19.78				

$\sum$ = 103.24

Table 6 Experimental test results and the replication variance

6. táblázat Kísérleti eredmények és az ismétlési variancia

Symbol	Experimental test	Scheffe's model
Y1	19.48	19.48
Y2	29.01	29.01
Y3	19.56	19.56
Y4	21.93	21.93
Y5	19.21	19.21
Y12	30.81	30.81
Y13	27.41	27.41
Y14	25.93	25.93
Y15	24.74	24.74
Y23	23.48	23.48
Y24	26.59	26.59
Y25	23.70	23.70
Y34	17.85	17.85
Y35	18.89	18.89
Y45	18.30	18.30
C1	21.85	23.14
C2	24.59	23.01
C3	22.59	21.36
C4	24.59	22.44
C5	24.44	17.97
C12	25.26	21.45
C13	25.93	24.20
C14	26.67	24.14
C15	24.79	22.56
C23	22.67	23.50
C24	19.14	18.60
C25	19.04	20.23
C34	19.73	18.95
C35	21.11	21.39
C45	18.30	21.14

Table 7 Experimental test and Scheffe's model results
7. táblázat Kísérleti és Scheffe modell eredmények

Symbol	Lab	Model	Lab-Model	(Lab-Model) ^ 2
C1	21.85	23.14	-1.29	1.67
C2	24.59	23.01	1.58	2.50
C3	22.59	21.36	1.23	1.52
C4	24.59	22.44	2.15	4.61
C5	24.44	17.97	6.48	41.94
C12	25.26	21.45	3.81	14.51
C13	25.93	24.20	1.73	2.98
C14	26.67	24.14	2.53	6.39
C15	24.79	22.56	2.23	4.96
C23	22.67	23.50	-0.83	0.70
C24	19.14	18.60	0.54	0.29
C25	19.04	20.23	-1.20	1.43
C34	19.73	18.95	0.78	0.61
C35	21.11	21.39	-0.27	0.08
C45	18.30	21.14	-2.84	8.06
	Total		**16.61**	**92.24**

Table 8 Student's t-test for the compressive strength
8. táblázat A nyomószilárdság Student tényező (t) változásának tesztje

References

[1] Oguaghamba, O. A. – Onyia, M. E.: Modified and generalized full cubic polynomial response surface methodology in engineering mixture design, Nigerian Journal of Engineering and Technology, 2019; 38 (1), 52-59

[2] Mlinarik, Lilla – Kopecsko, Katalin – Borosnyoi, Adorjan: Properties of cement mortars in fresh and hardened condition influenced by combined application of SCMs, Epitosanyag – Journal of Silicate Based and Composite Materials, Vol. 68, No. 2 (2016), 62-66 p. http://dx.doi.org/10.14382/epitoanyag-jsbcm.2016.11

[3] Scheffe, H.: Experiments with mixtures, Journal of Royal Statistical Society, 1958; Series B, 1958; 20: 344-366

[4] Scheffe H. : Simplex-centroid design for experiments with mixtures, Journal of Journal of the Royal Statistical Society", Series B, 1963; 25: 235-263

[5] House R. : Simplex lattice designs, 2017; retrieved from http://reliawiki.org/index.php/Mixture_Design on 10th August, 2017.

[6] Oguaghamba, O. A. – Mama, B. O.: Generalized Scheffe's second degree mathematical methods approach in engineering mixture design", Proceedings of 16th International Conference and AGM of Nigerian Institution of Civil Engineers (NICE) on Transforming national economy through sustainable civil engineering infrastructures- Engineering solutions to problematic soils and allied construction materials, Calabar, Nigeria, Oct. 24-26, 2018, 32-44

[7] Brown, L. J.: General blending models for mixture experiments: Design and analysis", An unpublished Ph.D thesis submitted to Faculty of Engineering and Physical Sciences, University of Manchester, United Kingdom, 2014

[8] Etuk, B. R. – Etuk, I. F. – Asuquo, L. O.:The feasibility of using sea shell ash admixtures for concrete, Journal of Environmental Sciences and Engineering, 2012; A1: 121-127

[9] Lerwattanaruk, P. – Makul, N. – Siripattarapravat, C.: Utilization of ground waste sea shells in cement mortars for masonry and plastering, Journal of Environmental Sciences and Management, 2012; 111: 133-141

[10] Liang Chou-Fu, - Wang Hung-Yu, : Feasibility of pulverized oyster shell as a cementing material, Advances in Materials Sciences and Engineering, Hindawi Publishing Corporation, 2013

[11] Wen-Ten, Kuo – Her-Yung, Wang – Chun-Ya, Shu – De-Sin, Su: Engineering properties of controlled low-strength material containing waste oyster shells, Construction and Building Materials, 2013; 46, 128-133

[12] Zhong, Bin-Yang – Zho, Qiang-Chan – Chan, Chang-Feng – Yan, Yu: Structure and property characterization of oyster shell cementing material, Chinese Journal of Struct. Chem., 2012; 31 (1), 85-92

[13] Ubachukwu, O. A. – Okafor, F. O.: Investigation of the supplementary cementitious potentials of oyster shell powder for eco-friendly and low-cost concrete, Electronic Journal of Geotechnical Engineering (EJGE), 2019, 24 (05), pp. 1297-1306.

[14] Nehme, Salem G.: Influence of supplementary cementing materials on conventional and self-compacting concretes, Epitoanyag – Journal of Silicate Based and Composite Materials, Vol. 67, No. 1 (2015), 28-33 http://dx.doi.org/10.14382/epitoanyag-jsbcm.2015.6

[15] BS12: Specification for Portland cement, British Standards Institution, London, 1996

[16] BS 812: Part 1: Method of determination of particle size and shape, British Standards Institution, London, 1975

[17] BS882: Specification for aggregates from natural sources for concrete, British Standards Institution, London, 1992

[18] BS3140: Methods of test for water for making concrete, including notes on the suitability of the water, British Standards Institution, London, 1980

[19] Okafor, F. O. – Oguaghamba, O. A.: Procedure for optimization using Scheffe's models, Journal of Engineering Science and Applications, 2010, 7 (1), 36-47

[20] Osadebe, N. N. – Ibearugbulem, O. M.: Application of Osadebe's alternative regression model in optimizing compressive strength of periwinkle shells-granite concrete, Nigerian Society of Engineers Technical Transaction, 2009, 43(1), 47-59

Ref.:
Ubachukwu, Obiekwe A. – **Okafor**, Fidelis O.: *Formulation of predictive model for the compressive strength of oyster shell powder-cement concrete using Scheffe's simplex lattice theory*
Építőanyag – Journal of Silicate Based and Composite Materials, Vol. 72, No. 6 (2020), 210–218. p.
https://doi.org/10.14382/epitoanyag-jsbcm.2020.34

Mechanical properties of fly ash modified asphalt treated with crushed waste glasses as fillers for sustainable pavements

Kennedy C. ONYELOWE ▪ Department of Civil Engineering, Michael Okpara University of Agriculture, Nigeria ▪ konyelowe@mouau.edu.ng
Michael ONYIA ▪ Department of Civil Engineering, Faculty of Engineering, University of Nigeria
Eze R. ONUKWUGHA ▪ Department of Civil Engineering, Faculty of Engineering, Federal Polytechnic, Nigeria
Duc BUI VAN ▪ Research Group of Geotechnical Engineering, Construction Materials and Sustainability, Hanoi University of Mining and Geology, Vietnam
Jesuborn OBIMBA-WOGU ▪ Department of Civil Engineering, Michael Okpara University of Agriculture, Nigeria
Chidozie IKPA ▪ Department of Civil Engineering, Faculty of Engineering, Alex Ekwueme Federal University, Nigeria

Érkezett: 2020. 03. 24. ▪ Received: 24. 03. 2020. ▪ https://doi.org/10.14382/epitoanyag-jsbcm.2020.35

Abstract

This research work investigated the effect of using fly ash as a modifier and utilizing crushed waste glasses (CWG) as fillers to enhance the mechanical properties of Asphalt for a sustainable pavement construction. The cost of pavement constructions is becoming overbearing on the developing countries and the need to develop more sustainable and green methods has become very imperative. With inclusion of waste materials like fly ash and CWG, enhanced and greener pavement is achieved. This is experimented in under laboratory conditions in order to improve the quality of representative asphalt for pavement construction using recycled waste materials. The scope of this research paper was on the investigation of the Marshall stability behaviour of the hot mix asphalt when mixed with recycled wastes. The asphalt, asphalt mixed with fly ash, and asphalt mixed with fly ash and crushed waste glass samples were tested and analysed with the Marshal Stability test, which is a major test for asphalt with admixtures. The results showed that at 15% by weight addition of fly ash in the modified asphalt, and 8% of CWG, the asphalt stability was observed to have increased substantially to 224.2 N/mm^2 compared to the control value of 216 N/mm^2 for stable pavements. The use of fly ash as a modifier in the asphalt road paving industry to mitigate the decrease in performance of the binder material due to exposure to traffic loads, climatic and environmental changes has generally produced favourable results consistent with those achieved by waste polymer modified asphaltic binders. This study demonstrated that incorporating fly ash resulted in improved rheological and performance characteristics while reducing cost and unfavourable environmental impacts.

Keywords: asphalt, fly ash, Marshal stability deformation, pavement, crushed waste glasses
Kulcsszavak: aszfalt, pernye, Marshall stabilitási deformáció, járófelület, zúzott üveghulladék

Kennedy C. ONYELOWE
He is a senior lecturer at the MOUAU, Nigeria, AE-FUNAI, Abakaliki, Nigeria and External Proposal Technical Reviewer, RIF, Makerere University, Uganda. His research interests include Geotechnical and Geoenvironmental Engineering. He is a member of several professional societies.

Michael ONYIA
He is a senior lecturer at the UNN, Nigeria and former head of department of Civil Engineering. His research interests include, structural engineering, materials engineering and geoenvironmental engineering.

Eze R. ONUKWUG HA
He is a chief lecturer and director at the FedPoNek, Owerri and his research interest is in water resources and environmental engineering

Duc BUI VAN
He is a senior researcher and lecturer at the HUMG and a strong member of the research group for sustainable construction materials.

Jesuborn OBI MBA -WOGU
He is a graduate assistant at the department of civil engineering with research interests in geotechnical and structural engineering

Chidozie IKPA
He is a lab technologist at the department of civil engineering, AE-FUNAI, Nigeria with research concentration in structural and construction materials.

1. Introduction

The use of environmentally friendly binders (ash, powder, geopolymer cements, etc.) derived from solid wastes under the influence of alkali activators for binding purposes has been practiced severally [1]. In as much as it is certain that human activity will never cease on the planet, there would always be an equivalent release of solid wastes (industrial, agricultural, household, and municipal, etc.) [1]. Hence, sustaining this technology wouldn't be a problem at all. Among the numerous derivatives of solid waste that have been utilized in various civil engineering works include palm oil fuel ash, fly ash, quarry dust, rice husk ash, coffee husk ash, paper ash, waste tire ash, palm fibre, palm kernel shell ash, snail shell ash, periwinkle shell ash/powder, oyster shell powder, biomass ash, bagasse ash, egg shell ash, sawdust, crushed waste ceramics, crushed waste plastics, crushed waste glasses, bio-peels, biochar, metallurgical slag (ground granulated blast furnace slag), iron ore tailings, palm nut fibre, glass fibres, etc. [1]. Improvement of asphalt pavement performances by means of additives to expand use over a wider range of temperatures and traffic loading has constantly been practiced by engineers. This modification of asphalt is commonly achieved through blending asphalt with manufactured products; such as polymers and some others. The use of fly ash to enhance the performance of asphalt concrete has been demonstrated but had not yet been adopted on a commercial scale [2]. Fly ash is a by-product of coal fired-furnaces at power generation facilities and is the non-combustible particulates removed from the flue gases [3]. The use of ASTM C 618 Class C fly ash has received most of the research focus [3]. It is derived when a subbituminous coal is burnt and it has obvious cementitious and pozzolanic properties. Class F fly ash and other Coal Combustion

Products (CCPs) warrant additional exploration for potential use as an ingredient in asphalt mixtures, especially the synergy between polymer modification and fly ash particles [4, 5]. Fly ash in asphalt bitumen can be considered an effective material in a viscoelastic matrix [1, 2]. Fillers for asphalt pavement applications are defined by AASHTO T190 and AASHTO T307 [6-8] as finely divided minerals, such as rock dust (e.g. granite and limestone), slag dust, hydrated lime, hydraulic cement, fly ash, loess, or other suitable mineral matter. The typical maximum particle size of fillers in asphalt is less than 75 microns. Although fillers, in general, usually represent less than 8% of Hot Mix Asphalt (HMA) by mass, the interactions of fillers with asphalt binder, and/or coarse and fine aggregates, affect the field performance. Furthermore, the use of fly ash in HMA has shown that it does not behave similar to typical fillers [8]. Fly ash has been used extensively in concrete production; however, there are limited applications in which fly ash has been used in asphalt pavements [7, 8]. Pavement engineers are interested in fly ash filler replacement because fly ash usage is important not only for improved performance, but also for economic, environmental and social benefits. Fly ash is an affordable, readily-available local material, and adding fly ash to asphalt mixtures does not require specialized equipment or changes for skilled constructors. Despite these benefits, the application of fly ash in asphalt technology has not yet become commonly accepted.

Glass waste is a viable material, due to its silicate-based composition for asphalt concrete that has been widely used in pavement that offers profound engineering and economic advantages, with a large amount of glass waste from industry forming subject of concern at both national and global levels, glass recycling by way of applications in commercial use in asphalt paving can save energy and decrease environmental waste. Early *glassphalt* projects used high percentages of glass (greater than 25% by weight of the mix) with coarse glass gradations (greater than 12.7 mm (1/2 in)). Current data suggest that the use of high glass percentages and large particles of glass probably contributed to most of the stripping and ravelling problems that were reported during the early test pavement demonstrations of the 1960s and 1970s. This can be attributed to the *"hydrophilic"* nature of glass. The high angularity of cullet, compared with rounded sand, can enhance the stability of asphalt mixes, where properly sized cullet is used. Stabilities comparable and, in many cases, better than those of conventional mixes have been reported, other beneficial characteristics include low absorption, low specific gravity and low thermal conductivity, which reportedly offer enhanced heat retention in mixes with glass. Proper mix design with suitable ingredients will ensure an improvement of the existing performance of roads. Various studies have been conducted to study the properties of mineral filler, especially the material passing 0.075 mm sieve (No. 200) and to evaluate its effect on the performance of asphalt paving mixtures in terms of consistency, void filling, resistance to displacement, water susceptibility, Marshall stability and mix strength. B.W. Ramme et al. and B. Baby *et al.* [9, 10], found that the behaviour of Hot Mix Asphalt (HMA) in different temperature conditions, depending on the variation of the admixture contents and the gradation of the aggregates, is improved in comparison with that of HMA mixtures.

This study aims at exploring the feasibility of using crushed waste glass fillers in improving the mechanical properties of fly ash modified asphalt by the determination of general performance of the stabilized materials through marshal stability testing.

2. Materials and methods

The crushed glass sample was collected from a Glass Industry located within Ogbor-hill environs in Aba, Abia state, while the fly ash was sourced from CIFA Industrial Company Atani Nike, Enugu state. Crushed waste glasses are waste materials derived as scrap loss during glass production and or as waste from mishandling and usage. These are known for their high composition of calcium oxide, silica and aluminates. Also, the fly ash, which is a byproduct of power generation and coal combustion is rich in aluminosilicates contents also. the aluminosilicates composition of the two waste materials constitute their preference as supplementary binders and modifiers due to their ability to enhance pozzolanic reactions. The asphalt was gotten from New Tunnel Asphalt Plant, Along the Isiala-Ngwa axis of the Enugu- Port Harcourt express road all in Nigeria. All the samples were collected at solid state before it was taking to the laboratory. The collected waste glass was crushed using a bulk density load apparatus for about 20 minutes repeatedly until desired particle size was achieved. The crushed glass was made to pass through a stack of BS sieve sizes according to known British test standard procedures with interest in the sieve no 22. The glass particles were made to pass through the sieve until the glass passing becomes finer. This procedure was repeated until the crushed glass wastes were exhausted.

In accordance with standard specifications [6, 7] in order to determine the optimum binder content for the aggregate mix type and traffic intensity otherwise called the Marshall test, about 1200gm of aggregate were blended in the desired proportions, measured and heated in the oven to the mixing temperature, bitumen was added at the mixing temperature to produce viscosity of 170 ± centi-stokes at various percentages and the mixture returned to the oven to be reheated to the compacting temperature (to produce viscosity of 280±30 centi-stokes). The sample was allowed to stand for the few hours to cool and the mass of the sample in air and when submerged is recorded respectively. This was to enable the measurement of density of the specimen, so as to allow calculation of the void properties. The sample is place in lower segment of the breaking head, the upper segment of the breaking head of the specimen is placed in position and the complete assembly is placed in position on the testing machine. The flow meter is placed over one of the posts and is adjusted to read zero, load is applied gently at a rate of 50 mm per minute until the maximum load reading is obtained. The maximum load reading in Newton is observed. At the same instant the flow as recorded on the flow meter in units of mm was also noted.

3. Results and discussion

The general behavior and analysis of the Marshal Stability test can be seen as presented in *Table 1*. The Marshall Stability result of three samples of asphalt was recorded showing the stability values, flow, height or thickness of the asphalt mould and the stability correction value of the samples. Finally, the average stability was determined by calculation as 216 N. This serves as the control MS value for the modified asphalt.

Sample	Stability (N)	Flow (mm)	Height (mm)	Stability correction factor (cf)	Corrected Stability (N)
1	200	0.1	64.5	0.96	192
2	210	0.2	61.5	1.04	218.4
3	218	0.1	60.7	1.09	237.6

Table 1 Marshall Stability result of asphalt
1. táblázat Aszfalt Marshall stabilitási vizsgálatának eredményei

$$\text{Average corrected stability} = \frac{192+218.4+237.6}{3} = 216$$

Fig. 1 presents the results of the three samples that were used to get a suitable corrected stability value for each Asphalt sample mixed with different percentages of Fly ash. It was observed that there was continuous increase in the corrected stability value with respect to increase in the percentage of fly ash sample [11-15]. At 15% fly ash mix, the highest number of corrected stability value was recorded. This substantial improvement was due to the cementing properties of the FA which enhanced carbonation and calcination reaction in the HMA thereby causing strengthening [3, 15-25].

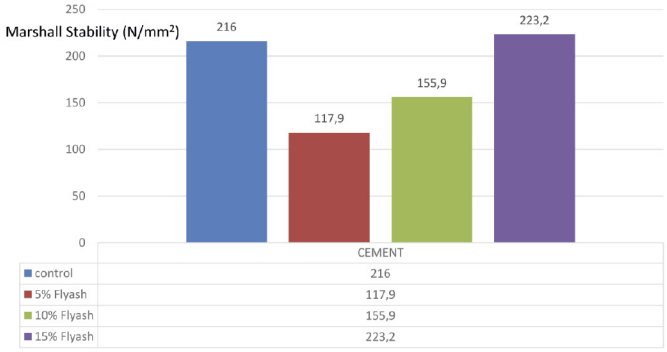

Fig. 1 Marshal stability test result of asphalt mixed with different percentages of fly ash
1. ábra Aszfalt Marshall stabilitási vizsgálatának eredményei különböző arányú pernye hozzáadása mellett

Results of the HMA treated with varying proportions of CWG and modified with 5%, 10% and 15% FA by weight of the mixture are presented in *Table 2* and discussed as follows;

i. it was observed that the result of asphalt mixed with a fixed fly ash percentage of 5 and treated with varying crushed waste glasses percentages showed that there was a reduction in the corrected stability value of the first control sample after crushed waste glass of 2% was added to the asphalt mix but there was increment when 4%, 6% and 8% of crushed waste glasses was added to the mix.

ii. for the asphalt sample mixed with 10% of fly ash and different percentages of crushed waste glass, it was observed that there is a reduction also in the corrected stability value of the first sample after crushed waste glass of 2% was added to the asphalt mix. This was followed by a constant increment at 4%, 6% and 8% of crushed waste glass sample and increased stability values.

iii. For the 15% Fly ash modified HMA and treated with different percentages of crushed waste glass, it was observed that there was a reduction in the corrected stability value for the first sample after crushed waste glass of 2% was added to the mix but there was substantial increment when 4%, 6% and 8% of crushed waste glass sample was added to the HMA mix.

The initial reductions recorded at the start of treatment for the HMA with 2% CWG was due to the reduced cementation due to lack of cementing properties from the CWG [26-30]. But then the recorded increase after the initial treatment was as a result filling pores in the asphalt by the CWG thereby improving the stability again [30-34]. However, the addition of FA maintained a consistent improvement pattern for the HMA stability. This shows that FA is a good modifier for asphalt mixes.

CWG proportion % by wt of HMA mix	MS of FA modified HMA with CWG as fillers		
	Fly Ash proportion % by wt of HMA mix		
	5	10	15
0	105.2	134.5	219.0
2	106.8	149.2	182.4
4	106.7	158.2	193.8
6	108.0	156.7	211.5
8	122.7	161.1	224.2

Table 2 Effect of FA and CWG on the HMA mix
2. táblázat FA és CWG hatása a HMA keveréken

4. Conclusions

Asphalt samples from table one was used as a control mix. This control was derived by getting the average corrected stability value of the three samples done. In view of the above, we observed that the average stability values of both 5% and 10% fly ash mixes were not up to that of the average control stability value; therefore, it had lesser resistance to deformation. At 15% Fly ash content by weight of asphalt cement, a higher resistance to permanent deformation and a higher stability value was observed as compared to the control mix value. Also, it was observed that at 8% waste glass content mixed with different percentages of fly ash modified asphalt, there was increase in the stability values which is a higher resistance to deformation but at 15% fly ash modified asphalt, 8% of waste glass was observed to have a greater average stability value of 224.2 than that of the control mixtures of 216. Hence, it can be concluded that at this percentage we have an optimum modified asphalt that will be able to stand the test of time in terms of durability and also a higher resistance to permanent deformation caused by applied loading. Generally, due to the silicate-based composition of the admixture, it can be accepted that at 8% CWG with 15% fly ash modified asphalt content, a good asphalt mix can be produced for use to achieve a more sustainable pavement construction.

5. Recommendation

After a close and thorough examination and investigation into the mechanical properties of a fly ash modified asphalt using crushed waste glass as filler, it was discovered that the fly ash modified asphalt gave more stability and it is easy to use in road or pavement construction. Therefore, it is recommended that the asphalt samples under investigation should be modified with fly ash due to its high silicate composition, which produces asphalt composite construction material and its quantity should be improved with crushed waste glass so as to meet the criteria for pavement structures that is to be used for highway purposes.

References

[1] Onyelowe, K. C. – Van, Duc Bui – Ubachukwu, Obiekwe – Ezugwu, Charles – Salahudeen, Bunyamin – Van, Manh Nguyen – Ikeagwuani, Chijioke – Amhadi, Talal – Sosa, Felix – Wu, Wei – Duc, Thinh Ta – Eberemu, Adrian – Duc, Tho Pham – Barah, Obinna – Ikpa, Chidozie – Orji, Francis – Alaneme, George – Amanamba, Ezenwa – Ugwuanyi, Henry – Sai, Vishnu – Kadurumba, Chukwuma – Selvakumar, Subburaj – Ugorji, Benjamin (2019): Recycling and Reuse of Solid Wastes; a Hub for Ecofriendly, Ecoefficient and Sustainable Soil, Concrete, Wastewater and Pavement Reengineering. International Journal of Low-Carbon Technologies. Vol. 14(3), pp. 440-451. https://doi.org/10.1093/Ijlct/Ctz028

[2] Peron, Hervé – Laloui, Lyesse – Hueckel, Tomasz – Hu, Liang Bo (2009): Desiccation cracking of soils, European Journal of Environmental and Civil Engineering, 13:7-8, 869-888, https://doi.org/10.1080/19648189.2009.9693159

[3] American Standard for Testing and Materials (ASTM) C618 (1978). Specification for Pozzolanas. ASTM International, Philadelphia, USA.

[4] Rebati, F, L. – Kandlial, P. S. – Brown E. R. – Lee.D.Y. – Kennedy, T. W. (2016): Hot Mix Asphalt Materials, Mixture Design and construction, National Asphalt Pavement Associaton Education Foundation, Lanham Mb

[5] Mohammed, Nazim – Ramjattan, Vitra – Maharaj, Harry and Rean (2016): Mechanistic Enhancement of Asphaltic materials using using fly ash. Journal of applied science 16:526-533

[6] AASHTO T 190-09 (2014): Standard method of test for resistance R-value and expansion pressure of compacted soils. American Association of State Highway and Transportation Officials, Washington DC.

[7] AASHTO T 307 (2014): Standard method of test for determining the resilient modulus of soils and aggregate materials. American Association of State Highway and Transportation Officials, Washington DC.

[8] A manual for design of Hot-mix Asphalt with commentary, Washington DC, The national Academies Press. https//doi.org/ 10.17220/14524

[9] Ramme, B. W. – Covi, A. – Faheem, A. – Soboilev, K. (2016): "Fly ash, An important ingredient for the use of Hot- mix asphalt concrete". Fourth International Conference on substanable construction materials and technologies. (SCMTA) Las Vegas USA. http// www.claisse.info/proccedings.htm

[10] Baby, M. – T.soly, M. – Baby, N. – Vishneye, S. Jacobs (2017): "Laboratory studies on waste Glass as fillers in bituminous mixes". International Research journals of Engineering and Technology (IRJET). Volume 4 issue 07, July 2017

[11] Abendeen, R. (2017): "Effect of Water glass on properties of Asphalt concrete mixes" Jordan Journal of Civil Engineering Volume II, Issue No1

[12] Kallas, B. F. – Puzinausakas, V. P. (1972): Flexural Fatigue Tests on Asphalt Paving Mixtures. Fatigue of Compacted Bituminious Aggregates Mixtures. American Society of Testing and Materials (ASTM), STP 508.

[13] Mix Design Methods for Asphalt, 6th ed., MS-02, Asphalt Institute. Lexington, KY.

[14] Ozsahin, T. S. – Oruc, S. Neural Network Mo. Resilient Modulus of emulsified Asphalt Mixtures for Construction and Building Materials, Vol. 22, 2008, pp. 1436-1445.

[15] Fakhri, M. – Ghanizadeh, A. R.: Ann Experimental Study on the Effect of Loading History Parameters on the Resilient Modulus of Coventional and Modified Asphalt Mixes. Construction and Building Materials, Vol.53, 2014, pp. 284-293.

[16] Hot Mix Asphalt Materials, Mixture Design, and Construction. National Asphalt Pavement Association Education Foundation. Lanham, MD.

[17] Shenoy, A.: 'Unifying asphalt rheological data using the material's volumetric-flow rate',J. Materials in Civil Engg. 13 (2001).

[18] Roberts, F. L., et al. (1996) Hot Mix Asphalt Materials, Mixture Design and Construction. 2nd Edition, NAPA Education Foundation, Lanham.

[19] Samtur., Harold R.: Quantitative Ecosystem Modeling Group, Institute for Environmental Studies, University of Wisconsin-Madison, 1974 - Glass waste

[20] Ben, M. D. – Jenkins, K. J. 2014. Performance of cold recycling materials with foamed bitumen and increasing percentage of reclaimed asphalt pavement. Road Materials and Pavement Design 15 (2): 348-371. DOI:10. 1080/14680629.2013.872051

[21] Brown, E. R. – Cross, S. A.: A national study of rutting in hot mix asphalt (HMA) pavements, National Center for Asphalt Technology, USA, 1992.

[22] Brown, S. F., 1997. Achievements and Challenges in Asphalt Pavement Engineering. ISAP 8th International Conference on Asphalt Pavements,

[23] D'Angelo, J., Harm, E., Bartoszek, J., Baumgardner, G., Corrigan, M., Cowsert, J., Harman, T., Jamshidi, M., Jones, W., Newcomb, D., Jaskuła, P. & Judycki, J. 2014. Durability of Asphalt Concrete Subjected to Deteriorating Effects of Water and Frost. J. Perform. Constr. Facil. https://doi.org/10.1061/(ASCE)CF.1943-5509.0000645, C4014004.

[24] Jenkins, K J. 2000. Mix Design Considerations for Cold and Half-Warm Bituminous Mixes with Emphasis on Foamed Bitumen. PhD Dissertation, Department of Civil Engineering, Faculty of Engineering, University of Stellenbosch, Stellenbosch, South Africa.

[25] Jenkins, K. J. – Molenaar, A. A. A. – de Groot, J. L. A. – Van de Ven, MFC. 2000. Optimisation and Application of Foamed Bitumen in Road Building. Doorwerth, Netherlands: Wegbouwkundige Werkdagen.

[26] Johnson, C. D. 1998. Waste glass as coarse aggregate for concrete. J. Testing Evaluation. 2: 344–350.

[27] Masaki, O. 1995. Study on the hydration hardening character of glass powder and basic physical properties of waste glass as construction material. Asahi Ceramic Foundation Annual Tech. Rep. pp.143-147.

[28] Prowell, B. – Sines, R. – Yeaton, B. 2008. Warm-Mix Asphalt: European Practice. FHWA Report No. FHWA-PL-08-007.

[29] Radziszewski, P. – Kowalski, K. – Król, J. – Sarnowski, M. – Piłat, J. 2014. Quality assessment of bituminous binders based on the viscoelastic properties: polish experience. Journal of Civil Engineering and Management 1 (20): 111-120. https://doi.org/10.3846/13923730.2013.843586.

[30] Asphalt Institute, 1996. Superpave TM Mix Design. Superpave Series SP-2, Lexington, Kentucky, USA.

[31] Vaitkus, A. – Cygas, D. 2009. Analysis and evaluation of possibilities for the use of warm mix asphalt in Lithuania. The Baltic Journal of Road and Bridge Engineering 4(2): 80-86. https://doi.org/10.3846/1822-427X.2009.4.80-86.

[32] Onyelowe, K. C. – Bui Van, D. – Dao-Phuc, L. – Onyelowe, F. – Ikpa, C. – Ezugwu, C. – Salahudeen, A. B. – Maduabuchi, M. – Obimba-Wogu, J. – Ibe, K. – Ihenna, L. (2020): Evaluation of index and compaction properties of lateritic soils treated with quarry dust based geopolymer cement for subgrade purpose. Epitőanyag– Journal of Silicate Based and Composite Materials, Vol. 72, No. 1, pp. 12–15. https://doi.org/10.14382/epitoanyag-jsbcm.2020.2

[33] Onyelowe, K. C. – Onyelowe, Favour Adaugo Deborah – Bui Van, Duc (2020). Overview of ash as supplementary cementitious silicate-based composite and construction material. Epitőanyag– Journal of Silicate Based and Composite Materials, Vol. 72, No. 3 (2020), pp. 80–85. https://doi.org/10.14382/epitoanyag-jsbcm.2020.13

[34] Onyelowe, K. C. – Bui Van, Duc – Ikpa, Chidozie – Osinubi, Kolawole – Eberemu, Adrian – Salahudeen, A. Bunyamin – Nnadi, Oscar C. – Chima, Moses C. – Obimba-Wogu, Jesuborn – Ibe, Kizito – Ugorji, Benjamin (2020). Resilient modulus and deviatoric stress of cemented soils treated with crushed waste ceramics (CWC) for pavement subgrade construction. Epitőanyag– Journal of Silicate Based and Composite Materials, Vol. 72, No. 3 (2020), pp. 86–90. https://doi.org/10.14382/epitoanyag-jsbcm.2020.14

Ref.:

Onyelowe, Kennedy C. – **Onyia**, Michael – **Onukwugha**, Eze R. – **Van**, Duc Bui – **Obimba-Wogu**, Jesuborn – **Ikpa**, Chidozie: *Mechanical properties of fly ash modified asphalt treated with crushed waste glasses as fillers for sustainable pavements*

Építőanyag – Journal of Silicate Based and Composite Materials, Vol. 72, No. 6 (2020), 219–222. p.

https://doi.org/10.14382/epitoanyag-jsbcm.2020.35

Polynomial relationship of compaction properties of silicate-based RHA modified expansive soil for pavement subgrade purposes

Kennedy Chibuzor ONYELOWE ▪ Department of Civil Engineering, Michael Okpara University of Agriculture, Nigeria ▪ konyelowe@mouau.edu.ng
Michael E. ONYIA ▪ Department of Civil Engineering, Faculty of Engineering, University of Nigeria
Eze R. ONUKWUGHA ▪ Department of Civil Engineering, Faculty of Engineering, Federal Polytechnic, Nigeria
Oscar C. NNADI ▪ Department of Civil Engineering, Michael Okpara University of Agriculture, Nigeria
Ifeanyichukwu C. ONUOHA ▪ Department of Environmental Technology, School of Environmental Sciences, Federal University of Technology, Nigeria
Fazal E. JALAL ▪ Geotechnical Engineering, Department of Civil Engineering, Shanghai Jiao Tong University, China

Érkezett: 2020. 02. 01. ▪ Received: 01. 02. 2020. ▪ https://doi.org/10.14382/epitoanyag-jsbcm.2020.36

Abstract

The effect of varying proportions of rice husk ash (RHA) on the compaction behaviour of modified soil has been investigated under laboratory conditions. Problematic soils exhibit undesirable characteristics that make them unsuitable for use as foundation materials due to their swell shrink properties. Clay dominant in montmorillonite and illite belongs to such group of soil due to the net negative cations at the surface when exposed to moisture. For this reason, such soils are modified in a stabilization process to improve their mechanical properties. In this research series of preliminary studies were carried out and it was discovered that the studied soil has 73.2% passing number 200 sieve, has liquid limit of 48% and plasticity index of 19%. This helped to classify the soil as A-7-6 soil according to AASHTO classification method. The soil was also classified as poorly graded soil and highly plastic. The dominant mineral is montmorillonite observed by scanning electron microscopy (SEM) method and due to its high affinity with moisture due to cation exchange, the soil swells and shrinks. The soil was treated with 2% to 30% by weight of solid with RHA and the results were observed. The results showed a steady decrease in the maximum dry density (MDD) of the RHA modified soil. The MDD did not reduce beyond the minimum value for clay soil, which is 1.20 g/cm^3. The decrease recorded in MDD was due to smaller specific gravity compared to the soil. Conversely, the optimum moisture content increased due to moulding moisture demand of the isomorphic net negative cation exchange. Though the cementing property of the RHA was due to the silicate-based aluminosilicates that provided bonding of the treated material, the blend will need a filler material to achieve a more appropriate densification. Finally, mathematical relationships of a polynomial form were proposed that summarized the total compaction behaviour of the RHA modified soil.

Keywords: polynomial relationship, compaction, silicate-based materials, rice husk ash, recycled solid waste material, composite construction materials
Kulcsszavak: polinomiális kapcsolat, tömörítés, szilikátalapú anyagok, rizshéj pernye, újrahasznosított hulladékanyagok, kompozik építőanyagok

Kennedy C. ONYELOWE
He is a senior lecturer at the MOUAU, Nigeria, AE-FUNAI, Abakaliki, Nigeria and External Proposal Technical Reviewer, RIF, Makerere University, Uganda. His research interests include Geotechnical and Geoenvironmental Engineering. He is a member of several professional societies.

Michael ONYIA
He is a senior lecturer at the UNN, Nigeria and former head of department of Civil Engineering. His research interests include, structural engineering, materials engineering and geoenvironmental engineering.

Eze R. ONUKWUG HA
He is a chief lecturer and director at the FedPoNek, Owerri and his research interest is in water resources and environmental engineering

Oscar C. NNADI
He is a graduate student of the department of civil engineering, MOUAU, Nigeria with research focus in Geotechnical Engineering.

Ifeanyichukwu C. ONUOHA
He is a doctoral candidate of the Department of Environmental Technology, FUTO, NIgeria with a research background in soil remediation and green and sustainable construction materials.

Fazal E. JALAL
He is a doctoral student of Shanghai Jiao Tong University, China with a research focus on artificial intelligence in geotechnical engineering.

1. Introduction

Road traffic is carried by the pavement, which in engineering terms is a horizontal structure supported by in situ natural material [1-4]. In order to design this structure, existing records must be examined and subsurface explorations also conducted [1]. The engineering properties of the in-situ soil are established, particularly with respect to strength, stiffness, durability, susceptibility to moisture, and propensity to shrink and swell over time [3-6]. The relevant properties are determined either by field tests (typically by measuring deflection under a loaded plate or the penetration of a rod), by empirical estimates based on the soil type, or by laboratory measurements [2]. The material is tested in its weakest expected condition, usually at its highest probable moisture content [5]. Probable performance under traffic is then determined [2]. Soils unsuitable for the final pavement are identified for removal, suitable replacement materials are earmarked, the maximum slopes of embankments and cuttings are established, the degree of compaction to be achieved during construction is determined, and drainage needs are specified [1]. However, in the case of problematic soils with undesirable characteristic, there has always been a standard need to modify the soils to improve the engineering properties required for a stable and durable foundation [7, 8]. Binders are the commonest in this effort, utilized to improve the quality of weak engineering soils [9]. Materials that exhibit such binding properties are known for either their calcium oxide content or silicate-based components like the rice husk ash (RHA) [10-13].

RHA is a primary agricultural product obtained from paddy. Rice milling produces a by-product known as husk which is surrounded by the paddy grain [14-16]. At the time of milling of paddy about 78% of weight constitutes rice, broken rice, bran and the remaining 22% of the weight of paddy is received as husk. For every 40 kg of rice 10 kg of husk is produced. The husk is disposed by dumping it heap in an open area near the mill or on the sides of the road to be burnt later [5]. Burning the rice husk produces about 15-20% weight of ash [5]. As the ash is very light, it is easily carried away by wind and water causing air pollution and water pollution [5, 6]. The large quantity of ash produced requires maximum areas for disposal. The husk is converted to ash by the process of incineration. The husk is generally used as fuel in the rice mills to produce steam for boiling. It contains about 75% of organic volatile matter and the rest 25% of the weight of the husk is converted into ash known as RHA during the burning process. This RHA in turn contains about 85% - 90% of amorphous silica. The maximum percentage of siliceous material contained in RHA showed that it has pozzolanic properties. Hence for every 997.9 kg of paddy milled, about 217.7 kg (22%) of husk is produced, and when it is fired in the boilers, about 54.4 kg (25%) of RHA is generated. This RHA is a great environmental hazard causing a negative impact on the land and the surrounding area in which it is dumped. There are many ways that are being thought for disposing it by making a commercial use with RHA. In the field of geo-environmental engineering, RHA has been found as a suitable geomaterial utilized in soil treatment due to its high composition of aluminosilicates [17-22]. Compaction characteristics of a test problematic soil treated with RHA was studied in this research making use of compaction curves (see *Fig. 1*) to propose relationships with the added binding material.

Compaction curves are invariable curves of polynomial function. A polynomial function is an equation with multiple terms that has variables and exponents. A graph of polynomial function contains a great deal of information which we can obtain the information by looking at the graph and equation. We can obtain the end behaviour of the graph if given the information or equation. By looking at the graph, we can determine the end behaviour, real and non-real zeros; if the graph is odd or even and the relative extrema. The end behaviour of a graph (compaction curve) is what is happening to the y-values (dry density) as the x-value (water content) increases and decreases.

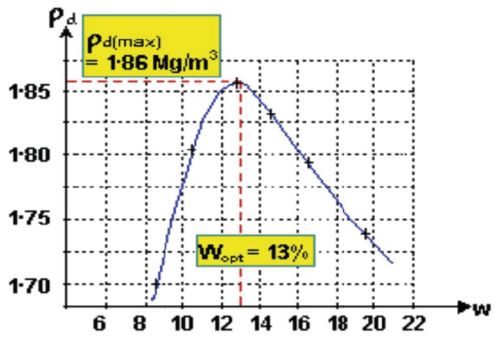

Fig. 1 A typical compaction curve [23]
1. ábra Tipikus tömörödési görbe [23]

When an expansive soil is densified under a constant compactive effort but with varying moisture content, a typical dry density versus water content relationship develops. The shape of the compaction curve is related strongly to the particle size distribution of the soil and compaction method utilised [24]. Compaction curves of expansive soils are essential to establish practical and reliable criteria for effective control of field compaction on most projects.

2. Materials and methods

2.1 Materials preparation

Soil

The test expansive soil was collected from Nbawsi, Nigeria located on 5°23′00′′N and 7°26′00′′E and on military grid reference system coordinates of 32NLL2641295260. 200 g of the sample was collected and prepared for use in the laboratory investigation.

Rice husk ash

Rice husk was collected from rice mills and local dumpsites in Abakaliki, Ebonyi State, Nigeria where the rice farming and milling is the most common occupation. These waste materials were sun dried and combusted to derive ash known as rice husk ash (RHA). The ash was then stored for use in the stabilization experiment.

2.2 Experimental methods

The basic tests that were conducted on the test soil for characterization and classification reasons are as follows:

- Particle size distribution (PSD): this was conducted with vertically arranged sieve sizes mounted on an automatic shaker in accordance with BS 1377-2 and Nigerian General Specification [25, 26].
- Consistency limits: this was conducted using a 2013 cassagrande apparatus on the untreated soil in accordance with BS 1377-2, and NGS [25, 26].
- Specific gravity test was conducted by pycnometer method in accordance with BS 1377-2, and NGS [25, 26].
- Chemical oxides composition test on the test soils and the test materials with XRF method in accordance with BS 1377-2 and Nigerian NGS [25, 26].
- California bearing ratio test (CBR) was conducted on the untreated and treated soils blended with. This was experimented with a 2015 S211 KIT CBR penetration machine, motorized 50 kN ASTM used to load the penetration piston into the soil sample at a constant rate of 1.27 mm/min (1 mm/min to BS Spec.) and to measure the applied loads and piston's penetrations at determined intervals with which CBR values were computed using Eq. (1) and results were obtained. This was experimented in accordance with British standards and AASHTO methods [1-4, 25, 26, 27].

$$CBR = \frac{P_T}{P_S} x100 \quad (1)$$

Where;

P_T = corrected unit test load corresponding to the chosen penetration from load penetration curve, P_T = the total standard load for the same depth of penetration which can be taken as 13.24 kN for 2.5 mm penetration and 19.96 kN for 5.0 mm penetration.

- And finally, standard Proctor compaction test was conducted on the untreated soil with 2016 ELE Automatic Compactor Machine in accordance with BS 1377-2, and NGS [25, 26] and on the rice husk ash modified soil in accordance with BS 1924 [27]. The rice husk was added and mixed with the soil in the proportion of 2 to 30% in increments of 2%.

3. Results and discussions

3.1 General behavior and classification of test materials

The preliminary tests conducted on the test materials were to enable a proper characterization of the materials and the basic classification protocol in a laboratory exercise. *Figs. 2-5* show the graphical results of the basic tests on the soil for particle size distribution, Atterberg limits, compaction and California bearing ratio. Results of the fundamental experiments show that the soil is classified as an A-7-6 soil according to AASHTO grouping. This classification is due to the fact that the percentage passing the number 200 sieve is greater than 36% (73.2%), the liquid limit of the soil is greater than 41% (48%) with a plasticity index greater than 11% (19%) and also a poorly graded soil (GP) according to the USCS. The soil is considered a silt-clay soil because more than 35% of the test specimen passed 0.0075 mm sieve. Generally, the soil is considered fair to poor in the rating for use as a subgrade material in accordance with AASHTO minimum requirements. *Table 1* shows the general information table for the classification data of the test soil and the additive which is rice husk ash. *Table 2* shows the chemical oxide composition of the test materials including those of ordinary Portland cement made by Dangote Industries to show the component differences between ordinary cement and rice husk ash. It can also be deduced from *Table 2* that rice husk ash derives its cementing properties from the silicate-based component of the ash as against the cement that derives its cementing property from calcium oxide (lime). It has been shown that the silicate composition in the rice husk ash is about 86% against about 64% lime present in ordinary cement. This high content of silicates contained in RHA is responsible for the cementitious ability of RHA when used to modify soils in a stabilization exercise. Sadly, the high content of sodium oxide present in the test soil is responsible for the soil's expansive and plastic behaviour. This contributes to the problematic behaviour, which soil exhibits that makes it unsuitable for use as subgrade material in pavement construction. However, this necessitated the stabilization exercise conducted with the rice husk ash to improve and modify the soil to make it more suitable for use as a pavement underlain.

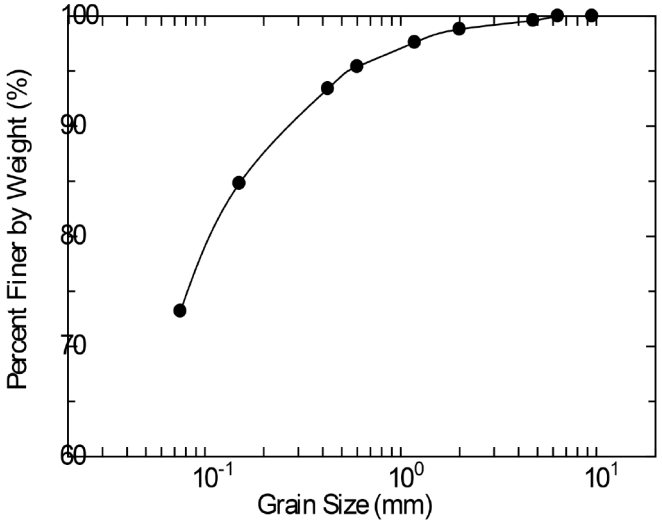

Fig. 2 Grain size distribution of study soil
2. ábra A vizsgált talaj szemcseméret-eloszlása

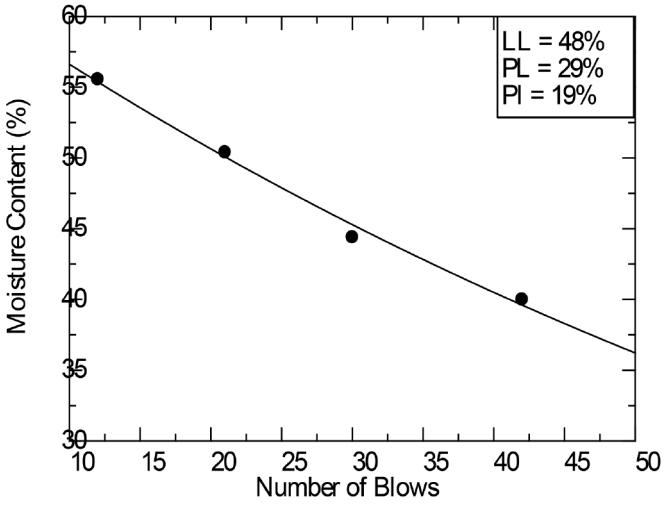

Fig. 3 Atterberg limits curve of the study soil
3. ábra A vizsgált talaj Atterberg határgörbéje

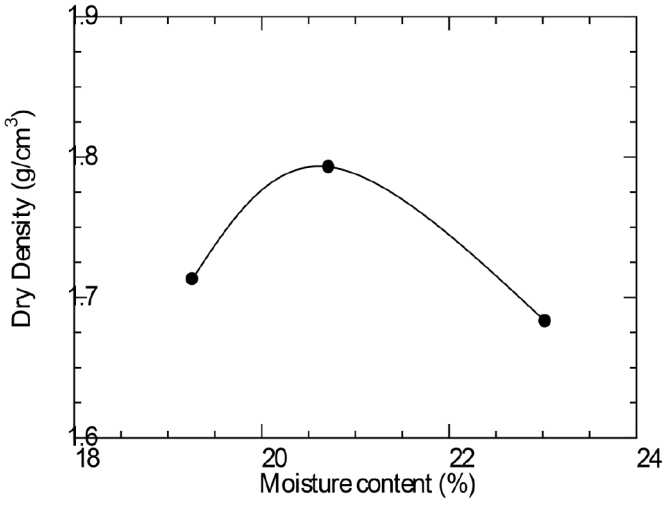

Fig. 4 Compaction curve of the study soil
4. ábra A vizsgált talaj tömörödési görbéje

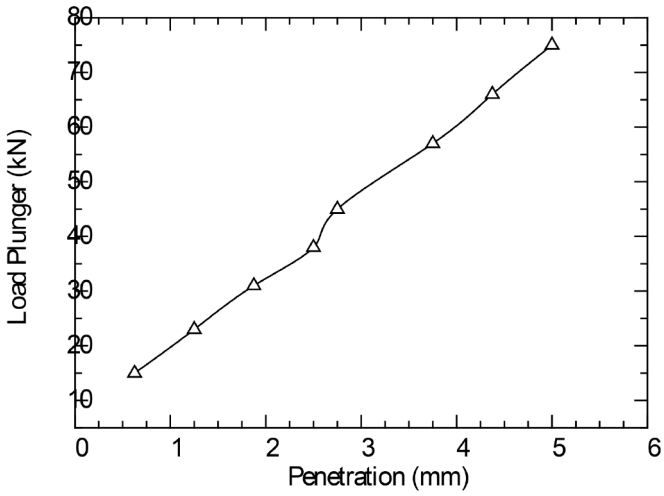

Fig. 5 California bearing ratio behaviour of study soil
5. ábra A vizsgált talaj kaliforniai teherbírási értékei

Property description of test soils and units	Values
% Passing sieve No. 200	73.2
NMC (%)	19
LL (%)	48
PL (%)	29
PI (%)	19
G_s	2.74
$G_s(rha)$	2.01
AASHTO Classification	A-7-6(14)
UCSC	GP/Cl
MDD (g/cm³)	1.80
OMC (%)	20.72
CBR (%)	40.6
Predominant Mineral	montmorillonite
Colour	reddish brown

Table 1 Basic properties of test soils
1. táblázat A vizsgált talaj alapvető tulajdonságai

3.2 Compaction behaviour of rice husk ash modified soil

The RHA was mixed with 2 to 30% in increment of 2% by weight of the solid with the soil and the behaviour of the soil with the increased proportion of the additive was observed. *Fig. 6* shows the dry density behaviour achieved at optimum moisture contents of the treated soil. From the graph, it can be deduced that the maximum dry density of the treated soils reduced with increase in the rice husk ash proportion while the moisture content increased as well (see *Figs. 7* and *8*). The increase in optimum moisture content was due to the increased hydration reaction with the increased addition of rice husk ash with its high content of aluminosilicates [10, 28]. This is also due to water penetrating the interlayer molecular spaces and concomitant adsorption [10]. Also, this is equally due largely to the type of exchangeable cations contained in the reactive interface between the clay soil and the rice husk ash mixed with moulding moisture [29-31]. The dry density reduced due to the fact that the specific gravity of RHA is less than that of soil. From, *Fig. 7*, a polynomial relationship has been proposed to monitor the behaviour of maximum dry density with respect to the proportions of rice husk ash. The polynomial relationship shows the parabolic behaviour of the studied soil when treated with rice husk as compacted at optimum moisture. These relationships are presented in Eq. 1 and 2 where Y represents both the maximum dry density and optimum moisture content in *Figs. 7* and *8*.

$$MDD = - 0.001RHA^2 - 0.0124RHA + 1.7699 \quad (1)$$

$$OMC = 0.0186RHA^2 - 0.1722RHA + 20.806 \quad (2)$$

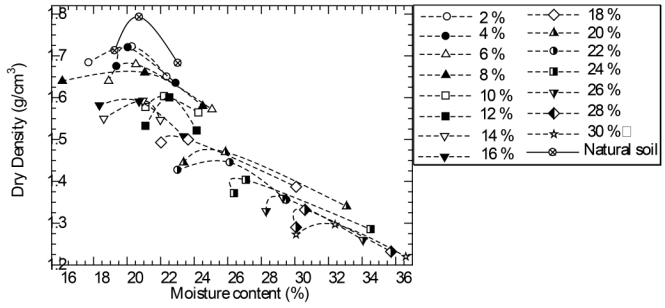

Fig. 6 Compaction curves relationship of rice husk ash modified soil
6. ábra A rizshéj pernye tartalom hatása a vizsgált talaj tömörödésére

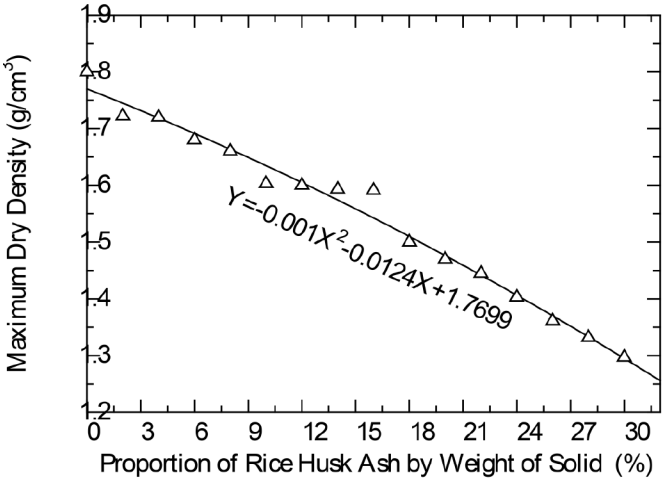

Fig. 7 Maximum dry density relationship with varying proportions of rice husk ash
7. ábra A rizshéj pernye tartalom hatása a maximális száraz sűrűségre

Materials	Oxides composition (content wt %)												
	SiO_2	Al_2O_3	CaO	Fe_2O_3	MgO	K_2O	Na_2O	TiO_2	LOI	P_2O_5	SO_3	IR	Free CaO
study soil	40.06	15.09	2.30	8.66	5.89	12.1	10.4	-	-	5.5	-	-	-
RHA	86.0	3.3	3.6	3.2	0.45	-	-	-	3.45	-	-	-	-
DOPC	21.45	4.45	63.81	3.07	2.42	0.83	0.20	0.22	0.81	0.11	2.46	0.16	0.64

**IR is Insoluble Residue, LOI is Loss on Ignition, RHA: rice husk ash, DOPC: dangote ordinary portland cement.*

Table 2 Oxides composition of the materials used in this paper
2. táblázat A vizsgált anyagok oxidos összetétele

The maximum dry density of the treated soil was at its lowest value at 30% by weight addition of RHA to the soil, which is 1.297 g/cm^3, a value still within the standard minimum value for clay soils (1.20 g/cm^3). The *Eq. 1* with R^2 equals 0.997 can be used to monitor the behaviour of the test soil when modified with RHA for the purpose of subgrade construction. However, RHA would require the assistance of another additive with higher specific gravity to achieve higher densification.

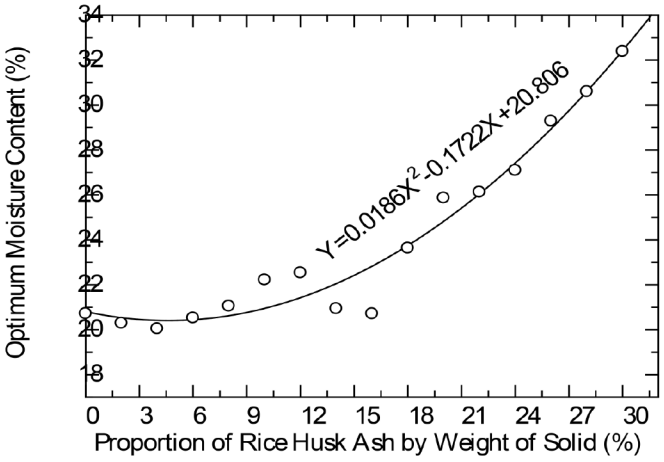

Fig. 8 Optimum moisture condition relationship of modified soil with varying proportion of rice husk ash
8. ábra A rizshéj pernye tartalom hatása a vizsgált talajok optimális nedvességtartalmára

4. Conclusion

The compaction characteristics of RHA modified expansive soil were studied in the laboratory and the following remarks can be made;

- The rice husk ash was observed to exhibit pozzolanic properties and served as a supplementary cementing material.
- The test soil was observed after preliminary experiments that it contains montmorillonite as the dominant mineral, which is responsible for the problematic nature of the soil due to its affinity with moisture.
- The blend of soil and rice husk ash in the modification exercise showed a decrease in the MDD of the treated soil and an increase in the OMC. This was due to the less specific gravity of the ash compared to that of the test soil and affinity for moisture in the hydration reaction that increased the OMC substantially. The silicates-based composition of the ash contributed to the pozzolanic reaction and enhanced the formation of flocs due to cation exchange of the isomorphous particles of the ash within the adsorbed complex phase.
- The RHA showed to be a good construction material to serve as a supplementary cementitious material because of its aluminosilicates content.
- The MDD polynomial relationship with the added admixture produced a correlation of 0.997 and this shows a good fit for the equation to be used in the design of stabilization experiments where RHA is utilized as a binder.

References

[1] AASHTO (1993). Guide for Design of Pavement Structures. American Association of State Highway and Transportation Officials (AASHTO), Washington DC.

[2] AASHTO (2005). Standard Specification for Transportation Materials and Methods of Sampling and Testing, Part II Methods of Sampling and Testing 25th Edition. American Association of State Highway and Transportation Officials, Washington DC.

[3] AASHTO T 190-09 (2014). Standard method of test for resistance R-value and expansion pressure of compacted soils. American Association of State Highway and Transportation Officials, Washington DC.

[4] AASHTO T 307 (2014). Standard method of test for determining the resilient modulus of soils and aggregate materials. American Association of State Highway and Transportation Officials, Washington DC.

[5] Onyelowe, K. C. – Bui Van, D. – Eberemu, A. O. – Xuan, M. N. – Salahudeen, A. B. – Ezugwu, C. – Van, M. N. – Orji, F. – Sosa, F. – Duc, T. T. – Amhadi, T. – Ikpa, C. – Ugorji, B. "Sorptivity, swelling, shrinkage, compression and durability of quarry dust treated soft soils for moisture bound pavement geotechnics". Journal of Materials Research and Technology, 8(4), 2019, 3529–3538. https://doi.org/10.1016/j.jmrt.2019.06.029

[6] Onyelowe, K. C. – Amhadi, T. – Ezugwu, C. N. – Onukwugha, E. – Ugwuanyi, H. – Jideoffor, I. – Ikpa, C. – Iro, U. – Ugorji, B. : Cemented Lateritic Soil as Base Material Improvement Using Compression. In book: Innovative Infrastructure Solutions using Geosynthetics, Proceedings of the 3rd GeoMEast International Congress and Exhibition, Egypt 2019 on Sustainable Civil Infrastructures – The Official International Congress of the Soil-Structure Interaction Group in Egypt (SSIGE), 2020c, pp. 58-67. https://doi.org/10.1007/978-3-030-34242-5_4

[7] Onyelowe, K. C. – Salahudeen, A. B. – Eberemu, A. O. – Ezugwu, C. N. – Amhadi, T. – Alaneme, G. : Oxides of Carbon Entrapment for Environmental Friendly Geomaterials Ash Derivation. In book: Recent Thoughts in Geoenvironmental Engineering, Proceedings of the 3rd GeoMEast International Congress and Exhibition, Egypt 2019 on Sustainable Civil Infrastructures – The Official International Congress of the Soil-Structure Interaction Group in Egypt (SSIGE), 2020a, pp. 58-67. https://doi.org/10.1007/978-3-030-34199-2_4

[8] Onyelowe, K. C. – Salahudeen, A. B. – Eberemu, A. O. – Ezugwu, C. N. – Amhadi, T. – Alaneme, G. – Sosa, F.: Utilization of Solid Waste Derivative Materials in Soft Soils Re-engineering. In book: Recent Thoughts in Geoenvironmental Engineering, Proceedings of the 3rd GeoMEast International Congress and Exhibition, Egypt 2019 on Sustainable Civil Infrastructures – The Official International Congress of the Soil-Structure Interaction Group in Egypt (SSIGE), 2020b, pp. 49-57. https://doi.org/10.1007/978-3-030-34199-2_3

[9] American Standard for Testing and Materials (ASTM) C618 (2014). Specification for Pozzolanas. ASTM International, Philadelphia, USA.

[10] Kotova, O. B. – Shushkov, D. A. – Gömze, L. A. – Kurovics, E. – Ignatiev, G. V. – Sitnikov, P. A. – Ryabkov, Y. I. – Vaseneva, I. N.: Composite materials based on zeolite-montmorillonite rocks and aluminosilicate wastes. Epitő anyag – Journal of Silicate Based and Composite Materials, Vol. 71 (4), 2019, Pp. 125–130. https://doi.org/10.14382/epitoanyag-jsbcm.2019.22

[11] El-Fakharany, M. E. – Ezzat, M. – Gad, A. – Ghafour, N. G. Abdel – Baghdady, A. R.: Performance of dolomitic cementitious mortars as a repairing material for normal concrete in Egypt. Építő anyag – Journal of Silicate Based and Composite Materials, Vol. 71 (2), 2019, Pp. 33–42. https://doi.org/10.14382/epitoanyag-jsbcm.2019.7

[12] Bui Van, D. – Onyelowe, K. C. – Phi Van Dang – Dinh Phuc Hoang – Nu Nguyen Thi – Wu, W. (2018). Strength Development of Lateritic Soil Stabilized by Local Nanostructured Ashes, Proceedings of China-Europe Conference On Geotechnical Engineering, SSGG, pp. 782–786, 2018. https://doi.org/10.1007/978-3-319-97112-4_175

[13] Edeh, Joseph Ejelikwu – Eberemu, Adrian Oshioname – Arigi, Abraham S. D. (2012). Reclaimed Asphalt Pavement Stabilized Using Crushed Concrete Waste as Highway Pavement Material, Advances in Civil Engineering Materials, 1 (1), 1–14, https://doi.org/10.1520/ACEM20120005.

[14] Little, D.N. – Males, E. H. – Prusinski, J. R. – Stewart, B. (2010). Cementitious Stabilization; Transportation in the New Millennium, Louisiana, USA, pp. 1-7.

[15] Janathan, Q. A. – Sanders, T. G. – Chenard, M. (2004). Road Dust Suppression; Effect on Unpaved Road Stabilization, JEST, Malaysia, vol. 1, pp. 21

[16.] Hasan, M. M. – Islam, M. R. – Tarefder, R. A. (2018). Characterization of subgrade soil mixed with recycled asphalt pavement. Journal of Traffic and Transportation Engineering, Vol. 5 (3), pp. 207-214. https://doi.org/10.1016/j.jtte.2017.03.007

[17] Onyelowe, K. C. (2012). Soil Stabilization Techniques and Procedures; A Clue for the Developing world-Nigeria, Global Journal of Engineering and Technology, GJET, India. Vol.5 (1) 65-69.

[18] Onyelowe, K. C. (2012). Geochemistry of Soil Stabilization, ARPN Journal of Earth Sciences, Vol. 1, Issue 2, Pp. 32-35.

[19] Onyelowe, K. C. – Okafor, F.O. (2013). Portland Cement/Quarry Dust Improvement of Olokoro Laterite for Road Base, World Journal of Engineering Science WJES, India. 1(4)133-143.

[20] Onyelowe, K. C. – Ubachukwu, O. A. (2015). Stabilization of Olokoro-Umuahia Lateritic Soil using Palm Bunch Ash (PBA) as Admixture, Umudike Journal of Engineering and Technology (UJET), Volume 1, Number 2, Pp. 67-77.

[21] Onyelowe, K. C. (2017). Solid Wastes Management (SWM) in Nigeria and their Utilization in the Environmental Geotechnics as an Entrepreneurial Service Innovation (ESI) for Sustainable Development. Int J Waste Resour 7: 282. ISSN: 2252-5211.

[22] Onyelowe, K. C. – Maduabuchi M. N. (2017). Palm Bunch Management and Disposal as Solid Waste and the Stabilization of Olokoro Lateritic Soil for Road Construction Purposes in Abia State, Nigeria. Int J Waste Resour Vol 7 Issue 2. https://doi.org/10.4172/2252-5211.1000279

[23] Onyelowe, K. C. – Duc Bui Van – Igboayaka, Clifford – Orji, Francis – Ugwuanyi, Henry (2018). Rheology of mechanical properties of soft soil and stabilization protocols in the developing countries-Nigeria. Materials Science for Energy Technologies. https://doi.org/10.1016/j.mset.2018.10.001

[24] Onyelowe, K. C. – Bui Van, D. (2018). Predicting Strength Behaviour of Stabilized Lateritic Soil- Ash Matrix using Regression Model for Hydraulically Bound Materials Purposes, International Journal of Pavement Research and Technology. https://doi.org/10.1016/j.ijprt.2018.08.004

[25] BS 1377 - 2, 3, (1990). Methods of Testing Soils for Civil Engineering Purposes, British Standard Institute, London.

[26] Nigeria General Specification/Federal Ministry of Works and Housing (1997). Testing for the selection of soil for roads and bridges, Vol. II.

[27] BS 1924, (1990). Methods of Tests for Stabilized Soil, British Standard Institute, London.

[28] Bui Van, D. – Onyelowe, K. (2018). Adsorbed complex and laboratory geotechnics of Quarry Dust (QD) stabilized lateritic soils. Environmental Technology & Innovation, 10, 355-363. https://doi.org/10.1016/j.eti.2018.04.005

[29] Salahudeen, A. B. – Eberemu, A. O. – Osinubi, K. J., (2014). Assessment of Cement Kiln Dust-Treated Expansive Soil for the Construction of Flexible Pavements. Geotechnical and Geological Engineering, an International Journal, 32:923-931. https://doi.org/10.1007/s10706-014-9769-0

[30] Szabó R. 2019. Control of mechanical properties of lignite fly ash based geopolymers by vibrating compression. Építő anyag – Journal of Silicate Based and Composite Materials, Vol. 71 (2), 2019, Pp. 66–71. https://doi.org/10.14382/epitoanyag-jsbcm.2019.12

[31] Khater, Hisham Mustafa Mohamed: Preparation and characterization of lightweight geopolymer composites using different aluminium precursors. Építőanyag – Journal of Silicate Based and Composite Materials, Vol. 70 (6), 2018, Pp. 186–194. https://doi.org/10.14382/epitoanyag-jsbcm.2018.33

Ref.:
Onyelowe, Kennedy Chibuzor – **Onyia**, Michael E. – **Onukwugha**, Eze R. – **Nnadi**, Oscar C. – **Onuoha**, Ifeanyichukwu C. – **Jalal**, Fazal E.: *Polynomial relationship of compaction properties of silicate-based RHA modified expansive soil for pavement subgrade purposes*
Építőanyag – Journal of Silicate Based and Composite Materials, Vol. 72, No. 6 (2020), 223–228. p.
https://doi.org/10.14382/epitoanyag-jsbcm.2020.36

GUIDELINE FOR AUTHORS

The manuscript must contain the followings: title; author's name, workplace, e-mail address; abstract, keywords; main text; acknowledgement (optional)**; references; figures, photos with notes; tables with notes; short biography** (information on the scientific works of the authors).

The full manuscript should not be more than 6 pages including figures, photos and tables. Settings of the word document are: 3 cm margin up and down, 2,5 cm margin left and right. Paper size: A4. Letter size 10 pt, type: Times New Roman. Lines: simple, justified.

TITLE, AUTHOR

The title of the article should be short and objective.

Under the title the name of the author(s), workplace, e-mail address.

If the text originally was a presentation or poster at a conference, it should be marked.

ABSTRACT, KEYWORDS

The abstract is a short summary of the manuscript, about a half page size. The author should give keywords to the text, which are the most important elements of the article.

MAIN TEXT

Contains: materials and experimental procedure (or something similar), results and discussion (or something similar), conclusions.

REFERENCES

References are marked with numbers, e.g. [6], and a bibliography is made by the reference's order. References should be provided together with the DOI if available.

Examples:

Journals:

[6] Mohamed, K. R. – El-Rashidy, Z. M. – Salama, A. A.: In vitro properties of nano-hydroxyapatite/chitosan biocomposites. *Ceramics International.* 37(8), December 2011, pp. 3265–3271, http://doi.org/10.1016/j.ceramint.2011.05.121

Books:

[6] Mehta, P. K. – Monteiro, P. J. M.: Concrete. Microstructure, properties, and materials. *McGraw-Hill*, 2006, 659 p.

FIGURES, TABLES

All drawings, diagrams and photos are figures. The **text should contain references to all figures and tables**. This shows the place of the figure in the text. Please send all the figures in attached files, and not as a part of the text. **All figures and tables should have a title**.

Authors are asked to submit color figures by submission. Black and white figures are suggested to be avoided, however, acceptable.

The figures should be: tiff, jpg or eps files, 300 dpi at least, photos are 600 dpi at least.

BIOGRAPHY

Max. 500 character size professional biography of the author(s).

CHECKING

The editing board checks the articles and informs the authors about suggested modifications. Since the author is responsible for the content of the article, the author is not liable to accept them.

CONTACT

Please send the manuscript in electronic format to the following e-mail address: femgomze@uni-miskolc.hu and epitoanyag@szte.org.hu or by post: Scientific Society of the Silicate Industry, Budapest, Bécsi út 122–124., H-1034, HUNGARY

We kindly ask the authors to give their e-mail address and phone number on behalf of the quick conciliation.

Építőanyag – *Journal of Silicate Based and Composite Materials*, Quarterly peer-reviewed periodical of the Hungarian Scientific Society of the Silicate Industry, SZTE.
http://epitoanyag.org.hu

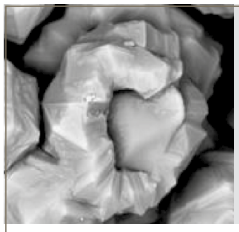

We are pleased to announce the organization of

ic-cmtp6

THE 6TH INTERNATIONAL CONFERENCE ON COMPETITIVE MATERIALS AND TECHNOLOGY PROCESSES

to be held in Hotel Palota in Miskolc-Lillafüred in May 3-7, 2021

The **ic-cmtp6** conference will be held in the wonderful palace of **Hotel Palota** in the exceptionally beautiful environment of **Beech Mountain** in **Miskolc-Lillafüred** in **Hungary**. In 2018 in the previous conference scientists had participated from **46** countries of **5** continents and the largest delegations have arrived from **Japan, Russian Federation, China, Czech Republic,** and **Korea**.

THE CONFERENCE SESSIONS

1. Advanced Ceramics and Nanoceramics
2. Advanced Composites and Nanocomposites
3. Advanced Materials for Bio- and Medical Applications
4. Advanced Materials for Extreme Applications
5. Advanced Nanomaterials and Nanocomposites
6. Advanced Optical Materials – Properties and Applications
7. Advanced Polymer-Clay Nanocomposites
8. Advanced Powder Metallurgy Materials
9. Advanced Processing and Characterization Methods for Nanocomposites
10. Bioelectronic Materials and Biosensors
11. Biomaterials Derived Ceramics and Nanocomposites
12. Clay Minerals and Organo-Clay Complexes
13. CO2 Capture and Fixing Materials and Methods
14. Glasses and Related Competitive Materials
15. Graphene – Properties and Applications
16. Hetero-Modulus and Hybrid Materials
17. Intelligence and Smart Materials – Structures, Properties and Applications
18. Interface as a Functional Material – Behavior, Function and Application
19. Light Weight Materials with Predesigned and Controlled Nanostructur
20. Materials and Methods to Capture and Fixing Radioactive Pollutants from Waters and Soils
21. Materials for Membranes and Catalysts
22. Materials for Biological Systems and Health
23. Materials for Energy Saving and Conservation
24. Materials for Harvesting Renewable Energy
25. Materials for Sensors and Actuators
26. Materials with Extreme Dynamic Strength
27. Mechanical Properties and Processing Technology of Advanced Materials
28. Minerals for Environmental and Medical Application
29. Nanomaterials Applied to Biomedical Applications and Nanomedicine
30. Nanomaterials for Electronic and Electrotechnical Applications
31. Novel Synthesis and Processing Technology
32. Polymer Derived Ceramics and Advanced Nanocomposites
33. Processing and Properties of Silicate Ceramics
34. Sol-Gel Technology in Materials Processing
35. Testing and Characterization of Materials – Methods, Equipment and Uncertainties
36. Traditional Ceramics and Building Materials
37. Traditional Ferrous and Nonferrous Metals

In case of pandemic quarantine of COVID-19 or other force majeure situation the conference ic-cmtp6 will be held in the same place in October 4-8, 2021.

Registration and further information: www.ic-cmtp6.eu